A review of the carotid artery and facial nerve canal systems in extant turtles (#49210)

First submission

Guidance from your Editor

Please submit by 13 Jun 2020 for the benefit of the authors (and your \$200 publishing discount).



Structure and Criteria

Please read the 'Structure and Criteria' page for general guidance.



Author notes

Have you read the author notes on the guidance page?



Raw data check

Review the raw data.



Image check

Check that figures and images have not been inappropriately manipulated.

Privacy reminder: If uploading an annotated PDF, remove identifiable information to remain anonymous.

Files

Download and review all files from the <u>materials page</u>.

19 Figure file(s)

3 Table file(s)

Structure and Criteria



Structure your review

The review form is divided into 5 sections. Please consider these when composing your review:

- 1. BASIC REPORTING
- 2. EXPERIMENTAL DESIGN
- 3. VALIDITY OF THE FINDINGS
- 4. General comments
- 5. Confidential notes to the editor
- Prou can also annotate this PDF and upload it as part of your review

When ready <u>submit online</u>.

Editorial Criteria

Use these criteria points to structure your review. The full detailed editorial criteria is on your guidance page.

BASIC REPORTING

- Clear, unambiguous, professional English language used throughout.
- Intro & background to show context.
 Literature well referenced & relevant.
- Structure conforms to <u>PeerJ standards</u>, discipline norm, or improved for clarity.
- Figures are relevant, high quality, well labelled & described.
- Raw data supplied (see <u>PeerJ policy</u>).

EXPERIMENTAL DESIGN

- Original primary research within Scope of the journal.
- Research question well defined, relevant & meaningful. It is stated how the research fills an identified knowledge gap.
- Rigorous investigation performed to a high technical & ethical standard.
- Methods described with sufficient detail & information to replicate.

VALIDITY OF THE FINDINGS

- Impact and novelty not assessed.
 Negative/inconclusive results accepted.
 Meaningful replication encouraged where rationale & benefit to literature is clearly stated.
- All underlying data have been provided; they are robust, statistically sound, & controlled.
- Speculation is welcome, but should be identified as such.
- Conclusions are well stated, linked to original research question & limited to supporting results.

Standout reviewing tips



The best reviewers use these techniques

Τ	p

Support criticisms with evidence from the text or from other sources

Give specific suggestions on how to improve the manuscript

Comment on language and grammar issues

Organize by importance of the issues, and number your points

Please provide constructive criticism, and avoid personal opinions

Comment on strengths (as well as weaknesses) of the manuscript

Example

Smith et al (J of Methodology, 2005, V3, pp 123) have shown that the analysis you use in Lines 241-250 is not the most appropriate for this situation. Please explain why you used this method.

Your introduction needs more detail. I suggest that you improve the description at lines 57-86 to provide more justification for your study (specifically, you should expand upon the knowledge gap being filled).

The English language should be improved to ensure that an international audience can clearly understand your text. Some examples where the language could be improved include lines 23, 77, 121, 128 - the current phrasing makes comprehension difficult.

- 1. Your most important issue
- 2. The next most important item
- 3. ...
- 4. The least important points

I thank you for providing the raw data, however your supplemental files need more descriptive metadata identifiers to be useful to future readers. Although your results are compelling, the data analysis should be improved in the following ways: AA, BB, CC

I commend the authors for their extensive data set, compiled over many years of detailed fieldwork. In addition, the manuscript is clearly written in professional, unambiguous language. If there is a weakness, it is in the statistical analysis (as I have noted above) which should be improved upon before Acceptance.



A review of the carotid artery and facial nerve canal systems in extant turtles

Yann Rollot Corresp., 1, Serjoscha W Evers 1, Walter G Joyce 1

Corresponding Author: Yann Rollot Email address: yann.rollot@gmail.com

The cranial circulation and innervation systems of turtles have been studied for more than two centuries and extensively used to understand their systematics. Although a significant number of studies related to these structures exists, global comprehension was hindered by poor sampling and a lack of synthetic studies that addressed both systems together. We here provide new insights regarding the carotid circulation and facial nerve innervation systems in a broad set of extant turtles using CT (computed tomography) scans, which allow us to trace the canals they form in bone and understand the interaction between both systems. We document that the palatine artery, including the lateral carotid canal, is absent in all pleurodires and carettochelyids and was likely reduced or lost several times independently within Testudinoidea. We also highlight osteological correlates for the location of the mandibular artery. We finally summarize variation regarding the placement of the mandibular artery, location of the geniculate ganglion, and placement of the hyomandibular and vidian nerves. A morphometric study confirms that the relative size of the carotid canals is correlated with one another. Our results have the potential for building new phylogenetic characters and investigating the circulation systems of fossil taxa, which are expected to shed light on the evolution of the circulation system of turtles and clarify some unresolved relationships between fossil turtle clades.

¹ Department of Geosciences, University of Fribourg, Fribourg, Switzerland



5

7

12

23

1 A review of the carotid artery and facial nerve canal systems in

2 extant turtles

4 Yann Rollot¹, Serjoscha W. Evers¹, Walter G. Joyce¹

6 ¹ Department of Geosciences, University of Fribourg, Fribourg, Switzerland

- 8 Corresponding Author:
- 9 Yann Rollot
- 10 Chemin de Musée 6, 1700 Fribourg, Switzerland
- 11 Email address: yann.rollot@gmail.com

13 Abstract

The cranial circulation and innervation systems of turtles have been studied for more than two 14 15 centuries and extensively used to understand their systematics. Although a significant number of studies related to these structures exists, global comprehension was hindered by poor sampling 16 and a lack of synthetic studies that addressed both systems together. We here provide new 17 insights regarding the carotid circulation and facial nerve innervation systems in a broad set of 18 extant turtles using CT (computed tomography) scans, which allow us to trace the canals they 19 form in bone and understand the interaction between both systems. We document that the 20 21 palatine artery, including the lateral carotid canal, is absent in all pleurodires and carettochelyids 22 and was likely reduced or lost several times independently within Testudinoidea. We also

highlight osteological correlates for the location of the mandibular artery. We finally summarize



PeerJ

24	variation regarding the placement of the mandibular artery, location of the geniculate ganglion,
25	and placement of the hyomandibular and vidian nerves. A morphometric study confirms that the
26	relative size of the carotid canals is correlated with one another. Our results have the potential for
27	building new phylogenetic characters and investigating the eirculation systems of fossil taxa,
28	which are expected to shed light on the evolution of the circulation system of turtles and clarify
29	some unresolved relationships between fossil turtle clades.
30	
31	INTRODUCTION
32	The vertebrate head is the primary body part for sensory perception and interaction with the
33	environment. Over the course of the last two centuries, two systems, the cranial nerve
34	innervation and the cranial arterial circulation, have been studied extensively across extant and
35	extinct tetrapods (e.g., Bojanus, 1819-21; Haughton, 1929; Shishkin, 1968; Lawson, 1970;
36	Starck, 1979; Evans, 1987; O'Keefe, 2001; Müller, Sterli & Anquetin, 2011; Pardo & Anderson,
37	2016). The cranial innervation system provides sensory cues to the brain while the carotid
38	circulation system provides blood to sensory and other organs. Therefore, differences in cranial
39	blood supply and innervation can give clues about the sensory capacities of animals (e.g.,
10	mechanoreception; Dehnhardt & Mauck, 2008; Muchlinski, 2008; George & Holliday, 2013),
11	their physiology (e.g., thermoregulation; Porter & Witmer, 2015; Yu, Ashwell & Shulruf, 2019),
12	the presence and type of cranial soft tissues in fossils (e.g., Benoit et al., 2018), as well as the
13	evolution of these features along stem-lineages (e.g., Benoit, Manger & Rubidge, 2016; Benoit et
14	al., 2018; Joyce et al., 2018; Evers, Barrett & Benson, 2019). Despite showing specific
15	adaptations that often relate to ecological specializations, both the nervous and carotid systems
16	are relatively conservative between major amniote clades in terms of their morphological



47	evolution (Kardong, 1998; Müller, Sterli & Anquetin, 2011) and can therefore be used to
48	examine variational patterns along deep diverging lineages, possibly providing phylogenetic
49	character support for specific divergences. Importantly, arteries and nerves are commonly
50	housed in bony canals for at least parts of their courses, and can thus be identified and analyzed
51	in specimens that lack soft tissues, such as dry museum specimens, or fossils. Therefore,
52	phylogenetic approaches have often focused on indirect evidence for the arterial circulation and
53	cranial innervation, namely the respective bony canals, which can readily be compared across
54	large specimen samples, including fossils. The difficulty here lies with the correct identification
55	(and thus, homology) of said canals.
56	Within turtles, variation pertaining to the carotid arterial system has been used as
57	phylogenetic characters since the seminal study of Gaffney (1975). On a gross scale, differences
58	have been found between early shelled stem-turtles such as Proganochelys quenstedtii from the
59	Late Triassic (Gaffney, 1990) and crown-group turtles (e.g., Sterli & de la Fuente, 2010; Rabi et
60	al., 2013). Within crown Testudines, the two major surviving clades, Pleurodira and Cryptodira,
61	have been found to have different carotid circulation patterns (Albrecht, 1967, 1976; Gaffney,
62	1975, 1979). Additionally, systematic differences between cryptodires and pleurodires have been
63	observed for the facial nerve system (Gaffney, 1975, 1979), which, for the system to have
64	experienced greater evolutionary change over time than other cranial nerves. Parts of the facial
65	nerve eourse share the same course as parts of the carotid arterial system (Albrecht, 1967, 1976;
66	Gaffney, 1979). The shared course of these systems potentially offers an explanation for the
67	relatively greater variability of the facial nerve system. In the past, most descriptive turtle studies
68	have focused on either carotid circulation (e.g., Sterli & de la Fuente, 2010) or cranial
69	innervation (e.g., Evers, Barrett & Benson, 2019) of single species, but hardly on both. However,



since the facial nerve and carotid circulation share some cranial canals, the question about 70 whether these structures evolve independently, or influence one another, has not been addressed. 71 Additionally, the identification of individual bony canals is hampered by the co-occurrence of 72 facial nerve and carotid arterial structures and has led to misidentifications in the past (Rollot, 73 Lyson & Joyce, 2018; Evers, Rollot & Joyce, in review). 74 75 An overview of cranial carotid arterial circulation 76 The main branching patterns of the carotid arterial circulation are conserved across amniotes. 77 78 The internal carotid artery arises from the common carotid artery and splits into a stapedial branch and a cerebral branch (e.g., Sedlmayr, 2002 for archosaurs including birds; Porter & 79 Witmer, 2015 for squamates; Porter, Sedlmayr & Witmer, 2016 for crocodilians; and Müller, 80 Sterli & Anguetin, 2011 for an amniote overview including stem-group taxa). In turtles, the 81 cerebral branch retains the name 'internal carotid artery' (e.g., McDowell, 1961; Gaffney, 1979; 82 Sterli et al., 2010; Rabi et al., 2013). The cerebral/internal carotid artery variously gives off 83 anteriorly directed arterial branches ('palatine artery' in turtles: e.g., Gaffney, 1979) (e.g., 84 Sedlmayr, 2002; Porter & Witmer, 2015), but otherwise enters and traverses the basic ranium 85 86 through the basisphenoid to exit into the pituitary fossa/sella turcica to supply blood to the brain (Sedlmayr, 2002; Müller, Sterli & Anguetin, 2011; Porter & Witmer, 2015; Porter, Sedlmayr & 87 Witmer, 2016). Additional anteriorly directed arteries, such as the infraorbital artery, may also 88 89 branch off the cerebral artery within the braincase (e.g., Porter & Witmer, 2015). Despite this conserved pattern of splitting into subordinate arteries, inconsistent nomenclature 90 91 across reptilian clades makes a deeper understanding of homology difficult. For instance, in 92 squamates and turtles, the artery that supplies the dorsal head region splits extracranially into two



94

95

96

97

98

99

100

101

102

103

104

105

106

107

108

109

110

111

112

113

114

115

major branches, one of which is the stapedial artery. The other branch enters the basic anium and splits again into two subordinate arteries, one that supplies blood to the brain, and one that typically supports the facial region. In the turtle literature, the term 'internal carotid artery' is used to refer to the arterial section that lies between the branching point of the stapedial artery. and the intracranial split (e.g., McDowell, 1961; Gaffney, 1979; Sterli et al., 2010; Rabi et al., 2013). Thus, in turtles, the 'internal carotid artery' gives rise to (i) the 'cerebral artery' that traverses the basisphenoid and enters the pituitary fossa to supply the brain with blood, and (ii) the 'palatine artery' that traverses the basic ranium anteriorly toward the facial region. In squamates, however, the term 'internal carotid artery' is used for the carotid section prior to the divergence of the stapedial artery (Porter & Witmer, 2015). The second branch that forms at this divergence is called the 'cerebral artery'. The 'cerebral artery' of squamates (= 'internal carotid artery' of turtles) then gives off the 'sphenopalatine artery' (= 'palatine artery' of turtles), and keeps its name for the remainder of its course into the brain (= 'cerebral artery' of turtles). In this study, we use the classic turtle nomenclature with regard to the splitting pattern of carotids, which gained influence primarily by the works of Albrecht (1967, 1976) and Gaffney (1972, 1979). Under this nomenclature, the internal carotid artery and stapedial artery diverge from one another in an extracranial position, with the stapedial artery entering the cavum acustico-jugulare. The stapedial artery usually gives off the mandibular artery, although many exceptions exist across turtles. For instance, the mandibular artery derives from the internal carotid artery in trionychids (Albrecht, 1967). The internal carotid artery travels medially toward the basic ranium and commonly, but not ubiquitously, splits into the cerebral and palatine arteries. The cerebral artery is always present and always traverses the basisphenoid and enters the sella turcica/pituitary fossa.



\mathbf{A}	history	of c	carotid	research	ı in	turtles

Early work on the carotid arterial system in turtles was mainly limited to the documentation of
carotid artery courses in single species (e.g., Bojanus, 1819-21; Nick, 1912; Shindo, 1914), or a
selection of related turtles (McDowell, 1961). Later, studies by Albrecht (1967, 1976) were the
first synthetic approaches to summarize variation of features related to carotid circulation across
clades. Albrecht's findings were further publicized by the landmark studies of Gaffney, who
introduced this character complex to turtle phylogenetics (e.g., Gaffney, 1975; Gaffney &
Meylan, 1988), and who advocated the use of osteological correlates of the arteries, namely the
canals and foramina, to identify carotid features in fossil turtles, particularly by providing
terminology (Gaffney, 1972) and comparisons across a large sample of turtles (Gaffney, 1979).
The importance of the cranial circulatory system in systematics has been highlighted now for
more than half a century and many studies have added and/or revised characters related to
carotids (e.g., Gaffney, 1975; Meylan & Gaffney, 1989; Jamniczky, 2008; Sterli & de la Fuente,
2010; Sterli et al., 2010; Rabi et al., 2013; Zhou & Rabi, 2015; Joyce et al., 2018; Evers &
Benson, 2019; Hermanson et al., 2020), although methods of character implementation have
significantly varied between studies (e.g., Joyce, 2007; Anquetin, 2012; Evers & Benson, 2019).
Several 'patterns' of circulation have been proposed, and other evolutionary scenarios have been
put forward. For instance, Meylan & Gaffney (1989) postulated the cerebral and palatine arteries
of turtles primitively had a similar size and were slightly smaller than the stapedial artery.
Gaffney (1975) also proposed that the three major groups of turtles recognized at the time (i.e.
pleurodires, cryptodires, and paracryptodires) each display a characteristic pattern for the
circulation system, with the discriminating feature being the position of the foramen posterius



140

141

142

143

144

145

146

147

148

149

150

151

152

153

154

155

156

157

158

159

However, most of these inferences were based on only a small sample of dissected taxa obtained during earlier studies (e.g., Albrecht, 1967, 1976), and patterns have been extrapolated from the few taxa studied to entire turtle groups (Gaffney, 1979; Jamniczky & Russell, 2007), without further verification. Paleontologists have been reporting patterns of cranial arterial circulation and innervation for extinct species. These studies recognized that the observed features cannot easily be fit into the framework established on the few extant turtles studied in the past. For example, although all crown-group turtles have their carotid arterial system fully embedded within the basicranium, fully or partially ventrally-open carotid systems appear in stem-group turtles, but also on the stem-lineages of various crown-group clades (e.g., Meylan & Gaffney, 1989; Sterli et al., 2010; Rabi et al., 2013). Rabi et al. (2013) proposed an updated, comprehensive nomenclatural system for the diversity of foramina and canals associated with the carotid system, but this nomenclature was not universally applied in recent turtle literature, despite its advantages. However, although this contribution figuratively cut the Gordian knot of confusing terminology by suggesting an internal consistent nomenclature, we here suggest two minor modifications to the names of the canals that contain the cerebral and palatine arteries (see Material and Methods below). The advent of CT-based studies has further led to a re-investigation of variation on a broad taxonomic and sampling scale of extant and extinct turtles (e.g., Paulina-Carabajal et al., 2017; Evers & Benson, 2019; Hermanson et al., 2020), challenging some of the more classic character concepts regarding the carotid system.

canalis carotici interni, i.e., the foramen through which the internal carotid artery enters the skull.

160

161

Facial nerve



162	Much less recent research has been done on the facial nerve (CN VII), despite the availability of
163	a broad historic literature describing nerve patterns in extant turtles (e.g., Bojanus, 1819-21;
164	Vogt, 1840; Kesteven, 1910; Gaupp, 1888; Hoffmann, 1890; Ruge, 1897; Siebenrock, 1897;
165	Bender, 1906; Noack, 1906; Ogushi, 1911, 1913a, 1913b; Hanson, 1919; Shiino, 1913; Nick,
166	1912; Shindo, 1914; Fuchs, 1931; van der Merwe, 1940; Soliman, 1964). The facial nerve
167	branches off the brain of turtles and exits the braincase via the fossa acustico-facialis on the
168	medial surface of the prootic. From this fossa, it extends laterally through a canal. Further
169	laterally, the facial nerve forms the geniculate ganglion, from which two major nerves emerge,
170	the anteriorly directed vidian/palatine nerve, and the posteriorly directed hyomandibular nerve
171	(Gaffney, 1979). Based on the comprehensive works of Siebenrock (1897), Shiino (1913), and
172	Soliman (1964), Gaffney (1975, 1979) suggested that the position of the geniculate ganglion of
173	the facial nerve differs between cryptodires and pleurodires, with cryptodires having the
174	geniculate ganglion positioned in the canal for the lateral head vein, i.e. the canalis cavernosus,
175	and pleurodires having the geniculate ganglion contact the internal carotid artery canal (=canalis
176	caroticus internus). Gaffney's (1979) interpretation was based on relatively few specimens, but
177	has largely remained unchallenged and been used in many phylogenetic studies of turtles.
178	Although deviations to Gaffney's (1979) clear-cut patterns have been known for a long time
179	(e.g., Gaffney, 1983), a more recent, systematic survey of CT scans reveals many more,
180	including a potentially novel position for the geniculate ganglion (Evers and Benson, 2019). As
181	historically terms were used interchangeably in the past, Rollot, Lyson & Joyce (2018) provided
182	a consistent nomenclature for the canals left by the facial nerve system. Here, we investigate the
183	facial nerve pattern on a broad taxonomic scale, and investigate how it is related to the carotid
184	arterial pattern, with which is partially shares canals.



Aims and objectives

For this contribution, we aim to document the carotid circulation pattern, as well as the course of the facial nerve, for all major clades of extant turtles. Our work is based on high-resolution micro-computed tomography (CT) scans of 66 extant turtle species. We focus on the position of foramina, the bones that form the canals and foramina, and the connections between these structures (i.e., canals). In addition to updating the standardized terminology for these features, we address the variation of these systems within and between clades and summarize patterns common to specific clades. We provide evidence for the repeated loss of some branches of the carotid arterial system and re-interpret canals that have been said to house the palatine artery in these turtles as actually housing the vidian nerve, a branch of the facial nerve. Our work provides an important step towards a comprehensive understanding of cranial arterial circulation and facial nerve patterns, which can aid in character construction for phylogenetic analyses.

Furthermore, with the inclusion of fossil data, our work will provide the basis for a comprehensive evolutionary understanding of cranial arterial circulation and innervation in turtles.

MATERIAL AND METHODS

CT-scanning and segmentation

For this study, we broadly sampled across the turtle tree to compile a set of 69 CT scans of the skulls of 66 extant turtle species (see Table 1). The vast majority of scans were previously published and are available at public repositories (Evers and Benson, 2018; Lautenschlager, Ferreira & Werneburg, 2018; Evers, 2019). The models generated are available on Morphobank





(http://morphobank.org/permalink/?P3732). The (para)basisphenoid, the left pterygoid, the carotid system, the canalis cavernosus, and the facial nerve system of 14 skulls representing the primary clades ("families") of extant turtles were segmented manually using the brush and lasso and interpolation tools of Amira 6.4.0 (https://www.fei.com/software) and final models were generated by exporting surfaces of the structures of interest.

213

214

215

216

217

218

219

220

221

222

223

224

225

226

227

228

229

230

208

209

210

211

212

Assessment of size relationships between 'medial' and stapedial blood flow

Albrecht (1976) hypothesized that reductions in the size of the stapedial artery of turtles are counterbalanced by increases in size of the palatine or orbital arteries ('medial' blood flow) to ensure the arterial blood supply for the facial region of the skull. In order to quantitatively and statistically assess this hypothesis, we measured the cross-sectional areas of the stapedial and carotid canals in Dragonfly 4.0 (https://www.theobjects.com/dragonfly/index.html) (see Table 2). For the internal carotid artery canal, the cross sectional area was measured close to the foramen posterius canalis carotici interni. For the stapedial, palatine, and cerebral artery canals, the cross sectional area was measured close to their respective exit foramina. In all cases, measurements were taken orthogonal to the orientation of the canal. These measurements provide approximate estimates of blood flow, as arterial canal diameter is proportional to arterial size in turtles (Albrecht 1976, Jamnicky and Russell, 2004). To test if the reduction of the stapedial artery has an effect on the 'medial' blood flow, we performed phylogenetic generalized least squares regression (PGLS; Grafen, 1989; Rohlf, 2001) of the log₁₀-transformed internal carotid arterial cross-sectional area on the respective measurement for the stapedial artery. PGLS is a modification of ordinary least squares regression (OLS), which takes into account the expected co-variance structure of residuals that is the result of phylogenetic non-independence of



231	the input data (e.g., Felsenstein, 1985; Grafen, 1989; Symonds & Blomberg, 2014). The expected
232	variances and co-variances of traits among species follow a Brownian motion model of trait
233	evolution in PGLS and related methods like phylogenetic independent contrasts (e.g.,
234	Felsenstein, 1985; Pagel, 1997, 1999), although different models of trait evolution can be used in
235	PGLS. The strength of the phylogenetic correlation was estimated under maximum likelihood
236	during the model fitting using variable Pagel's lambda (Revell, 2010; Motani & Schmitz, 2011).
237	Pagel's lambda is a parameter that describes the model of evolution, with values of 1 indicating
238	that trait evolution occurred under Brownian motion, whereas a value of 0 means there is no
239	phylogenetic signal in the residuals of the regression. PGLS was performed in R with the gls()
240	function of the package ape (Paradis & Schliep, 2018), and the corPagel option for setting the
241	correlation structure of the model. Because of phylogenetic correlation in the error structure of a
242	PGLS, the coefficient of correlation R ² cannot be easily defined for phylogenetic regressions
243	(Ives, 2018). Here, we use a generalized form of R ² described by Nagelkerke (1991), which is
244	derived by comparison of the log-likelihood of the model with that of a null model ($\log_{10}(CCI)$ ~
245	1). As the phylogenetic input for the PGLS, we used the dated phylogeny of Pereira et al. (2017),
246	which we pruned to match our taxon sample. Two species in our sample, Kinixys erosa and
247	Pseudemys floridana, were not included in the study of Pereira et al. (2017). We re-assigned the
248	tip-labels of two closely related species, Kinixys belliana and Pseudemys texana, in the tree of
249	Pereira et al. (2017) to those of our sampled species. This procedure assumes that <i>Kinixys erosa</i>
250	(or Pseudemys floridana) is closer related to Kinixys belliana (or Pseudemys texana) than to any
251	other turtle in the tree, which is justified by the circumstance that the monophyly of neither the
252	species of Kinixys nor Pseudemys are disputed, and by the fact that we sampled only one species
253	of each genus in our study. For the regression analysis, we chose the internal carotid artery as





255

256

257

258

259

260

261

262

263

264

265

266

267

268

269

270

271

272

representing 'medial' blood flow, as opposed to the combined values of the cerebral and palatine arteries. This allowed us to include taxa for which the palatine artery has no osteological correlate but is present (i.e. chelonioids; see Results). Additionally, this procedure allowed the inclusion of podocnemidids. Although podocnemidids provide no reliable estimation for the cross-sectional area of the internal carotid artery, as the artery extends through the enlarged cavum pterygoidei (see Results), these turtles could be included by taking the cross-sectional areas of the cerebral artery instead. This can be justified, as the palatine artery is absent in podocnemidids (see Results), and thus the cerebral artery canal represents the internal carotid artery in terms of cross-sectional area (=blood flow). Although interesting for questions we liked to address, we had to exclude taxa with completely reduced stapedial arteries for the analysis (n=2), as the logarithm of zero is undefined. Additionally, we excluded *Kinosternon baurii* after an initial run of analyses including it. K. baurii has a strongly reduced stapedial artery size in absolute numbers (two orders of magnitude smaller than in other kinosternids), and has a proportionally extremely large internal carotid artery (same order of magnitude than other kinosternids), leading to an extreme positive residual when included into a regression. It can, therefore, be statistically defined as an outlier with large leverage on the regression line. Although the data for K. baurii strongly supports the notion that internal carotid artery size is strongly increased when the stapedial artery size is strongly reduced (see Discussion), we conservatively excluded the taxon. Our sample in total was thus n=63.

273

274

Nomenclature and Homology



As our primary source of information are skulls, we are not able to observe the cranial circulation and innervation systems directly, but rather ean only assess their former presence by



particular Albrecht (1967, 1976). The vast majority of our assessments are, nevertheless, 278 uncontroversial. We therefore shorten our descriptions by not justifying explicitly why we 279 believe a particular canal to be filled by a particular soft structure. Instead, we only provide 280 separate justifications in the text for the rare cases where our conclusions differ from previously 281 282 published ones. The dissections of Albrecht (1967, 1976) documented strong variation in the organization of 283 the cranial blood supply of turtles, which are interchangeably fed by branches of the internal 284 carotid artery and the stapedial artery. For instance, the sensory organs and tissues of the snout 285 region (i.e., "the palate") are mostly supplied by the stapedial branch in chelydrids, testudinoids, 286 and pleurodires, by the palatine branch in kinosternoids, by a mixture of the stapedial and 287 palatine branches in chelonioids, but by the orbital branches of the cerebral branch in 288 trionychids. Conversely, the mandible is fed by the stapedial branch in chelydrids, pleurodires, 289 290 and testudinoids, but by the palatine branch in kinosternoids, chelonioids, and trionychids. So, while the terms "cerebral" and "stapedial" are somewhat misleading, as they disguise the fact that 291 tissues other than the brain and stapes are often fed by them, the term "palatine" is positively 292 misleading, as the relevant artery, if present, does not feed the palate at all in many turtles. The 293 situation is especially problematic in trionychids, where the "palatine artery" only feeds the 294 mandible, while the palate is entirely fed by a large subordinate branch of the "cerebral artery." 295 296 The nomenclatural system of Rabi et al. (2013) created nomenclatural clarity by providing separate names for all possible canals and openings formed by the internal carotid system, but 297 298 accidentally introduced a new source of confusion by selecting names for the canals that negate 299 the homology of the vessels that they contain. As the system is still relatively new, we here take

explicit reference to the canals they left in bone in combination with published dissections, in



301

302

303

304

305

306

307

308

309

310

311

312

313

314

315

316

317

318

319

320

321

322

the opportunity to provide minor adjustments, by replacing the terms canalis caroticus cerebralis with canalis caroticus basisphenoidalis and canalis caroticus palatinum with canalis caroticus lateralis. We select these terms as they have historic precedence. The term canalis caroticus basisphenoidalis connects to the term "foramen caroticum basisphenoidale," which was introduced by Gaffney (1983) for the posterior opening of the carotid canal that punctures the basisphenoid (e.g., the internal carotid canal of Gaffney, 1983, but the cerebral canal of Rabi et al., 2013). Although this term was sometimes applied to the fenestra caroticus of Rabi et al. (2013) (e.g., Meylan & Gaffney, 1989; Brinkman & Peng, 1996; Sukhanov, 2000), it was mostly used for this foramen in subsequent descriptions of basal turtles (e.g., Gaffney, 1990; Gaffney & Meylan, 1992; Gaffney and Ye, 1992; Brinkman & Peng, 1993; Gaffney, 1996; Sukhanov, 2000). The term canalis caroticus lateralis, on the other hand, had been used consistently over the course of the entire 20th century (Gaffney, 1972, 1979), but had been replaced purposefully by Rabi et al. (2013), as the name of the canal did not make reference to the arteries it contained. However, as highlighted above, the replacement term "palatine canal" is just as confusing, as the vessels held in this canal do not feed the palate in many turtles. In addition to reconnecting to the historic literature, these newly established names have the advantage by being purely positional and by not implying what vessels they contain. This nomenclature therefore only highlights the homology that exists to the basic branching pattern seen in the carotid system of turtles. As the artery held in the canalis caroticus basisphenoidalis universally feeds the brain, we here retain the term "cerebral artery," even though other structures may be fed as well by subordinate branches that diverge off the cerebral artery within the sella turcica. For the artery held in the canalis caroticus lateralis, we will try to be specific, where possible, by reference to Albrecht (1967, 1976). However, in anticipation of the needs of paleontologists, who cannot know what



tissues are fed by the arteries passing the lateral canal, we suggest the informal term "lateral 323 branch of the internal carotid canal." 324 In addition to the modifications provided for the nomenclature of the cranial arterial 325 circulation system, we also add the terms 'proximal' and 'distal' to some aspects of the 326 innervation system. Although the usage of 'proximal' and 'distal' are unusual in a cranial 327 328 context, we find these terms useful to refer to distinct sections of nerves within the cranium. The 'proximal' part of a nerve is close to its origin, i.e. the brain or its ganglion, whereas 'distal' 329 portions are further away from its origin and close to the innervated tissue. Our modified list for 330 the definitions of all canals we discuss and criteria on how to recognize them is as follows: 331 Cavum cranii – We here restrict the meaning of the term cavum cranii from referring to the 332 entire space from the fossa nasalis to the foramen magnum (Gaffney, 1972) to the space filled by 333 brain tissues only. 334 Canalis caroticus internus – The bony canal that contains the main branch of the internal 335 336 carotid artery from the foramen posterius canalis carotici interni to the split into its two primary subarteries (Rabi et al., 2013). Whenever the split of the internal carotid artery cannot be 337 identified, typically because of the absence of a formed canalis caroticus lateralis, the canalis 338 339 caroticus internus is defined as the portion of the canal that does not yet traverse the basisphenoid, as opposed to the canalis caroticus basisphenoidalis, which is defined as the 340 341 portion of the canal that is located inside the basisphenoid. Additional structures might be 342 contained in the canalis caroticus internus, in particular the vidian nerve, but this is not reflected in the name. The canalis caroticus internus typically traverses the skull at the junction of the 343 344 basisphenoid with the pterygoid and/or prootic in the posterior prolongation of the canalis 345 caroticus basisphenoidalis.



Foramen posterius canalis carotici interni – The posterior foramen to the canalis caroticus
internus, which serves as the entry of the internal carotid artery into the skull (Rabi et al., 2013).
Canalis caroticus basisphenoidalis – The canal that contains the cerebral artery from the
split of the carotid artery into its primary branches to the foramen anterius canalis carotici
basisphenoidalis (canalis caroticus cerebralis of Rabi et al., 2013). Whenever the split of the
internal carotid artery cannot be identified, the canalis caroticus basisphenoidalis is defined as
the portion of the canal that traverses the basisphenoid, as opposed to the more posteriorly
located canalis caroticus internus, which is located outside of the basisphenoid. No other
structures are known to traverse this canal. The canalis caroticus basisphenoidalis typically
penetrates the basisphenoid at mid-length and universally exits the basisphenoid within the sella
turcica. The canalis caroticus basisphenoidalis is the largest canal to pierce the basisphenoid.
Foramen anterius canalis carotici basisphenoidalis – The anterior opening of the canalis
caroticus basisphenoidalis (foramen anterius canalis carotici cerebralis of Rabi et al., 2013),
universally located within the sella turcica of the basisphenoid.
Canalis caroticus lateralis – The bony canal that contains the lateral branch of the internal
carotid canal, typically the palatine artery, from the split of the carotid artery into its two primary
branches to the foramen anterius canalis carotici lateralis (canalis caroticus palatinum of Rabi et
al., 2013). The vidian nerve may traverse part of this canal. The canalis caroticus lateralis
typically punctures the skull at the junction of the basisphenoid with the pterygoid and exits
within the sulcus cavernosus and near the anterior opening of the latter.
Foramen anterius canalis carotici lateralis – The anterior exit of the lateral branch of the
internal carotid artery, typically the palatine artery, located near the anterior exit of the sulcus
cavernosus (foramen anterius canalis carotici palatinum of Rabi et al., 2013).



369	Canalis carotico-pharyngealis – A single or series of bony canals in the pterygoid that
370	contain the arteria carotico-pharyngealis. The arteria carotico-pharyngealis arises at the base of
371	the palatine artery, enters the canalis carotico-pharyngealis to extend ventrally through the
372	pterygoid, and exits the skull through the foramen carotico-pharyngeale (Albrecht, 1967).
373	Foramen carotico-pharyngeale – The ventral exit of the arteria carotico-pharyngealis
374	located on the ventral surface of the pterygoid.
375	Canalis cavernosus – The bony canal that contains the lateral head vein (Gaffney, 1972). The
376	distal portion of the hyomandibular nerve may traverse this canal as well. Additionally, the
377	mandibular artery may traverse this canal in some turtle clades. The canalis cavernosus is
378	generally a large and straight canal that obliquely traverses the skull lateral to and outside of the
379	braincase to exit within the cavum acustico-jugulare.
380	Canalis nervus facialis – The bony canal that contains the facial nerve prior to its split at the
381	geniculate ganglion into the vidian and hyomandibular branches (Rollot, Lyson & Joyce, 2018).
382	The canal is recognized as the structure laterally penetrating the prootic from the fossa acustico-
383	facialis. It may end within the canalis cavernosus, the canalis caroticus internus, or at its split
384	into the vidian and hyomandibular nerves.
385	Canalis nervus hyomandibularis proximalis – The bony canal that is laterally continuous
386	with the canalis nervus facialis, and exits into the canalis cavernosus. This canal contains the
387	proximal part of the hyomandibular branch of the facial nerve, but is only present in turtles in
388	which the geniculate ganglion is not positioned within the canalis cavernosus.
389	Canalis nervus hyomandibularis distalis – The bony canal that originates within the wall of
390	the canalis cavernosus posterior to the connection of the canalis nervus facialis or canalis nervus
391	hyomandibularis proximalis. The canal extends posteriorly, paralleling the canalis cavernosus,



392	and exits into the cavum acustico-jugulare. It contains the distal portion of the hyomandibular
393	branch of the facial nerve, and is only present in some turtles.
394	Canalis pro ramo nervi vidiani – The bony canal that contains the posterior (=proximal)
395	portion of the vidian nerve to the exclusion of the other primary nerves and blood vessels defined
396	herein (Rollot, Lyson & Joyce, 2018). In living turtles, the canal, when present, connects the
397	geniculate ganglion to the canalis caroticus internus and traverses the prootic and pterygoid
398	along its way.
399	Canalis nervus vidianus – The bony canal that contains the anterior (=distal) portion of the
400	vidian nerve to the exclusion of the other primary nerves and blood vessels defined herein
401	(Rollot, Lyson & Joyce, 2018). The canal typically originates from the canalis caroticus lateralis
402	and anteroposteriorly traverses the pterygoid or palatine to open towards the foramen palatinum
403	posterius. Numerous accessory canals may branch from this canal that innervate the dorsal or
404	ventral side of the pterygoid or palatine.
405	Foramen anterius canalis nervi vidiani – The anterior exit of the canalis nervus vidianus
406	(Rollot, Lyson & Joyce, 2018). The foramen is typically located posterior to the foramen
407	palatinum posterius, but can be split into multiple foramina arranged on the dorsal or ventral
408	surfaces of the pterygoid or palatine.
409	Foramen arteriomandibulare – A separate, anterior exit for the mandibular artery from the
410	canalis cavernosus into the temporal fossa. It is located just posterior to the foramen nervi
411	trigemini.
412	
413	RESULTS
414	Chelidae (Fig. 1)



In all chelids studied, the internal carotid artery enters the skull from ventral. The foramen
posterius canalis carotici interni is formed by the prootic in <i>Phrynops hilarii</i> and <i>Hydromedusa</i>
tectifera, by the basisphenoid and the prootic in Chelus fimbriatus, by the prootic and quadrate in
Chelodina oblonga and Phrynops geoffroanus, and by the basisphenoid, prootic and quadrate in
Emydura subglobosa. These observations differ from those of Siebenrock (1897), who identified
the prootic in chelids as being the main bone forming the foramen posterius canalis carotici
interni, with occasional contributions from the basisphenoid. Albrecht (1976) similarly described
the foramen posterius canalis carotici interni as only being formed by the prootic and
basisphenoid in the chelids he studied. The apparent variation in bone contributions to this
foramen was recently coded by Evers and Benson (2018) as separate characters. The internal
carotid artery is directed anteromedially and the canalis caroticus internus is formed by the
prootic and basisphenoid in Chelus fimbriatus, P. hilarii, and H. tectifera, by the quadrate,
prootic, and basisphenoid in Chelodina oblonga and P. geoffroanus, and by the quadrate, prootic,
basisphenoid and pterygoid in E. subglobosa. Again, this contrasts with Albrecht (1976), who
noted that the canalis caroticus internus is only formed by the prootic and basisphenoid. We have
not been able to observe a canalis caroticus lateralis in any of our specimens. This as first glance
seems to contrast with Albrecht (1976), who stated that a canalis caroticus lateralis is present in
all the chelids he observed, except for Chelus fimbriatus. A close reading of Albrecht (1976),
however, reveals that he did not observe the palatine or any other artery in any chelid in his
sample and that the canal he termed the lateral carotid canal mostly crossed the pterygoid, opens
posterior to the foramen palatinum posterius, not the sulcus cavernosus, and contains the vidian
nerve only. Albrecht's (1976) observations therefore support our conclusion that the palatine
artery and canalis caroticus lateralis are completely absent in chelids. In contrast to Albrecht



(1976), we are able to trace the passage of the vidian nerve in <i>Chelus fimbriatus</i> , which confirms
similar observations made by Gaffney (1979: fig. 23). Hermanson et al. (2020) recently observed
the foramen anterius canalis carotici lateralis in chelids, but we are able to confirm from the CT
scans used in this study that this is the foramen anterius canalis nervi vidiani instead. The canalis
carotico-pharyngealis is absent. The canalis caroticus basisphenoidalis, herein defined by its
entry into the basisphenoid due to the absence of the canalis caroticus lateralis, and the foramen
anterius canalis carotici basisphenoidalis are formed by the basisphenoid. The foramina anterius
canalis carotici basisphenoidalis are widely-spaced. The canalis stapedio-temporalis is the largest
canal in all observed chelids, ranging from ten times bigger than any carotid canal in P. hilarii, to
two times the size of them in E. subglobosa. The canalis caroticus internus is the smallest canal
in Chelodina oblonga, E. subglobosa, and P. hilarii, whereas the canalis caroticus
basisphenoidalis is the smallest in <i>Chelus fimbriatus</i> , <i>H. tectifera</i> , and <i>P. geoffroanus</i> (Table 2).
There is no trace in bone of the mandibular artery in our sample. This is consistent with
Albrecht's (1976) conclusion that the (internal) mandibular artery of chelids branches from the
stapedial artery after its exit from the foramen stapedio-temporale.
The canalis cavernosus originates posterior to the foramen stapedio-temporalis in Chelodina
oblonga, E. subglobosa, and H. tectifera, but at the level of the foramen stapedio-temporalis in
Chelus fimbriatus, P. hilarii and P. geoffroanus. The canalis cavernosus is formed by the
quadrate, prootic, and basisphenoid in Chelodina oblonga, by the prootic, pterygoid,
basisphenoid, and parietal in <i>Chelus fimbriatus</i> , by the quadrate and prootic in <i>E. subglobosa</i> ,
and by the quadrate, prootic, and pterygoid in P. hilarii, P. geoffroanus, and H. tectifera. The
foramen cavernosum itself is formed by the prootic and pterygoid. In Chelus fimbriatus, the
lateral head vein is fully enclosed by bone a second time anterior to the foramen nervi trigemini,





462

463

464

465

466

467

468

469

470

471

472

473

474

475

476

477

478

479

480

481

482

483

cavernosus connects to a large ventrolaterally directed canal that opens on the ventral surface of the pterygoid, and which we call the 'chelid canal' herein. Siebenrock (1897) observed this canal in all chelids and interpreted it as containing a branch of the carotid artery, but dissections made by Albrecht (1976) on *Chelodina* sp. and *Mesoclemmys nasuta* showed that the canal only contains connective tissue. The facial nerve extends laterally from the cavum cranii to the canalis caroticus internus through the canalis nervus facialis, which is formed by the prootic. The geniculate ganglion is inferred to be in contact with the canalis caroticus internus in all observed chelids. The hyomandibular branch extends posterolaterally through the prootic in its own canal, the canalis nervus hyomandibularis proximalis, for most of its length. In *Chelodina oblonga* and *E*. subglobosa, the quadrate contributes to the canalis nervus hyomandibularis proximalis posteriorly. In all observed taxa but E. subglobosa, the canalis nervus hyomandibularis proximalis connects to the canalis cavernosus posteriorly, close to the position of the columella auris. In E. subglobosa, however, the canalis nervus hyomandibularis proximalis does not connect to the canalis cavernosus and directly joins the cavum acustico-jugulare. As already discussed above, Albrecht (1976) suggested that the palatine artery is absent and that the vidian nerve extends through the canalis caroticus lateralis, but we here conclude based on the same observations that the lateral carotid canal is absent and that the vidian nerve traverses the canalis nervus vidianus. In *Chelus fimbriatus* (Fig. 1), the vidian nerve emerges from the geniculate ganglion and does not enter the canalis caroticus internus, but rather directly enters the canalis nervus vidianus which crosses the prootic and pterygoid to join the sulcus cavernosus at the level of the foramen nervi trigemini. The path is generally similar in other chelids, but in P. hilarii, P.

a feature not observed in other chelids. In all observed chelids but E. subglobosa, the canalis



485

486

487

488

489

490

491

492

493

494

495

496

497

498

499

geoffroanus, and H. tectifera, the vidian nerve partially enters the canalis caroticus internus, whereas in *Chelodina oblonga* and *E. subglobosa* the vidian nerve fully enters the canalis caroticus internus before splitting from it again further to the anterior. The vidian nerve passes for this part of the vidian canal through the prootic, pterygoid, and basisphenoid in *Chelodina* oblonga and H. tectifera, through the prootic and pterygoid in Chelus fimbriatus, E. subglobosa, P. hilarii, and P. geoffroanus. The basisphenoid contribution to this canal had previously been already noted for Chelus fimbriatus and Chelodina longicollis by Siebenrock (1897). In E. subglobosa, P. geoffroanus, and H. tectifera, no trace of the vidian nerve is visible inside the bone anterior to the foramen nervi trigemini, so the vidian nerve probably lies inside the sulcus cavernosus. In *Chelus fimbriatus* and *P. hilarii*, the vidian nerve re-enters the skull anteriorly through the lateral wall of the sulcus cavernosus. In *Chelus fimbriatus*, the vidian nerve extends anteriorly along the pterygoid-parietal suture for a long distance and at its anterior end, splits into two short canals that leave the skull posterolaterally to the descending process of the parietal. The foramen anterius canalis nervi vidiani is formed by the pterygoid and parietal. A similar pattern is visible in *Chelodina oblonga*, except that the portion of the vidian nerve that is enclosed by bone is much shorter.

500

501

502

503

504

505

506

Podocnemididae (Fig. 2)

The main branch of the internal carotid artery is never tightly enclosed by bone in the observed podocnemidids, so a true foramen posterius canalis carotici interni is absent, at least if a tight enclosure is used as a definitional criterion. Instead, podocnemidids possess an enlarged cavity, the podocnemidoid fossa (Lapparent de Broin & Werner, 1998) or cavum pterygoidei (Gaffney, Tong & Meylan, 2006), through which the carotid artery extends and that is additionally filled by



508

509

510

511

512

513

514

515

516

517

518

519

520

521

522

523

524

525

526

527

528

529

muscle tissue (Albrecht, 1976). As the internal carotid artery is not enclosed by bone, it is difficult to make clear statements regarding the circulation pattern of the carotid artery in our specimens. We can only identify with confidence a short canalis caroticus basisphenoidalis that is formed by the basisphenoid. These observations broadly agree with those of Siebenrock (1897), though with different nomenclature, as he interprets the entry of the cavum pterygoidei as the foramen posterius canalis carotici interni. Albrecht (1976) described a small artery splitting from the internal carotid artery in *Podocnemis sextuberculata* that he hypothesized to be a possible, vestigial palatine artery, but he was not able to identify similar structures in the other podocnemidids he dissected. This small artery splits into two branches, one supplying the muscle inside the cavum pterygoidei, one joining the canalis cavernosus to supply tissue within the sulcus cavernosus. Albrecht (1976) also noted the presence of the foramen anterius canalis carotici lateralis in all of the podocnemidids he observed. We identify a large, irregularly shaped fenestra between the cavum pterygoidei and the sulcus cavernosus in specimens of *Peltocephalus dumerilianus* and *Podocnemis unifilis* that may correspond to the foramen anterius canalis carotici lateralis of Albrecht (1976). Given that Albrecht (1976) only observed a blood vessel that passes this fenestra in one out of four podocnemidids in his sample and that this vessel does not feed tissues related to the palate, we conclude that the palatine artery is not present in extant podocnemidids. The canalis caroticopharyngealis are absent. The foramina anterius canalis carotici basisphenoidalis are widely-spaced. The canalis stapedio-temporalis is the largest canal, being five times larger than the canalis caroticus basisphenoidalis in Peltocephalus dumerilianus and two times larger than it in Podocnemis unifilis (Table 2). We are not able to find any traces of a mandibular artery in our sample of podocnemidids. This is consistent with Albrecht's (1976) observation that the external and internal mandibular arteries



531

532

533

534

535

536

537

538

539

540

541

542

543

544

545

546

547

548

549

550

551

552

of podocnemidids branch off the stapedial artery prior to and after its passage through the canalis stapedio-temporale, respectively.

The canalis cavernosus originates at the level of the foramen stapedio-temporalis in all podocnemidids and is formed by the quadrate and prootic. The foramen cavernosum is formed by the prootic and pterygoid.

The facial nerve canal is short and extends mediolaterally through the prootic. At mid-distance between the canalis cavernosus and the fossa acustico-facialis, i.e. within the prootic, the facial nerve canal bifurcates into two branches, indicating the position of the geniculate ganglion and the split of the facial nerve into the hyomandibular and vidian branches. In Peltocephalus dumerilianus, the hyomandibular branch extends posterolaterally through the prootic through a canalis nervus hyomandibularis proximalis. This canal coalesces with the canalis cavernosus. For most of its distal course along the canalis cavernosus, the hyomandibular nerve extends along a sulcus in the wall of the canalis cavernosus. However, the sulcus becomes a proper canalis nervus hyomandibularis distalis in the posterior-most section of the canalis cavernosus, just before entering the cavum acustico-jugulare. In *Podocnemis unifilis*, a short but distinct canalis nervus hyomandibularis distalis joining the cavum acustico-jugulare is present. The vidian nerve of Peltocephalus dumerilianus extends ventrally through the canalis pro ramo nervi vidiani, which is formed by the prootic, to enter the cavum pterygoidei. The vidian nerve is then inferred to first traverse the cavum pterygoidei to then pierce the full anteroposterior length of the pterygoid, where it splits into several branches. These branches extend through the pterygoid, palatine, and parietal, and exit the skull through various foramina formed by these bones. The path is inferred to be similar in *Podocnemis unifilis*, but the vidian nerve first crosses the above-mentioned fenestra to enter the sulcus cavernosus before entering the pterygoid and only splits into two branches within



that bone. The lateral one extends through the pterygoid and its anterior foramen is formed by the pterygoid and the palatine. The medial one extends through the pterygoid, palatine, and parietal, and its anterior foramen is formed by the palatine and parietal. Siebenrock (1897) noted for *Erymnochelys madagascariensis* that the vidian nerve exits the prootic posteromedially to cross the cavum pterygoidei (his canalis caroticus internus), and then enters the pterygoid, traverses it in its own canal, and exits the pterygoid on its dorsal surface, posterior to the orbit and medial to foramen palatinum posterius. Albrecht (1976) noticed that the vidian nerve mainly runs through the pterygoid as well.

Pelomedusidae (Fig. 3)

In *Pelomedusa subrufa* and *Pelusios subniger*, the carotid artery enters the skull from ventral and the foramen posterius canalis carotici interni is formed by the basisphenoid and the prootic. The internal carotid artery is directed anteromedially and extends through the prootic and the basisphenoid. The canalis caroticus internus intersects with the facial nerve system at the inferred position of the geniculate ganglion dorsally in the prootic close to the foramen posterius canalis carotici interni. This intersection with the facial nerve system is superficial so that the vidian nerve never fully enters the canalis caroticus internus. The intersection occurs in the prootic in *Pelusios subniger* and along the prootic-basisphenoid suture in *Pelomedusa subrufa*. This slightly differs from Albrecht's (1976) observations, who noted that this intersection occurred only in the prootic in both species. In *Pelomedusa subrufa*, the intersection is exposed ventrally. The canalis caroticus lateralis, as previously observed by Albrecht (1976), and canalis carotico-pharyngealis are absent. The canalis caroticus basisphenoidalis, herein defined as beginning with the entry of the carotid system into the basisphenoid, and foramen anterius canalis carotici basisphenoidalis are formed



by the basisphenoid. The foramina anterius canalis carotici basisphenoidalis are widely-spaced. 576 The canalis stapedio-temporalis is the largest canal, being four times larger than the canalis 577 caroticus internus and canalis caroticus basisphenoidalis in Pelomedusa subrufa, and about three 578 times larger than them in *Pelusios subniger* (Table 2). 579 Albrecht (1976) documented that the mandibular artery of pelomedusids branches from the 580 581 stapedial artery after its passage through the stapedio-temporal canal. Evers & Benson (2019), on the other hand, reported the presence of a foramen arteriomandibulare for *Pelomedusa subrufa*, 582 which suggests passage of the mandibular artery through the sulcus cavernosus. After restudying 583 the same CT scans as used by Evers & Benson (2019), however, we support the initial conclusion 584 of Albrecht (1976), as the reported foramen arteriomandibulare appears to be an ontogenetic 585 artifact (see Discussion for more details). 586 The canalis cavernosus starts slightly posterior to the foramen stapedio-temporalis in *Pelusios* 587 subniger, but at the level of the foramen stapedio-temporalis in *Pelomedusa subrufa*. In *Pelusios* 588 subniger, the canalis cavernosus extends anteromedially through the prootic, whereas in 589 Pelomedusa subrufa, the quadrate contributes to the lateral border of the canalis cavernosus for 590 much of its path. The foramen cavernosum is formed by the prootic in both species. 591 592 The facial nerve extends laterally from the braincase toward the canalis caroticus internus through the prootic. The geniculate ganglion is inferred to contact the canalis caroticus internus 593 in both species and the canalis pro ramo nervi vidiani is absent. In *Pelusios subniger*, a long 594 595 canalis nervus hyomandibularis proximalis is present and directed posterolaterally through the prootic. The canalis nervus hyomandibularis proximalis joins the ventral part of the canalis 596 cavernosus at the level of the bifurcation between the canalis cavernosus and canalis stapedio-597 598 temporalis. In *Pelomedusa subrufa*, the hyomandibular branch almost directly enters the canalis



cavernosus and is therefore mainly visible as a sulcus alongside the wall of the latter. At the level of the contact between the geniculate ganglion and the internal carotid artery, the vidian nerve leaves the canalis caroticus internus. In *Pelusios subniger*, the split of the facial nerve occurs near the dorsal part of the canalis caroticus internus and the vidian nerve directly enters a separate canalus nervus vidianus. This canal first shortly extends through the prootic and along a trifurcation formed by the prootic, pterygoid, and basisphenoid. The vidian nerve then continues anteriorly through the pterygoid and the foramen anterius canalis nervi vidiani is formed by the pterygoid. In *Pelomedusa subrufa*, the split of the facial nerve occurs on the dorsolateral part of the canalis caroticus internus and for a short distance, the vidian nerve extends through the canalis caroticus internus. The vidian nerve then branches off the canalis caroticus internus and travels out of the skull, ventral to the prootic and basisphenoid, before re-entering the skull through the pterygoid via a canalis nervus vidianus. The vidian nerve then extends anteriorly through the pterygoid, and the foramen anterius canalis nervi vidiani is formed by the pterygoid.

Carettochelyidae (Fig. 4)

The internal carotid artery enters the skull close to the posterior end of the basisphenoid and the foramen posterius canalis carotici interni is formed by the pterygoid only. The canalis caroticus internus extends anteromedially mostly through the pterygoid, and enters the basisphenoid, at which point it transforms into the canalis caroticus basisphenoidalis, considering that the lateral carotid canal is absent. The canalis pro ramo nervi vidiani joins the canalis caroticus internus halfway along its path. Somewhat anterior to this connection, just before the origin of the canalis caroticus basisphenoidalis, and along the pterygoid/basisphenoid suture, the vidian nerve leaves the canalis caroticus internus laterally to form the vidian canal. The canalis caroticus lateralis is



623

624

625

626

627

628

629

630

631

632

633

634

635

636

637

638

639

640

641

642

643

644

absent. Joyce, Volpato & Rollot (2018) previously noted the absence of this canal and speculated by reference to trionychids, where the mandibular artery passes through the lateral carotid canal, that the mandible of *Carettochelvs insculpta* may be fed from the cerebral artery instead. CT scans of a stained specimen available to us, however, clarify that the mandible of Carettochelys insculpta is fed by the mandibular artery, which branches off the stapedial artery and extends through the canalis cavernosus and the posteriorly elongated trigeminal foramen. The only recently reported foramen arteriomandibulare apparent in carettochelyids (Evers and Benson, 2019) serves as an excellent osteological correlate. A canalis carotico-pharyngealis is absent. The canalis caroticus basisphenoidalis is formed by the basisphenoid. The foramina anterius canalis carotici basisphenoidalis are widely separated and formed by the basisphenoid. The canalis stapediotemporalis, canalis caroticus internus, and canalis caroticus basisphenoidalis are relatively large and roughly equal-sized (Table 2). The canalis cavernosus posteriorly starts at the level of the foramen stapedio-temporalis and is very short. For most of its path, the canalis cavernosus is bordered by the quadrate laterally and ventrolaterally, and by the prootic dorsally, medially and ventromedially. Shortly before anteriorly exiting the skull laterally to the braincase, the pterygoid minorly contributes to the ventral limit of the canalis cavernosus. The foramen cavernosum is formed by the quadrate, prootic, and pterygoid. The facial nerve course of Carettochelys insculpta was already described in detail by Joyce, Volpato & Rollot (2018) based on the same specimen and CT scans. The facial nerve extends laterally from the cavum cranii through the prootic. At two-thirds of the distance between the fossa acustico-facialis and the canalis cavernosus, the canalis nervus facialis splits into canals for the vidian and hyomandibular branches. The aforementioned stained specimen confirms a geniculate ganglion position within the prootic, although the position is close to the wall of the canalis



cavernosus and not as deeply within the prootic as in many pleurodires. The hyomandibular nerve extends laterally along its own proximal canal through the prootic for a short distance and joins the canalis cavernosus, form which it further extends posteriorly within a sulcus. The canalis pro ramo nervi vidiani is small, extends through the prootic and pterygoid, and connects to the canalis caroticus internus halfway along its length. The vidian nerve leaves the canalis caroticus internus laterally at the basisphenoid/pterygoid suture. Its proximal parts are located in the pterygoid, the most distal portions fully in the palatine. The canalis nervus vidianus ends in a series of various small canals that open on the dorsal and ventral surfaces of the palatine.

Trionychidae (Fig. 5)

In all observed taxa, the internal carotid artery enters the skull from ventral and the foramen posterius canalis carotici interni is formed by the pterygoid only. The canalis caroticus internus is formed by the pterygoid and basisphenoid in all trionychid specimens with minor contributions of the prootic in *Amyda cartilaginea*, *Apalone mutica*, *Apalone spinifera*, *Chitra indica*, *Cyclanorbis senegalensis*, and *Pelodiscus sinensis*. Jamniczky & Russell (2007) only identified the basisphenoid and pterygoid as contributing to the canalis caroticus internus in *Ap. mutica* and *Trionyx triunguis*. In *Am. cartilaginea*, *Chitra indica*, *P. sinensis*, and *Cycloderma frenatum*, the internal carotid artery is exposed dorsally, i.e. in the floor of the cavum acustico-jugulare, for a short distance between the foramen posterius canalis carotici interni and the canalis pro ramo nervi vidiani. The canalis pro ramo nervi vidiani enters the canalis caroticus internus midway and the vidian nerve follows the path of the canalis caroticus lateralis. In *Cycloderma frenatum*, the vidian nerve splits directly from the canalis caroticus internus instead of following the path of the canalis caroticus lateralis. The split of the internal carotid artery into its two subbranches, in



669

670

671

672

673

674

675

676

677

678

679

680

681

682

683

684

685

686

687

688

689

this case the cerebral and mandibular arteries (Albrecht, 1967), occurs at the same level as the sella turcica. The canalis caroticus lateralis and canalis caroticus basisphenoidalis are short. Indeed, the canalis caroticus lateralis is shortened to the length of a fenestra. The mandibular artery joins the sulcus cavernosus through this fenestra, which is formed by the pterygoid and basisphenoid in Am. cartilaginea, Ap. mutica, Ap. spinifera, Chitra indica, and P. sinensis, but only by the pterygoid in Cyclanorbis senegalensis, Cycloderma frenatum and L. punctata. The canalis carotico-pharyngealis is absent, as observed by Albrecht (1967). In all examined trionychids, the cerebral branch exits through the sella turcica. The foramina anterius canalis carotici basisphenoidalis are widely-spaced and formed by the basisphenoid. The canalis caroticus basisphenoidalis is larger than the canalis stapedio-temporalis and canalis caroticus lateralis in all observed trionychids. However, some differences as to which canal is the smallest are apparent across taxa. The canalis caroticus lateralis is the smallest in Am. cartilaginea, C. indica, and Cycloderma frenatum, whereas the canalis stapedio-temporalis is the smallest in Ap. mutica, Cyclanorbis senegalensis, L. punctata, and P. sinensis. The canalis stapedio-temporalis and canalis caroticus lateralis are equal-sized in Ap. spinifera (Table 2). This corroborates Albrecht (1976), who noted that trionychids have a small stapedial artery and a large carotid artery, but slightly differs from Jamniczky & Russell (2007), who identified a foramen anterius canalis carotici lateralis that is larger than the foramen anterius canalis carotici basisphenoidalis in Ap. mutica and Trionyx triunguis. The structures we identify in trionychids are identical to the ones identified by Albrecht (1967, 1976). The canalis cavernosus starts at the level of the foramen stapedio-temporalis or slightly posterior to it. The canalis cavernosus is formed by the pterygoid, prootic, and quadrate in all



691

692

693

694

695

696

697

698

699

700

701

702

703

704

705

706

707

708

709

710

711

712

observed taxa except Cycloderma frenatum, in which the canalis cavernosus is only bordered by the prootic and pterygoid. The foramen cavernosum is formed by the prootic and pterygoid. The facial nerve extends laterally from the fossa acustico-facialis through the prootic. The geniculate ganglion is inferred to be located in the canalis cavernosus in Ap. spinifera, Ap. mutica, Am. cartilaginea, and P. sinensis, but in between the canalis cavernosus and canalis caroticus internus in Chitra indica, Cyclanorbis senegalensis, Cycloderma frenatum, and L. punctata. This observation contradicts Gaffney (1979), who stated that the geniculate ganglion is always in contact with the canalis cavernosus in cryptodires. The geniculate ganglion gives off two branches in all observed trionychids but Cyclanorbis senegalensis, the ventral one being the vidian nerve, and the lateral one being the hyomandibular branch. In Cyclanorbis senegalensis, a third branch is present that runs anteriorly along the prootic-pterygoid suture to join the sulcus cavernosus. The distal portion of the hyomandibular branch is fully confluent with the canalis cavernosus in Am. cartilaginea, is present as a sulcus connected to the canalis cavernosus in Ap. spinifera, Ap. mutica, and P. sinensis, and extends posterolaterally through its own canalis nervus hyomandibularis proximalis along the prootic-pterygoid suture in *Chitra indica*, Cyclanorbis senegalensis, Cycloderma frenatum and L. punctata. In all observed trionychids, the vidian nerve is contained in the canalis pro ramo nervi vidiani and extends ventrally from the geniculate ganglion through the prootic and pterygoid to join the canalis caroticus internus midway. In all taxa but Cycloderma frenatum, the vidian branch likely initially follows the course of the canalis caroticus internus, but then passes through the fenestra-like canalis caroticus lateralis to enter the sulcus cavernosus. From there, the nerve pierces either the pterygoid or the palatine to form the canalis nervus vidianus. In Cycloderma frenatum, the vidian branch leaves the canalis caroticus internus laterally between the canalis pro ramo nervi vidiani



714

715

716

717

718

719

720

721

722

723

724

725

726

727

728

and canalis caroticus lateralis and then joins the sulcus cavernosus. Bender (1906) described a similar pattern in *Apalone ferox*, noting that the vidian nerve enters a canal formed by the basisphenoid and pterygoid (our canalis caroticus internus) and runs anteriorly along the suture made by these two bones. The vidian nerve then bifurcates, runs anteriorly along the pterygoidpalatine suture, and connects with the maxillary branch of the trigeminal nerve (V_2) outside of the bone to form the sphenopalatine ganglion, at the level of the contact between the pterygoid and the maxilla. Our observations for trionychids in general correspond to those of Ogushi (1911) for P. sinensis and Shiino (1913) for the vidian nerve in Am. cartilaginea. In all of our specimens, the vidian nerve connects with at least one ventral canalis carotico-pharyngeale. The canalis nervus vidianus is formed by the palatine in Ap. spinifera, Chitra indica, P. sinensis, and Cyclanorbis senegalensis, by the pterygoid and palatine in Ap. mutica, Am. cartilaginea and L. punctata, and by the pterygoid, palatine and parietal in Cycloderma frenatum. In Ap. spinifera, Am. cartilaginea, and P. sinensis, the canalis nervus vidianus splits into several smaller canals that exit the skull on the dorsal and ventral surfaces of the palatine. Much of this variation was previously noted by Meylan (1987) for a broader sample. The foramen anterius canalis nervi vidiani is formed by the palatine in all observed trionychids.

729

730

731

732

733

734

735

Kinosternidae (Fig. 6)

In all observed kinosternids, the internal carotid artery initially enters the skull through the fenestra postotica and then passes through a groove within the cavum acustico-jugulare that is roofed by the prootic, as previously noted by Evers and Benson (2019). The actual foramen posterius canalis carotici interni is formed by the pterygoid and prootic, and the canalis caroticus internus is formed by the pterygoid, prootic, and basisphenoid. This slightly differs from the



737

738

739

740

741

742

743

744

745

746

747

748

749

750

751

752

753

754

755

756

757

observations of Siebenrock (1897), who did not mention the involvement of the basisphenoid in the formation of the canalis caroticus internus. Jamniczky & Russell (2007) only mentioned the pterygoid as forming the foramen posterius canalis carotici interni, and the basisphenoid and pterygoid as forming the canalis caroticus internus in *Kinosternon baurii* and *Staurotypus* salvinii. The canalis pro ramo nervi vidiani connects to the canalis caroticus internus just before its split into its palatine and cerebral branches (Albrecht, 1976). The canalis caroticus lateralis and canalis caroticus basisphenoidalis are short. The canalis caroticus lateralis joins the sulcus cavernosus. The canalis caroticus lateralis and foramen anterius canalis carotici lateralis are formed by the prootic, pterygoid, and basisphenoid in Sternotherus minor, Kinosternon subrubrum, and Staurotypus salvinii, by the pterygoid and basisphenoid in K. baurii, and only by the pterygoid in *Kinosternon scorpioides*. Two canalis carotico-pharyngealis are present in K. scorpioides and Staurotypus salvinii. The cerebral branch exits at the sella turcica. The canalis caroticus basisphenoidalis and foramen anterius canalis carotici basisphenoidalis are formed by the basisphenoid. The foramina anterius canalis carotici basisphenoidalis are widely separated. The canalis caroticus lateralis has a greater cross-section than the canalis caroticus basisphenoidalis and canalis stapedio-temporalis in all observed kinosternids, and the canalis stapedio-temporalis, which is absent in K. scorpioides, is the smallest canal in K. baurii, K. subrubrum, Staurotypus salvinii, and Sternotherus minor (Table 2). With the exception of K. baurii, for which Jamniczky and Russell (2007) were not able to identify the canalis stapediotemporalis and foramen stapedio-temporalis, the relative canal sizes we observe in our specimens confirm the observations of McDowell (1961), Albrecht (1967, 1976), and Jamniczky & Russell (2007).



759

760

761

762

763

764

765

766

767

768

769

770

771

772

773

774

775

776

777

778

779

780

The mandibular artery branches from the palatine artery within the sulcus cavernosus and exits through the trigeminal foramen (Albrecht, 1967). It is therefore not surprising that we cannot find any osteological correlates for this artery beyond the enormous size of the anterior foramen of the lateral carotid canal.

The canalis cavernosus starts posterior to the foramen stapedio-temporalis and is formed by the quadrate, prootic, and pterygoid. The foramen cavernosum is formed by the prootic and pterygoid.

The facial nerve extends ventrolaterally from the cavum cranii to the canalis cavernosus through the prootic. The geniculate ganglion is inferred to be located in the canalis cavernosus and gives off two branches in all observed kinosternids. The hyomandibular nerve extends posterolaterally within the canalis cavernosus, visible as a sulcus in K. subrubrum, K. baurii, K. scorpioides, and Sternotherus minor, but undistinguishable from the canalis cavernosus in Staurotypus salvinii. In all observed kinosternids, the vidian nerve is contained in a short canalis pro ramo nervi vidiani that extends ventrally through the prootic and pterygoid to join the canalis caroticus internus. In Sternotherus minor, K. subrubrum, K. baurii, and K. scorpioides, the vidian nerve extends within the canalis caroticus internus and then anteriorly within the canalis caroticus lateralis, from which it exits into the sulcus cavernosus. Slightly more anteriorly in the sulcus cavernosus, approximately at the level of the dorsum sellae of the basisphenoid, the vidian nerve enters its own canal. This canal, the canalis nervus vidianus, is formed by the pterygoid and palatine, with some contributions of the parietal in K. baurii, and of the epipterygoid in K. scorpioides. Within the palatine, the vidian nerve splits into several branches. One of these branches extends to the foramen palatinum posterius, while the others either get lost in the porosity of the bone, or connect to the dorsal or ventral surfaces of the palatine (likely forming, respectively, the foramina arteriae anteriovidianae



782

783

784

785

786

787

788

789

790

791

792

793

794

795

796

797

798

799

800

and foramina arteriaevidianae of Albrecht, 1967). In Staurotypus salvinii, a canal leaves the canalis caroticus internus ventrolaterally and merges with a canal coming from ventral. This complex then fuses with another canal coming from the canalis caroticus internus, and the resulting canal divides more anteriorly into two branches. The largest one runs anterodorsally and joins the sulcus cavernosus anterior to the foramen anterius canalis carotici lateralis. The smallest one runs anteriorly through the pterygoid and palatine, likely corresponding to the canal for the vidian nerve. The vidian nerve exits the skull on the ventromedial side of the palatine, posterior to the anterior end of the pterygoid. More anteriorly, the vidian nerve likely re-enters the skull, merges with unidentified canals, and exits near the foramen palatinum posterius inside the palatine. The pattern we observe for the vidian nerve differs in two respects from the descriptions of McDowell (1961) and Albrecht (1967). Firstly, McDowell (1961) only mentioned the pterygoid as the bone forming the vidian canal, whereas we observed a higher complexity of the innervation pattern, with the palatine, parietal, and epipterygoid contributing to the formation of the canalis nervus vidianus. Secondly, Albrecht (1967) noted that some branches of the vidian nerve leave the canalis pro ramo nervi vidiani to run anteriorly through the pterygoid, and anteriorly connect with other branches of the vidian nerve that exit the canalis caroticus lateralis. Although we cannot exclude that Albrecht (1967) indeed observed that in the specimens he dissected, we have not been able to observe this pattern in our specimens and the canalis nervus vidianus is either exclusively connected to the sulcus cavernosus (Sternotherus minor, K. subrubrum, K. baurii, and K. scorpioides), or the canalis caroticus internus (Staurotypus salvinii).

801

802

Dermatemydidae (Fig. 7)



804

805

806

807

808

809

810

811

812

813

814

815

816

817

818

819

820

821

822

823

824

825

In *Dermatemys mawii*, the internal carotid artery enters the skull through the fenestra postotica. The posterior course of the internal carotid artery can be inferred from a dorsally open trough in the pterygoid. The internal carotid artery only becomes fully enclosed by bone within the cavum acustico-jugulare, where the prootic covers the pterygoid to form the actual foramen posterius canalis carotici interni. The internal carotid artery is bordered by the prootic, pterygoid, and basisphenoid. The canalis pro ramo nervi vidiani enters the internal carotid canal about mid-length. Slightly posterior to the split into the canalis caroticus lateralis and canalis caroticus basisphenoidalis, a small canal of unclear function or homology connects the canalis caroticus internus to the canalis cavernosus on the right side of the available specimen. The split of the canalis caroticus internus into the canalis caroticus basisphenoidalis and canalis caroticus lateralis occurs along the pterygoid-basisphenoid suture. The canalis caroticus lateralis is short and formed by the prootic, pterygoid, and basisphenoid. The herein contained palatine artery (Albrecht, 1976) joins the sulcus cavernosus by the way of the foramen anterius canalis carotici lateralis, which is formed by the pterygoid and basisphenoid. A canalis carotico-pharyngealis is absent. The canalis caroticus basisphenoidalis extends anteromedially through the basisphenoid and joins the braincase via the widely-spaced foramina anterius canalis carotici basisphenoidalis, which are formed by the basisphenoid. The canalis caroticus lateralis is about four times bigger in cross section than the canalis caroticus basisphenoidalis (Table 2), and the canalis stapedio-temporalis and foramen stapedio-temporalis are absent, possibly explaining the particularly large diameter of the canalis caroticus lateralis. The canalis cavernosus posteriorly starts slightly anterior to the columella auris. The canalis cavernosus is formed by the quadrate, prootic, and pterygoid. The foramen cavernosum is formed by the prootic and pterygoid.



827

828

829

830

831

832

833

834

835

836

837

838

839

840

841

842

843

844

845

846

847

We are unaware of any literature that explicitly discusses the placement of the mandibular artery in *Dermatemys mawii*. Its branching from the stapedial artery posterior to the stapedial canal and exit through the trigeminal foramen is suggested by a lateral sulcus within the canalis cavernosus. This sulcus is otherwise only apparent in turtles for which the mandibular artery traverses through the canalis cavernosus. However, the large diameter of the lateral carotid canal, on the other side, suggests that the mandible is perhaps partially or fully fed from the palatine artery as well. The taxa that phylogenetically bracket *Dermatemys mawii* do not provide any further evidence, as the mandible is fed by the stapedial artery in chelydrids, but by the palatine artery in kinosternids. As we believe the division of the canalis cavernosus and the relative size of the lateral carotid canal to be a useful osteological correlates, we reconstruct *Dermatemys mawii* as having a split mandibular artery, as seen in Cheloniidae (Fig. 7D). This issue will need to be resolved in the future, however, by reference to wet specimens. The facial nerve canal extends ventrolaterally from the cavum cranii to the canalis cavernosus through the prootic. As there are no osteological indications for the split of the facial nerve to occur prior to the facial canal joining the canalis cavernosus, the position of the geniculate ganglion is inferred to be within the latter. And as no osteological correlate for the hyomandibular branch of the facial nerve could be identified within the canalis cavernosus, its course is inferred to be posteriorly directed within that structure. A small canalis pro ramo nervi vidiani is visible on the right side only in the available specimen that extends along the prootic-pterygoid suture and joins the canalis caroticus internus mid-length. The vidian nerve is then inferred to follow the path of the canalis caroticus internus and the canalis caroticus lateralis into the sulcus cavernosus. Anterior to the rostrum basisphenoidale and posteroventromedially to the processus inferior parietalis, the



vidian nerve leaves the sulcus cavernosus ventrolaterally to enter the canalis nervus vidianus, extends anteriorly through the palatine, and ends at the foramen palatinum posterius.

850

851

852

853

854

855

856

857

858

859

860

861

862

863

864

865

866

867

868

869

870

848

849

Chelydridae (Fig. 8)

The internal carotid artery enters the skull slightly anterior to the level of the columella auris through the fenestra postotica. The artery forms a dorsally exposed sulcus within the cavum acustico-jugulare in *M. temminckii*, but not in *Chelydra serpentina*. The foramen posterius canalis carotici interni within the cavum acustico-jugulare is formed by the prootic and pterygoid in Chelydra serpentina, but only by the pterygoid in Macrochelys temminckii, as noted by Siebenrock (1897). The canalis caroticus internus is formed by the prootic, pterygoid, and basisphenoid. This slightly differs from Siebenrock (1897) who only described the prootic and pterygoid as the bones forming this canal in C. serpentina, and only the pterygoid in M. temminckii, and from Jamniczky & Russell (2007), who noted that the canalis caroticus internus traverses the pterygoid and basisphenoid in C. serpentina. The canalis pro ramo nervi vidiani connects the canalis cavernosus to the canalis caroticus internus about mid-length of the later. In both observed chelydrids, the split of the canalis caroticus internus into the canalis caroticus lateralis and canalis caroticus basisphenoidalis occurs at the pterygoid-basisphenoid suture. The canalis caroticus lateralis is much longer than the canalis caroticus basisphenoidalis. The palatine artery (Albrecht, 1976) runs anteriorly through the canalis caroticus lateralis, which extends first through the pterygoid and then along the pterygoid-basisphenoid suture in M. temminckii, but only along the pterygoid-basisphenoid suture in C. serpentina. The palatine artery then exits its canal through the foramen anterius canalis carotici lateralis, formed by the pterygoid and basisphenoid. This contrasts with Albrecht (1976), who noted that the foramen anterius canalis



872

873

874

875

876

877

878

879

880

881

882

883

884

885

886

887

888

889

890

891

892

893

carotici lateralis is only formed by the pterygoid in chelydrids. A canalis carotico-pharyngealis is present in both taxa. The canalis caroticus basisphenoidalis extends anteromedially through the basisphenoid and opens within the sella turcica. The foramina anterius canalis carotici basisphenoidalis are widely-spaced in C. serpentina but close together in M. temminckii. The canalis stapedio-temporalis is the largest canal and the canalis caroticus lateralis the smallest in terms of diameters in both specimens. The canalis stapedio-temporalis is about five times larger than the canalis caroticus basisphenoidalis in C. serpentina, and ten times larger in M. temminckii, and more than ten times larger than the canalis caroticus lateralis in both specimens (Table 2). These canal proportions corroborate the results of McDowell (1961), Albrecht (1976), and Jamniczky & Russell (2007). The canalis cavernosus posteriorly starts at the level of the foramen stapedio-temporalis. It is short in C. serpentina, but long in M. temminckii. The canalis cavernosus is formed by the quadrate, prootic, and pterygoid, and houses the geniculate ganglion. The foramen cavernosum is formed by the prootic and pterygoid. A dorsal groove within the large canalis cavernosus provides an osteological correlate for the presence of two parallel lying vessels, which we interpret as the ventromedially located lateral head vein and the dorsolaterally located mandibular artery, which exits the canalis cavernosus through the trigeminal foramen (Albrecht, 1976). The facial nerve canal extends ventrolaterally from the fossa acustico-facialis to the canalis cavernosus through the prootic. The geniculate ganglion is inferred to be positioned within the canalis cavernosus and gives off two branches. The hyomandibular branch has no osteological correlate in M. temminckii, but its course remains visible in C. serpentina as a sulcus in the wall of the canalis cavernosus. In C. serpentina, the canalis pro ramo nervi vidiani is short and located



895

896

897

898

899

900

901

902

903

904

905

906

907

908

909

910

911

912

913

914

915

916

along the prootic-pterygoid suture, whereas it is long in M. temminckii and formed by the pterygoid only. The vidian nerve enters the internal carotid canal at mid-length in both taxa. In C. serpentina, the vidian nerve leaves the canalis caroticus internus just posterior to the split of the canalis caroticus internus into the canalis caroticus lateralis and canalis caroticus basisphenoidalis. The canalis nervus vidianus is long but narrow in diameter, extends anteriorly through the pterygoid, and connects to small exiting canals along its path. The main vidian canal opens onto the dorsal surface of the pterygoid, anterior to the foramen anterius canalis carotici lateralis, and posteromedially to the anterior limit of the processus inferior parietalis. Siebenrock (1897) described the vidian nerve of C. serpentina as extending through a groove lateral to the internal carotid artery, being posterodorsally covered by the prootic, and posteriorly starting from the foramen jugulare anterius, and that the vidian nerve runs through the canalis caroticus lateralis and foramen anterius canalis carotici lateralis. Albrecht (1976) similarly stated that the canal we identify as the vidian canal does not connect to the canalis caroticus internus and that no nerve is contained in it. Our observations differ from these descriptions as our specimen clearly exhibits a canalis nervus vidianus distinct from the canalis caroticus lateralis and that is connected to the canalis caroticus internus, as previously suggested by Gaffney (1972a) for this taxon, even though it is hard to distinguish and sometimes barely visible in the CT scans. In M. temminckii, two small canals ventrally leave the canalis caroticus internus near its posterior end and pass through the pterygoid to eventually merge through detours with a canal that runs anteriorly through the pterygoid, lateral to the canalis caroticus internus, to connect with a branch of the canalis caroticopharyngeale, and to merge with the canalis caroticus lateralis close to the foramen anterius canalis carotici lateralis. This system of canals may have held the vidian nerve. This conclusion differs from Albrecht (1976) who described the canalis nervus vidianus in M. temminckii as connecting



to the canalis caroticus internus and bifurcating from it slightly posterior to the split of the canalis caroticus internus into the canalis caroticus lateralis and canalis caroticus basisphenoidalis. His canalis nervus vidianus then runs anteriorly through the pterygoid and opens into the orbit at the anterior end of the crista pterygoidea.

921

922

923

924

925

926

927

928

929

930

931

932

933

934

935

936

937

938

939

917

918

919

920

Cheloniidae (Fig. 9)

In all observed cheloniids, the internal carotid artery enters the skull from posterior at the posteroventral part of the pterygoid. The foramen posterius canalis carotici interni is formed by the pterygoid. In Eretmochelys imbricata, Chelonia mydas, and Natator depressus, the canalis caroticus internus is formed by the pterygoid and basisphenoid, but only by the pterygoid in Lepidochelys olivacea and Caretta caretta. In E. imbricata and Chelonia mydas, a narrow and short canal leaves the canalis caroticus internus dorsally at about half of its length to join the cavum labyrinthicum. In E. imbricata, Chelonia mydas, and N. depressus, the canalis pro ramo nervi vidiani connects the canalis cavernosus to the canalis caroticus internus, but in L. olivacea and Caretta caretta no canalis pro ramo nervi vidiani is visible. Unlike in all other turtles, the internal carotid artery exits the basicranium to enter the sulcus cavernosus prior to its split into subordinate arteries in all observed cheloniids. This had previously been inferred by Zangerl (1953) for Chelonia mydas and observed in dissected specimens of the same species by Albrecht (1976), and then observed for cheloniids more widely by Evers & Benson (2019). The position of the canalis caroticus basisphenoidalis provides osteological evidence for this unusual constellation. This canal usually diverges off the canalis caroticus internus within the basicranium and at the basisphenoidpterygoid suture. In cheloniids, however, the canalis caroticus basisphenoidalis diverges from the sulcus cavernosus into the basisphenoid. Therefore, a short part of the internal carotid artery must



941

942

943

944

945

946

947

948

949

950

951

952

953

954

955

956

957

958

959

960

961

be inferred to extend dorsally uncovered within the sulcus cavernosus across all cheloniids. Consequentially, the palatine artery, the presence of which has been confirmed for at least Chelonia mydas by Albrecht (1976), is never encased in a canal in cheloniids, confirming observations by Evers & Benson (2019), who reported this condition to be present in all extant cheloniids and *Dermochelys coriacea*, but not in all extinct cheloniids. A characteristic commonly used in turtle systematics (and first used explicitly by Shaffer et al., 1997) is the spacing of the foramina anterius canalis carotici basisphenoidalis, which in most turtles are widely spaced across the sella turcica, but come close together in cheloniids and some extinct turtles, such as plesiochelyids (Gaffney, 1976). Recently, Evers & Benson (2019) defined a third passage for the cerebral arteries, based on the observation that right and left arteries converge within the basisphenoid and exit through a single median foramen anterius canalis carotici basisphenoidalis in L. olivacea, Caretta caretta, and N. depressus, but not in other extant cheloniids. Here, we confirm these observations. As the palatine artery is never encased in a bony canal, the identification of the canals traversing the pterygoid as being the canalis carotico-pharyngealis is not fully certain. However, respectively one and two canals in E. imbricata and Caretta caretta connect the ventral surface of the pterygoid to the portion of the sulcus cavernosus in which the carotid artery lies, making them plausible candidates for being the canalis carotico-pharyngealis. The canalis stapedio-temporalis is about twice as large as the canalis caroticus internus and about four to five times larger than the canalis caroticus basisphenoidalis in all observed cheloniids (Table 2). Although we cannot infer the diameter of the palatine artery in the absence of a formed canalis caroticus lateralis, observations made by Albrecht (1976) show that the palatine artery is larger than the cerebral artery.



963

964

965

966

967

968

969

970

971

972

973

974

975

976

977

978

979

980

981

982

983

984

The canalis cavernosus starts at the level of the foramen stapedio-temporalis. The canalis cavernosus is formed by the quadrate, prootic and pterygoid and the foramen cavernosum is formed by the prootic and pterygoid. Albrecht (1976) reported that the mandible of chelonioids is fed by two separate branches, a vestigial one originating from the stapedial artery and a larger one fed by the palatine artery. We find osteological evidence of the latter in the form of a sulcus within the canalis cavernosus, combined with a foramen arteriomandibulare that is present in *Chelonia* mydas, but not in other cheloniids. In contrast to Albrecht (1976), however, we note that the foramen arteriomandibulare does not form a short canal in C. mydas, but rather represents a small fenestra to the canalis cavernosus. In addition, the lateral sulcus within the canalis cavernosus in our specimen is suggestive of a large mandibular artery. This is further supported by the dried remains of the mandibular artery in our specimen of Eretmochelys imbricata. Although further studies on wet specimens will need to further clarify this issue, we reconstruct chelonioids as having similarly sized anterior and posterior mandibular arteries. The facial nerve canal extends ventrolaterally from the fossa acustico-facialis to the canalis cavernosus through the prootic. The position of the geniculate ganglion is inferred to be located in the canalis cavernosus, where it gives off the vidian and hyomandibular nerves. Whereas a sulcus for the hyomandibular nerve is visible in the wall of the canalis cavernosus in L. olivacea and Chelonia mydas, the hyomandibular branch of the facial nerve has no osteological correlate in E. imbricata, Caretta caretta, and N. depressus, and is thus inferred to be fully contained within the canalis cavernosus. The canalis pro ramo nervi vidiani is present in E. imbricata, Chelonia mydas, and N. depressus, formed by the pterygoid, and connects the canalis cavernosus to the canalis caroticus internus. No canalis pro ramo nervi vidiani is visible in the specimens we used for L. olivacea and Caretta caretta and the path of the vidian nerve is therefore unclear in these two taxa.



No canalis nervus vidianus is visible in any observed cheloniids. Siebenrock (1897) noted that the vidian nerve of *Caretta caretta*, *Chelonia mydas*, and *E. imbricata* is contained in the sulcus in which the internal carotid artery lies once it has joined the sulcus cavernosus, and Soliman (1964) clearly shows a vidian nerve in his illustrations of the cranial nerves in *Eretmochelys imbricata*. In the absence of separate canals for the vidian nerve, we infer that this nerve usually passes through the canalis caroticus internus and then through the sulcus cavernosus, but does not form an anterior vidian canal.

Dermochelyidae (Fig. 10)

The internal carotid artery enters the skull from posterior through the fenestra postotica. The actual foramen posterius canalis carotici interni is positioned deeply within the cavum acustico-jugulare and formed by the prootic and pterygoid. Unlike in most cryptodires, in which the foramen posterius canalis carotici interni and canalis caroticus internus are ventrally deeply embedded within the pterygoid bone, the internal carotid artery of *Dermochelys coriacea* seems to have a more dorsally positioned, superficial course with regard to the pterygoid. In particular, the foramen posterius canalis carotici interni and canalis caroticus internus are formed by raised ridges on the dorsal surface of the pterygoid, the lateral of which is the comparatively shallow extension of the crista pterygoidei. The crista pterygoidei and the medial ridge are then roofed by the prootic to form the canalis caroticus internus. The canalis caroticus internus then continues between the pterygoid and prootic for a short distance, before the canal becomes encased by the basisphenoid and pterygoid more anteriorly. These observations differ from Albrecht (1976), who stated that the internal carotid artery is only surrounded by the pterygoid. As in cheloniids, the internal carotid artery joins the sulcus cavernosus and the split into the palatine and cerebral branches is not



1009

1010

1011

1012

1013

1014

1015

1016

1017

1018

1019

1020

1021

1022

1023

1024

1025

1026

1027

1028

1029

1030

covered by bone (Nick, 1912; Albrecht, 1976; Evers & Benson, 2019). No canalis caroticus lateralis, canalis caroticus basisphenoidalis, and canalis carotico-pharyngealis are present in our specimens. The absence of an ossified canalis caroticus basisphenoidalis in D. coriacea is unique among extant turtles, although it has been observed in at least one fossil turtle (Evers & Joyce, 2020). In D. coriacea, osteological correlates for a short cerebral artery sulcus exist nonetheless. Directly anteromedial to the basicranial exit of the canalis caroticus internus, the lateral surface of the basisphenoid shows a weak but broad sulcus ventrally to the vestigially developed clinoid processes. This sulcus is interpreted as an incompletely ossified, anteriorly open canalis caroticus basisphenoidalis, and its broad size indicates that the cerebral artery is relatively large in diameter. Although the path for the cerebral artery was thus not fully enclosed by bone in the specimens we examined, Albrecht (1976) noticed on the specimen he examined that a canalis caroticus basisphenoidalis was present, supporting statements by Nick (1912). D. coriacea is known for its incomplete ossification pattern. For instance, much of the lateral side of the braincase, which, in other turtles, is ossified by a ventrally tall descending process of the parietal, remains cartilaginous in D. coriacea (Nick, 1912), and much of the hyoid skeleton remains entirely cartilaginous (Schumacher, 1973). Therefore, it is possible that completely ossified canalis caroticus basisphenoidalis develop in particularly old and well ossified individuals, so that our observations are not necessarily in contrast to those of Albrecht (1976) or Nick (1912). The canalis stapediotemporalis is about three times larger than the canalis caroticus internus in both specimens (Table 2). The canalis cavernosus of *Dermochelys coriacea* is located lateral to the canalis caroticus internus and connects the cavum acustico-jugulare with the subtemporal region of the skull. The

canalis cavernosus is formed by the pterygoid, quadrate, and prootic and is extremely short. The



foramen cavernosum is positioned distinctly posterior to the position of the anteriorly unossified trigeminal foramen. A distinct sulcus cavernosus, as developed in most turtles anterior to the foramen cavernosum, is not developed in *D. coriacea*, but the course of the vena capitis lateralis is still inferred to pass anteriorly along the dorsal surface of the pterygoid based on the position of the foramen cavernosum. We are unaware of studies that clarify the source of the mandibular artery in *D. coriacea*, but also find no clear osteological correlates that would suggest origin from the stapedial artery versus one of the arteries of the internal carotid.

The facial nerve canal extends ventrolaterally from the fossa acustico-facialis through the prootic. The canalis nervus facialis exits the prootic in a position anterodorsal to the divergence point of the canalis caroticus internus and the canalis cavernosus. The geniculate ganglion is inferred to contact the canalis caroticus internus. The canalis pro ramo nervi vidiani is therefore absent and the vidian nerve directly enters the canalis caroticus internus. The hyomandibular nerve joins the canalis cavernosus via a very short canalis nervus hyomandibularis proximalis and then leaves no osteological correlate within the posterior section of the canalis cavernosus. No canalis nervus vidianus is visible, but Nick (1912) observed the vidian nerve paralleling the course of the internal carotid artery and, once the internal carotid artery has joined the sulcus cavernosus and split into the cerebral and palatine branches, paralleling the course of the palatine artery. This provides evidence for our interpretations of the facial nerve system in *Dermochelys coriacea*.

Platysternidae (Fig. 11)

The internal carotid artery enters the skull anterior to the level of the columella auris and through the fenestra postotica. A short, dorsally open sulcus in the pterygoid leads within the cavum acustico-jugulare to the foramen posterius canalis carotici interni, which is formed by the



pterygoid. The canalis caroticus internus is formed by the prootic, pterygoid, and basisphenoid. The canalis pro ramo nervi vidiani enters the canalis caroticus internus about mid-length. The canalis caroticus lateralis is absent in our specimen, which confirms Albrecht's (1976) observations, but contradicts Jamniczky & Russell (2007). The canal that Jamniczky & Russell (2007) identify as the canalis caroticus lateralis is herein identified as the canalis nervus vidianus instead (see below). A canalis carotico-pharyngealis is absent. The canalis caroticus basisphenoidalis, herein defined once the internal carotid artery enters the basisphenoid, is mainly formed by the basisphenoid, with ventral contributions of the pterygoid. The narrowly-spaced foramina anterius canalis carotici basisphenoidalis are formed by the basisphenoid. The canalis stapedio-temporalis is three times larger than the canalis caroticus internus and canalis caroticus basisphenoidalis (Table 2). The relative proportions between the canalis stapedio-temporalis and canalis caroticus basisphenoidalis corroborate the results of Jamniczky & Russell (2007).

The canalis cavernosus starts posteriorly at the level of the foramen stapedio-temporalis and is bordered by the quadrate, prootic, and pterygoid. The lateral wall of the canalis cavernosus is incompletely ossified in our specimen, exposing the canal along the lateral pterygoid-prootic-quadrate surfaces toward the subtemporal fossa. The foramen cavernosum is formed by the prootic and pterygoid. The placement of the mandibular artery within the canalis cavernosus is suggested by a faint groove alone its lateral side, but we are unaware of dissections that unambiguously document this path. Evers and Benson (2019) reported the presence of a foramen arteriomandibulare. We are able to confirm the presence of symmetric openings between the canalis cavernosus and the temporal fossa in our specimen, the same as employed by Evers and Benson (2019), but note that the anterior wall of the canalis cavernosus is extremely thin and that the "foramina" are elongate slits. The study of other specimens should clarify if these indeed



1078

1079

1080

1081

1082

1083

1084

1085

1086

1087

1088

1089

1090

1091

1092

1093

1094

1095

1096

1097

represent the exit foramina of the mandibular artery or the incomplete ossification of the anterior wall of the canalis cavernosus in this particular specimen.

The canalis nervus facialis extends laterally from the fossa acustico-facialis to the canalis cavernosus through the prootic. The position of the geniculate ganglion is inferred to be within the canalis cavernosus, where it gives off the hyomandibular and vidian nerves. The hyomandibular nerve has no osteological correlate within the canalis cavernosus. The vidian nerve enters the canalis pro ramo nervi vidiani, extends ventrolaterally along the prootic-pterygoid suture, and joins the canalis caroticus internus at about its mid-length. Anteriorly, the vidian nerve exits the canalis caroticus internus at the level of the foramen nervi trigemini just posterior to its transformation into the cerebral canal. The vidian nerve extends anteriorly through the pterygoid and leaves the skull on the lateral surface of the pterygoid, anteroventrally to the foramen nervi trigemini. More anteriorly, ventral to the anterior end of the epipterygoid, the vidian nerve likely re-enters the skull on the lateral surface of the pterygoid, and runs anteriorly through the pterygoid and palatine. At its anterior end, the canalis nervus vidianus merges with canals coming from ventral and then splits into two branches. The medial branch joins the dorsal surface of the palatine and the lateral one joins the foramen palatinum posterius. Jamniczky & Russell (2007) identified the canalis nervus vidianus as being the canal for the palatine artery, but its location within the pterygoid, its exit towards the foramen palatinum posterius, the reported likely absence of the palatine artery in this taxon (Albrecht, 1967), and its correspondence with the vidian nerve canal of other testudinoids support our identification instead. The foramina anterius canalis nervi vidiani are formed by the pterygoid and palatine.

1098

1099

Emydidae (Fig. 12)



1101

1102

1103

1104

1105

1106

1107

1108

1109

1110

1111

1112

1113

1114

1115

1116

1117

1118

1119

1120

1121

1122

The internal carotid artery enters the skull through the fenestra postotica in *Emydoidea* blandingii, Emys orbicularis, Deirochelys reticularia, Glyptemys insculpta, Graptemys geographica, Pseudemys floridana, and Terrapene ornata, but in a relatively more ventral position in Clemmys guttata, Glyptemys muhlenbergii, and Terrapene coahuila. The foramen posterius canalis carotici interni is formed by the prootic, pterygoid, and basisphenoid in C. guttata, D. reticularia, Emydoidea blandingii, Gl. insculpta, and T. ornata, by the prootic and pterygoid in Emys orbicularis, Gr. geographica, Gl. muhlenbergii, and T. coahuila, and by the pterygoid and basisphenoid in *P. floridana*. This differs from Siebenrock (1897) and McDowell (1961) who only identified the pterygoid and prootic as the bones forming the foramen posterius canalis carotici interni in these emydids. The canalis caroticus internus is formed by the prootic, pterygoid, and basisphenoid in all observed emydids but *P. floridana*, in which the carotid artery extends along the pterygoid-basisphenoid suture for its entire length. According to Jamniczky & Russell (2007), the canalis caroticus internus of *Chrysemys picta* and *Emys orbicularis* is formed by the basisphenoid and pterygoid bones only. Siebenrock (1897) also noted for *Trachemys* ornata that the foramen posterius canalis carotici interni is formed by the pterygoid and the canalis caroticus internus by the pterygoid and basisphenoid. The canalis pro ramo nervi vidiani enters the internal carotid canal in all emydids but Gl. muhlenbergii, in which the vidian nerve takes a short-cut by directly entering the canalis caroticus lateralis. In all observed emydids, the split of the canalis caroticus internus into the canalis caroticus lateralis and canalis caroticus basisphenoidalis occurs along the pterygoid-basisphenoid suture. The palatine artery extends anteriorly through the canalis caroticus lateralis along the pterygoid-basisphenoid suture and joins the sulcus cavernosus slightly posteriorly to the anterior end of the rostrum basisphenoidale. In Gr. geographica, the anterior portion of the palatine artery shifts laterally



1124

1125

1126

1127

1128

1129

1130

1131

1132

1133

1134

1135

1136

1137

1138

1139

1140

1141

1142

1143

1144

1145

and extends through the pterygoid only. The palatine artery is exposed ventrally for a short distance in C. guttata, D. reticularia, Gl. muhlenbergii, T. coahuila, and T. ornata through an unnamed fenestra. Albrecht (1967) noted the presence of a canalis carotico-pharyngealis in *Trachemys scripta*. Here, we confirm the presence of one canalis carotico-pharyngealis in D. reticularia, Emydoidea blandingii, Emys orbicularis, Gl. insculpta, and P. floridana, and two canalis carotico-pharyngealis in Gr. geographica. In C. guttata, Gl. muhlenbergii, T. coahuila, and T. ornata, no canalis carotico-pharyngealis is visible but this might be due to the ventral exposure of the palatine artery. The cerebral artery extends anteromedially through the basisphenoid and joins the sella turcica along widely-spaced foramina anterius canalis carotici basisphenoidalis. The canalis stapedio-temporalis is the largest canal and the canalis caroticus lateralis the smallest in all observed emydids, with the canalis stapedio-temporalis being about ten times larger (Table 2). However, some variation occurs regarding the size of the canalis caroticus basisphenoidalis in comparison with the canalis caroticus lateralis. For instance, the canalis caroticus basisphenoidalis of *D. reticularia* is ten times larger than the canalis caroticus lateralis, whereas the canalis caroticus basisphenoidalis and canalis caroticus lateralis of Gr. geographica have a similar size. The eventual split occurring between the canalis nervus vidianus and canalis caroticus lateralis is likely to change the size of the canalis caroticus lateralis anterior to this split, as in *T. ornata* or *D. reticularia*, in which the canalis caroticus lateralis becomes much smaller anterior to the separation with the canalis nervus vidianus. Our results differ from Jamniczky & Russell (2007) who found equally sized canalis caroticus lateralis and canalis caroticus basisphenoidalis in *Emys orbicularis*. The morphology of the canalis cavernosus is very similar in all observed emydids. The canalis

cavernosus starts at the level of the foramen stapedio-temporalis and is formed by the quadrate,



1147

1148

1149

1150

1151

1152

1153

1154

1155

1156

1157

1158

1159

1160

1161

1162

1163

1164

1165

1166

1167

1168

presence of the mandibular artery can be inferred from a sulcus located along the lateral wall of the canalis cavernosus (Albrecht, 1967). The facial nerve extends ventrolaterally from the fossa acustico-facialis to the canalis cavernosus through the prootic. The position of the geniculate ganglion is inferred to be within the canalis cavernosus in all emydids, giving off the hyomandibular and vidian nerves. The hyomandibular nerve has no osteological correlate within the canalis cavernosus in Gl. insculpta, Gl. muhlenbergii, and P. floridana. However, in C. guttata, D. reticularia, Emydoidea blandingii, Emys orbicularis, Gr. geographica, T. coahuila, and T. ornata, the course of the hyomandibular nerve can be seen as a sulcus in the wall of the canalis cavernosus. The vidian nerve of all emydids but Gl. muhlenbergii extends through the canalis pro ramo nervi vidiani to join the canalis caroticus internus, and is bordered by the prootic and pterygoid, with minor contributions of the basisphenoid in C. guttata, Emys orbicularis, Gl, insculpta, and P. floridana. This slightly differs from Shiino (1913), who did not mention the basisphenoid as forming parts of the canalis pro ramo nervi vidiani in C. guttata. In Gl. muhlenbergii, the vidian nerve does not join the canalis caroticus internus and extends through the prootic and pterygoid to merge anteriorly with the canalis caroticus lateralis. The vidian nerve is then inferred to follow the course of the canalis caroticus lateralis into the sulcus cavernosus. Anterior to the foramen anterius canalis caroticus lateralis, at the level of the anterior margin of the descending process of the parietal, an extremely short canal that might contain a portion of the vidian nerve crosses the pterygoid medio-laterally. In C. guttata, Emydoidea blandingii, and Emys orbicularis, the vidian nerve is inferred to pass through the canalis caroticus internus and canalis caroticus lateralis to join the sulcus cavernosus, and anteriorly pierces the pterygoid to enter the canalis nervus

prootic and pterygoid. The foramen cavernosum is formed by the prootic and pterygoid. The



1170

1171

1172

1173

1174

1175

1176

1177

1178

1179

1180

1181

1182

1183

1184

1185

1186

1187

1188

1189

1190

1191

vidianus that is formed the pterygoid and epipterygoid in C. guttata, by the pterygoid, epipterygoid, and parietal in *Emydoidea blandingii*, and *Emys orbicularis*. The foramen anterius canalis nervi vidiani is formed by the pterygoid and epipterygoid in C. guttata, by the pterygoid and parietal in *Emydoidea blandingii*, and by the epipterygoid, palatine, and parietal in *Emys* orbicularis. D. reticularia exhibits a specific pattern on each side. On the left side, the vidian nerve splits from the canalis caroticus internus posterior to its split into the canalis caroticus lateralis and canalis caroticus basisphenoidalis, and the canalis nervus vidianus is formed by contributions of the prootic, pterygoid, basisphenoid, epipterygoid and parietal. On the right side, the vidian nerve is inferred to follow the course of the canalis caroticus internus and canalis caroticus lateralis, then splits from the canalis caroticus lateralis to extend through its own canal which is formed by the pterygoid, epipterygoid, and parietal. The foramina anterius canalis nervi vidiani are formed by the epipterygoid and parietal, and located ventrolaterally to the anterior margin of the processus inferior parietalis. In Gl. insculpta, anterior to the canalis pro ramo nervi vidiani, the vidian nerve remains distinguishable from the canalis caroticus internus for a short distance as a hump located on the lateral side of the latter. The vidian nerve then splits from the canalis caroticus internus, extends anteriorly along the pterygoid-basisphenoid suture, and joins the posterior portion of the canalis caroticus lateralis. Posterior to the foramen anterius canalis carotici lateralis, the vidian nerve diverges from the canalis caroticus lateralis to extend through the pterygoid and exits the skull ventrolaterally to the anterior margin of the processus inferior parietalis. In Gr. geographica, P. floridana, T. coahuila and T. ornata, the vidian nerve is inferred to follow the course of the canalis caroticus internus and canalis caroticus lateralis, then splits from the latter posterior to or at the level of the foramen anterius canalis carotici lateralis, and extends anteriorly through the canalis nervus vidianus. The canalis nervus vidianus and



foramen anterius canalis nervi vidiani are formed by the pterygoid and palatine in *Gr.* geographica, and by the pterygoid and epipterygoid in *T. coahuila* and *T. ornata*. The canalis nervus vidianus of *P. floridana* is formed by the pterygoid and palatine, but the foramen anterius canalis nervi vidiani by the palatine only. Siebenrock (1897) noted that the canalis nervus vidianus of *Trachemys ornata* is formed by the pterygoid and palatine. Albrecht (1967) described a different pattern for the vidian nerve in *Trachemys scripta*, *Chrysemys picta*, and *Pseudemys concinna*. In these taxa, some branches of the vidian nerve enter a canal that Albrecht (1967) calls 'posterior canalis nervi vidiani' and that extends anterolaterally from the canalis pro ramo nervi vidiani close to the canalis carotico-pharyngeale. The other branches of the vidian nerve follow the course of the canalis caroticus internus and canalis caroticus lateralis. Some of these latter branches then join the branches of the 'posterior canalis nervi vidiani' via the canalis carotico-pharyngeale, and together, run anteriorly through his 'anterior canalis nervi vidiani' then opens into the foramen palatinum posterius.

Testudinidae (Fig. 13)

In all examined testudinids, the internal carotid artery enters the skull through the fenestra postotica. A sulcus for the internal carotid artery is present on the dorsal side of the pterygoid in all observed specimens but *Aldabrachelys gigantea*. The foramen posterius canalis carotici interni is formed within the cavum acustico-jugulare by the prootic and pterygoid in *Agrionemys horsfieldii*, *Al. gigantea*, *Gopherus agassizii*, *Gopherus polyphemus*, *Indotestudo elongata*, *Indotestudo forstenii*, *Malacochersus tornieri*, and *Testudo marginata*, by the pterygoid in *Gopherus flavomarginatus*, by the prootic, pterygoid, and basisphenoid in *Kinixys erosa*, and by



1216

1217

1218

1219

1220

1221

1222

1223

1224

1225

1226

1227

1228

1229

1230

1231

1232

1233

1234

1235

1236

1237

the quadrate, prootic, pterygoid, and basisphenoid in *Psammobates tentorius*. The canalis caroticus internus is formed by the prootic, pterygoid, and basisphenoid in all observed testudinids but P. tentorius, in which the quadrate posterolaterally contributes to it. Jamniczky & Russell (2007) did not mention the prootic as contributing to the canalis caroticus internus of G. polyphemus and Ag. horsfieldii. The canalis caroticus internus contacts the canalis pro ramo nervi vidiani in Ag. horsfieldii Al. gigantea, G. agassizii, G. flavomarginatus, G. polyphemus, I. forstenii, M. tornieri, P. tentorius, but not in I. elongata, K. erosa, and T. marginata. The canalis caroticus lateralis and canalis carotico-pharyngealis are absent in all observed testudinids, with exception of a highly asymmetric specimen of *Manouria impressa*, which possess a canalis caroticus lateralis on the right side, but not on the left side. The canal on the right side appears to be a 'regular' canalis caroticus lateralis in the sense that it is in the expected position of such a canal in the basisphenoid-pterygoid suture, and that it extends toward an exiting foramen within the sulcus cavernosus. The canal size is similar to that in geoemydids. As this specimen appears to display a congenital abnormality, we disregard it from further consideration, but note that it may be informative in better understanding how the cranial circulation patterns originate during development (see Discussion). Our identification of the only canal that splits from the canalis caroticus internus as being the canalis nervus vidianus rests upon three criteria that are encountered in all observed testudinids. First, this canal always extends anteriorly in a relative lateral position through the pterygoid. Second, the canal does not extend along the pterygoid/basisphenoid suture, as in all turtles with an unambiguous canalis caroticus lateralis. And third, the canal never connects to the sulcus cavernosus, whereas the canalis caroticus lateralis, when present in other turtles, connects to the sulcus cavernosus via the foramen anterius canalis caroticus lateralis along the pterygoid/basisphenoid suture. These criteria also imply that



the palatine artery is likely absent in the taxa we observed. However, its presence has been
highlighted in several studies. Shindo (1914) noted the presence of a very small palatine artery in
Testudo graeca, splitting from the canalis caroticus internus close to the foramen anterius canalis
carotici basisphenoidalis, and running anteriorly with the vidian nerve through the palatine.
McDowell (1961) made a similar statement for the testudinids he dissected, observing a vestigial
palatine artery in Gopherus berlandieri and T. graeca that runs through its own canal separate
from the vidian nerve. Albrecht (1976) mentioned the palatine artery as being present but
vestigial in G. flavomarginatus, G. polyphemus, M. tornieri, and Chelonoidis nigra, but these
claims are not based on dissections and he did not provide detailed descriptions about where the
palatine canal is located. Jamniczky & Russell (2007) finally stated that the canalis caroticus
lateralis and foramen anterius canalis carotici lateralis are absent in G. polyphemus. Several
possibilities exist to explain these differences. First, it is possible that the presence of the palatine
artery is highly polymorphic, but the systematic absence in our sample makes that somewhat
unlikely. Second, it is possible that Shindo (1914) and McDowell (1961) misidentified the vidian
nerve as the palatine artery and that the palatine artery is systematically absent. Third, it is
possible that the palatine artery of tortoises regularly follows the course of the vidian nerve into
the palatine, as hinted by Shindo (1914). Our criteria of homology may therefore have tricked us
to have concluded the palatine artery to be systematically absent. Future studies using wet
specimens will need to clarify this issue.
The cerebral artery extends anteromedially through the basisphenoid in all testudinids to join
the sella turcica, with exception of G. flavomarginatus, where the artery runs along the
pterygoid-basisphenoid suture before entering the basisphenoid. The foramina anterius canalis
carotici basisphenoidalis are widely spaced. The canalis stapedio-temporalis is overall the largest



1262

1263

1264

1265

1266

1267

1268

1269

1270

1271

1272

1273

1274

1275

1276

1277

1278

1279

1280

1281

1282

1283

canal and the canalis caroticus basisphenoidalis the smallest in all observed taxa (Table 2). However, as in emydids, some variation occurs. The canalis stapedio-temporalis of G. agassizii is more than ten times larger than the canalis caroticus basisphenoidalis, whereas the canalis stapedio-temporalis of *I. forstenii* is only slightly larger than the canalis caroticus basisphenoidalis. The canalis caroticus basisphenoidalis of *I. forstenii* is also slightly larger than the canalis caroticus internus, whereas the canalis caroticus basisphenoidalis is always smaller than the canalis caroticus internus in other observed testudinids. Our measurements contradict Jamniczky & Russell (2007) who described the canalis stapedio-temporalis to be equally sized to the canalis caroticus internus and canalis caroticus basisphenoidalis in G. polyphemus. The canalis cavernosus posteriorly starts at the level of the foramen stapedio-temporalis. In M. tornieri, the lateral wall of the canalis cavernosus is partially unossified, exposing it along the subtemporal fossa. The canalis cavernosus of testudinids is formed by the quadrate, prootic, and pterygoid. The mandibular artery of testudinoids splits off the stapedial artery within the cavum acustico-jugulare, passes through the canalis cavernosus, and exits the skull through the trigeminal foramen (McDowell, 1961; Albrecht, 1967). The passage within the canalis cavernosus is typically visible as a lateral sulcus. McDowell (1961) noted, however, that the mandibular artery exits at an earlier point through a separate foramen that he named the foramen arteriomandibulare. The variable presence of this foramen was utilized by Crumly (1982, 1994) to infer phylogenetic relationships among tortoises. Here, we confirm the presence of the foramen in G. polyphemus and additionally report it for G. agassizii, G. flavomarginatus, Al. gigantea, and K. erosa. This foramen is formed by the quadrate and pterygoid in Gopherus spp., by the quadrate in Al. gigantea, and by the quadrate, prootic, and pterygoid in K. erosa. The mandibular artery of M. tornieri (on the right side) and T. marginata is not contained in the



1285

1286

1287

1288

1289

1290

1291

1292

1293

1294

1295

1296

1297

1298

1299

1300

1301

1302

1303

1304

1305

1306

canalis cavernosus for a short distance between the foramen stapedio-temporalis and the foramen cavernosum and likely extends through its own canal. In Ag. horsfieldii, I. forstenii, I. elongata, and P. tentorius, no separate mandibular artery foramen is evident, indicating that the arteria mandibularis passes anteriorly through the canalis cavernosus and then exits the skull through the trigeminal foramen. The foramen cavernosum is formed by the prootic and pterygoid. The facial nerve extends laterally through the prootic from the fossa acustico-facialis to the canalis cavernosus in Ag. horsfieldii, G. agassizii, G. flavomarginatus, G. polyphemus, K. erosa, M. tornieri, and T. marginata, and the geniculate ganglion is inferred to be within the canalis cavernosus. The geniculate ganglion is inferred to be located medially to the canalis cavernosus and dorsally to the canalis caroticus internus in Al. gigantea, I. elongata, and I. forstenii. P. tentorius exhibits asymmetry, as the geniculate ganglion is located in between the canalis cavernosus and canalis caroticus internus on the right side, but contacts the canalis caroticus internus on the left side. The geniculate ganglion gives off the hyomandibular and vidian nerves. The hyomandibular nerve has not osteological correlate within the canalis cavernosus in G. flavomarginatus and I. elongata, but its course can be seen as a sulcus in the wall of the canalis cavernosus in Ag. horsfieldii, G. agassizii, I. forstenii, K. erosa, M. tornieri, P. tentorius, and T. marginata, and it extends through its own canalis nervus hyomandibularis distalis Al. gigantea and G. polyphemus. In all observed testudinids but K. erosa, and T. marginata, the vidian nerve extends through the canalis pro ramo nervi vidiani to connect with the canalis caroticus internus, and leaves the latter more anteriorly to extend through the canalis nervus vidianus. The canalis pro ramo nervi vidiani is formed by the prootic and pterygoid in Ag. horsfieldii, Al. gigantea, G. agassizii, G. flavomarginatus, G. polyphemus, I. elongata, and I. forstenii, but only by the prootic in M. tornieri and P. tentorius. The vidian nerve of K. erosa and T. marginata extends



1308

1309

1310

1311

1312

1313

1314

1315

1316

1317

1318

1319

1320

1321

1322

ventromedially from the geniculate ganglion but does not join the canalis caroticus internus and instead directly enters the canalis nervus vidianus. Additional variation exists regarding the bones forming the canalis nervus vidianus and foramina anterius canalis nervi vidiani. The canalis nervus vidianus is formed by the prootic, pterygoid, and palatine in Ag. horsfieldii, G. polyphemus, and M. tornieri, by the pterygoid, epipterygoid, and palatine in Al. gigantea, by the pterygoid and palatine in G. agassizii, I. elongata, and P. tentorius, by the pterygoid, epipterygoid, palatine, and parietal in G. flavomarginatus, by the pterygoid in I. forstenii, by the prootic, pterygoid, palatine, and parietal in *K. erosa*, and by the prootic, pterygoid, epipterygoid, palatine, and parietal in T. marginata. In G. agassizii, the vidian nerve exits the skull anteroventrally to the foramen nervi trigemini for a short distance, before re-entering it by piercing the lateral surface of the palatine. The foramina anterius canalis nervi vidiani are formed by the pterygoid and palatine in Ag. horsfieldii, M. tornieri, and P. tentorius, by the epipterygoid and palatine in Al. gigantea, by the palatine in G. agassizii, G. polyphemus, and I. elongata, by the palatine and parietal in G. flavomarginatus and K. erosa, by the pterygoid in I. forstenii, and by the epipterygoid, palatine, and parietal in *T. marginata*. Gaupp (1888) noted that the canalis nervus vidianus of *Testudo graeca* is formed by the basisphenoid and pterygoid.

1323

1324

1325

1326

1327

1328

1329

Geoemydidae (Fig. 14)

In all observed geoemydids, the internal carotid artery enters the skull through the fenestra postotica. A sulcus for the internal carotid artery is formed on the dorsal side of the pterygoid. The foramen posterius canalis carotici interni is located within the cavum acustico-jugulare and formed by the prootic and the pterygoid in all taxa in our sample but *Geoclemys hamiltonii*, where it is only formed by the pterygoid. This slightly differs from Siebenrock (1897) and



1331

1332

1333

1334

1335

1336

1337

1338

1339

1340

1341

1342

1343

1344

1345

1346

1347

1348

1349

1350

1351

1352

McDowell (1961) who only identified the pterygoid as forming the foramen posterius canalis carotici interni in Cyclemys dentata, Geoclemys hamiltonii, and Morenia sp. McDowell (1961) also noted that the opisthotic contributes to the foramen posterius canalis carotici interni of Batagur sp., which is not the case in the specimen of Batagur baska we studied. The canalis caroticus internus is formed by the prootic, pterygoid, and basisphenoid in all observed geoemydids but Geoclemys hamiltonii, in which the canalis caroticus internus is formed by the pterygoid and basisphenoid only. Jamniczky & Russell (2007) noted that the canalis caroticus internus of Cuora amboinensis and Rhinoclemmys pulcherrima is formed by the basisphenoid and pterygoid. The canalis pro ramo nervi vidiani enters the internal carotid canal in all geoemydids but Cyclemys dentata, Geoemyda spengleri, and Rhinoclemmys melanosterna. The canalis caroticus internus splits into the canalis caroticus lateralis and canalis caroticus basisphenoidalis in all sampled taxa but Malayemys subtrijuga, Pangshura tecta, and R. melanosterna, where the lateral canal appears to be absent. Jamniczky & Russell (2007) noted the absence of the canalis caroticus lateralis and foramen anterius canalis carotici lateralis in Cu. amboinensis and R. pulcherrima. The canalis caroticus lateralis extends anteriorly along the pterygoid-basisphenoid suture in B. baska, Cu. amboinensis, Cv. dentata, Geoclemys hamiltonii, Geoemyda spengleri, Mauremys leprosa, and Mo. ocellata, and the foramen anterius canalis carotici lateralis is formed by the pterygoid and basisphenoid in these taxa. In S. crassicollis, the canalis caroticus lateralis and foramen anterius canalis carotici lateralis are formed by the pterygoid only. The canalis carotico-pharyngealis is absent in all observed specimens but Cu. amboinensis, in which one canalis carotico-pharyngealis is present. The canalis caroticus basisphenoidalis and foramen anterius canalis carotici basisphenoidalis are formed by the basisphenoid in all geoemydids but S. crassicollis, in which the pterygoid posteriorly contributes



1354

1355

1356

1357

1358

1359

1360

1361

1362

1363

1364

1365

1366

1367

1368

1369

1370

1371

1372

1373

1374

1375

to the canalis caroticus basisphenoidalis. The foramina anterius canalis carotici basisphenoidalis are widely separated. In all observed geoemydids, the canalis stapedio-temporalis is the largest canal and the canalis caroticus lateralis, when present, the smallest (Table 2). As in emydids and testudinids, some variation regarding canal size occurs. The canalis stapedio-temporalis is generally nearly ten times larger than the canalis caroticus lateralis, if present, but this difference is more important in Cy. dentata and Geoemyda spengleri, in which the canalis caroticus lateralis is greatly reduced, and in *Malayemys subtrijuga*, *P. tecta*, and *R. melanosterna*, in which the canalis caroticus lateralis is absent. Moreover, the canalis stapedio-temporalis is about five times larger than the canalis caroticus basisphenoidalis in B. baska and Cu. amboinensis, but only twice as large as the canalis caroticus basisphenoidalis in Malayemys subtrijuga and R. melanosterna, as noted by Jamniczky & Russell (2007) in Rhinoclemmys pulcherrima. The canalis cavernosus starts at the level of the foramen stapedio-temporalis. The canalis cavernosus is formed by the quadrate, prootic, and pterygoid in all observed geoemydids. Siebenrock (1897) described a similar pattern for the mandibular artery of Cy. dentata as in testudinids, but this is not the case in our specimen. However, a distinct protrusion is visible on the lateral wall of the canalis cavernosus of this specimen that likely corresponds to the mandibular artery. The foramen cavernosum is formed by the prootic and the pterygoid. The canalis nervus facialis extends laterally through the prootic from the fossa acusticofacialis to the canalis cavernosus. The position of the geniculate ganglion is inferred to be within the canalis cavernosus in all observed geoemydids but Mauremys leprosa, in which the geniculate ganglion is not in contact with the canalis cavernosus, and R. melanosterna, in which the geniculate ganglion contacts the canalis caroticus internus. The geniculate ganglion gives off the hyomandibular and vidian nerves. The course of the hyomandibular nerve is visible as a



1377

1378

1379

1380

1381

1382

1383

1384

1385

1386

1387

1388

1389

1390

1391

1392

1393

1394

1395

1396

1397

1398

sulcus in all observed geoemydids but Mo. ocellata, in which the hyomandibular nerve has no osteological correlate within the canalis cavernosus and is inferred to follow the course of it. In all geoemydids but Cv. dentata, Geoemyda spengleri, and R. melanosterna, the vidian nerve extends through the canalis pro ramo nervi vidiani to join the canalis caroticus internus. Three patterns for the vidian nerve can be identified for the taxa exhibiting a canalis pro ramo nervi vidiani. In *Malayemys subtrijuga* and *P. tecta*, the vidian nerve leaves the canalis caroticus internus anterior to the canalis pro ramo nervi vidiani to enter the canalis nervus vidianus. In Mauremys leprosa and Mo. ocellata, the vidian nerve leaves the canalis caroticus internus, and anteriorly enters the canalis caroticus lateralis to extend into the sulcus cavernosus, and then leaves the latter laterally, anterior to the foramen anterius canalis carotici lateralis. In B. baska, Cu. amboinensis, Geoclemys hamiltonii, and S. crassicollis, the vidian nerve is inferred to extend through the canalis caroticus internus and canalis caroticus lateralis into the sulcus cavernosus, and then enters the canalis nervus vidianus anterior to the foramen anterius canalis carotici lateralis. The vidian nerve of Geoclemys hamiltonii is laterally exposed for a short distance. Cv. dentata and Geoemyda spengleri diverge from these patterns by having a vidian nerve that respectively merges with one and two canals originating from the posterior portion of the canalis caroticus internus. The vidian nerve of Geoemyda spengleri also shortly runs through the canalis caroticus lateralis. As the facial nerve system of R. melanosterna connects to the canalis caroticus internus, the canalis pro ramo nervi vidiani is absent and the vidian nerve directly joins the canalis caroticus internus, follows the course for the internal carotid artery for a short distance, and enters the canalis nervus vidianus. As in testudinids, a substantial amount of variation exists about the bones forming the canalis nervus vidianus and foramina anterius canalis nervi vidiani. The canalis nervus vidianus is formed by the pterygoid and palatine in B.



baska and P. tecta, by the pterygoid, palatine, and parietal in Cu. amboinensis, Geoclemys hamiltonii, Malayemys subtrijuga, Mo. ocellata, and S. crassicollis, by the prootic, pterygoid, and parietal in Cy. dentata, by the prootic and pterygoid in Geoemyda spengleri, by the pterygoid, epipterygoid, and parietal in Mauremys leprosa, and by the pterygoid, epipterygoid, palatine, and parietal in R. melanosterna. The foramina anterius canalis nervi vidiani are formed by the palatine in B. baska, Mo. ocellata, P. tecta, and R. melanosterna, by the pterygoid and parietal in Cu. amboinensis, by the parietal in Cy. dentata and Mauremys leprosa, by the palatine and parietal in Geoclemys hamiltonii, Malayemys subtrijuga, and S. crassicollis, and by the pterygoid in Geoemyda spengleri.

DISCUSSION

Summary of carotid canal system

Internal carotid artery: All extant turtles have an internal carotid artery that is fully enclosed in a canalis caroticus internus that extends anteriorly into the basicranium. The sole exception are podocnemidids, where the internal carotid artery passes through a large opening, the cavum pterygoidei, which is unique to that clade. The highly derived placement of podocnemidids within Testudines strongly suggests that this is a secondary modification. We note here, that it is a matter of semantic preference if the foramen posterius canalis carotici interni is thought to be present in podocnemidids, but modified (e.g., sensu Gaffney, Tong & Meylan, 2006), or absent due to the presence of a cavum pterygoidei (as defined herein). Our study therefore do not provide novels insights that contradict previous ones. The pterygoid bone is always involved in the formation of the foramen posterius canalis carotici interni in cryptodires but never contributes to this foramen in extant pleurodires. This generalization, of



1423

1424

1425

1426

1427

1428

1429

1430

1431

1432

1433

1434

1435

1436

1437

1438

1439

1440

1441

1442

1443

1444

course, only applies in the strict sense of the foramen posterius canalis carotici interni employed herein, as the enlarged cavum pterygoidei of podocnemidis has a clear contribution from the pterygoid and has been interpreted as the foramen posterius canalis carotici interni by others (e.g., Siebenrock, 1897). Incidentally, a contribution from the pterygoid is apparent in the stem pleurodire *Notoemys laticentralis* (Lapparent de Broin, de la Fuente & Fernandez, 2007). This may suggest that a pterygoid contribution is plesiomorphic for crown Testudines. Cerebral artery: Little variation exists for the cerebral artery in extant turtles outside of Chelonioidea. All examined taxa have a canalis caroticus basisphenoidalis that extends through the basisphenoid and exits in the sella turcica. The only exception to this is found in Dermochelys coriacea, in which the canalis caroticus basisphenoidalis is anteriorly unossified, a feature that has otherwise only been reported in one fossil turtle (Evers & Joyce, 2020). The exiting foramina for the cerebral artery, the foramina anterius canalis carotici basisphenoidalis, are paired across the skull midline in nearly all species of extant turtles. Only in three species of cheloniids (Lepidochelys olivacea, Caretta caretta, Natator depressus), the left and right canalis caroticus basisphenoidalis merge within the basisphenoid and exit the sella turcica via a single, median foramen (see also Hooks, 1998; Evers, Barrett & Benson, 2019 for fossil occurrences of this feature). Otherwise, variation regarding the cerebral circulation is limited to the spacing of the foramina anterius canalis carotici basisphenoidalis (Hirayama, 1998). In our sample, the foramina anterius canalis carotici basisphenoidalis are widely-spaced in all turtles but Macrochelys temminckii, platysternids, and the remaining chelonioids, in which these openings are rather narrowly-spaced. The repeated loss of the lateral carotid canal: We observe the complete loss of the lateral carotid canal in all pleurodires (contra Albrecht, 1967, 1976; Gaffney, Tong & Meylan, 2006;



1446

1447

1448

1449

1450

1451

1452

1453

1454

1455

1456

1457

1458

1459

1460

1461

1462

1463

1464

1465

1466

1467

Hermanson et al., 2020), carettochelyids (see also Joyce, Volpato & Rollot, 2018), platysternids, testudinids, and some geoemydids. A canalis caroticus lateralis is furthermore absent in chelonioids, but not a result of the absence of the palatine artery, but due to its anterior displacement (see also Zangerl, 1953; Albrecht, 1976; Gaffney, 1979; Evers & Benson, 2019). Several authors have previously noticed the absence of the canalis caroticus lateralis in some pleurodires, but the special embedding of the internal carotid artery within the cavum pterygoidei in podocnemidids makes assessments for that clade difficult. In particular, whereas previous authors, such as Gaffney, Tong & Meylan (2006) or Hermanson et al. (2020), interpreted the fenestra between the cavum pterygoidei and sulcus cavernosus to be a trough let for the palatine artery, we instead hypothesize the absence of a palatine artery for podocnemidids. Our assessment is largely based on the dissection study of Albrecht (1976), who only found a vestigial blood vessel to pass this fenestra in one out of six specimens. Our re-interpretation is more parsimonious than the interpretation of Hermanson et al. (2020), who inferred a loss of the palatine artery in Pelomedusoides, its reappearance in Podocnemidoidae, and yet another loss for stereogenyine podocnemidids. Additionally, we re-interpret the 'canalis caroticus lateralis' of chelids by Hermanson et al. (2020; figured for *Hydromedusa tectifera*) to be the canalis nervus vidianus instead. As a result, the absence of the lateral carotid canal, which is ultimately based on the loss of the palatine artery, is a likely synapomorphy of Pleurodira. Within Trionychia, we infer the independent loss of the palatine artery for carettochelyids (see also Joyce, Volpato & Rollot, 2018). Interestingly, the artery that extends through the short canalis caroticus lateralis in trionychids does not serve the function of a 'regular' palatine artery, but instead supplies the mandible (Albrecht, 1967). Thus, the lateral carotid canal of trionychids, although present according to our observations, fulfills a different role and complicates





1469

1470

1471

1472

1473

1474

1475

1476

1477

1478

1479

1480

1481

1482

1483

1484

1485

1486

1487

1488

1489

1490

assessment on its homology. We provide our reasoning for concluding that the mandibular artery of trionychids is a repurposed palatine artery below (see discussion of mandibular artery). In addition to the definite reductions in pleurodires and carettochelyids, the canalis caroticus lateralis is lost several times within testudinoids, which generally show the largest amount of variation. As the canalis caroticus lateralis is absent in *Platysternon megacephalum*, but present in all emydids, there seems to have been one independent loss within Emysternia. Within geoemydids, the canalis caroticus lateralis is generally present, with exception of *Malayemys* subtrijuga, Pangshura tecta, and Rhinoclemmvs melanosterna, which represent several independent losses of the palatine artery based on current geoemydid in-group relationships (e.g., Garbin, Ascarrunz & Joyce, 2018). The canalis caroticus lateralis is absent in all testudinids we examined, with the exception of a highly unusual specimen of *Manouria impress* (SMF 69777; Fig. 15), which has an asymmetrical arterial pattern with a 'regular' canalis caroticus lateralis on the left side, but none on the right side. The occurrence of the palatine artery had been mentioned by Shindo (1914), McDowell (1961), and Albrecht (1976) for some testudinids. Thus, although the vast majority of testudinid specimens examined herein show no evidence for the presence of the palatine artery, it is possible that this feature is highly polymorphic within testudinids. To address this further, studies focusing on intraspecific variation regarding the palatine artery are necessary, which is beyond the scope of this contribution. We note, however, that the canalis caroticus lateralis is extremely small in diameter whenever it is present (Table 2). In summary, a highly reduced to absent palatine artery appears to be a common feature of all extant testudinoids. Although the palatine artery is present in extant chelonioids (Albrecht, 1976), the internal carotid artery of these turtles enters the sulcus cavernosus prior to its split into the palatine and



1492

1493

1494

1495

1496

1497

1498

1499

1500

1501

1502

1503

1504

1505

1506

1507

1508

1509

1510

1511

1512

1513

cerebral branches, so that the palatine artery is never encased in a bony canal (Zangerl, 1953: Albrecht, 1976; Gaffney, 1979; Evers & Benson, 2019). However, the condition likely evolved independently in dermochelyids and extant cheloniids, as stem-group cheloniids show a regular bifurcation pattern with a regularly enclosed palatine artery (Evers, Barrett & Benson, 2019). The mandibular artery: The mandible of turtles is typically supplied by a large artery that variously originates from different parts of the carotid arterial system (Albrecht, 1967, 1976). These different origins make it difficult to homologize arteries, but the term 'mandibular artery' has historically been used for all variants of mandible-supplying arteries (e.g., Gaffney, 1979) and we generally adhere to this practice. However, as the mandible is sometimes supplied by two arteries from two sources, we here follow the convention of Albrecht (1967, 1976) by distinguishing between an anterior and posterior mandibular artery. The mandibular artery is mostly supplied by the stapedial artery in pleurodires, carettochelyids, chelydrids, and testudinoids, by the palatine artery in kinosternids, but by both sources in cheloniids (McDowell, 1961; Albrecht, 1967, 1976). In trionychids, the mandibular artery takes the same proximal course as the palatine artery of other turtles (i.e., via the lateral carotid canal), but then only supplies the mandible and does not send a branch anteriorly to supply the facial region (Albrecht, 1967). This raises the question of whether the 'mandibular artery' of trionychids is a modified palatine artery (in which case the palatine artery is present in trionychids), or neomorphic (in which case the palatine artery of trionychids was lost). This distinction is important for the reconstruction of the plesiomorphic condition for both crown Cryptodira and crown Testudines. Currently, unpublished CT scans of stem trionychians available to us (e.g., Basilemys sp.; Adocus sp.) indicate that a 'regular' palatine artery was present in stem-trionychians. This suggests that the mandibular artery of trionychids indeed is a palatine artery in which the





1515

1516

1517

1518

1519

1520

1521

1522

1523

1524

1525

1526

1527

1528

1529

1530

1531

1532

1533

1534

1535

1536

change has occurred at least a second time, within kinosternids, but in that clade the palatine artery retains its 'regular' function and only adds the role of supplying the mandible (Albrecht, 1967). In turtles in which the mandibular artery branches off the stapedial artery, this branching point can occur either before the stapedial artery enters the canalis stapedio-temporale (as reported for cryptodires in which the mandible is supplied by a branch of the stapedial artery: Albrecht, 1967; Gaffney, 1979), or after it has left the foramen stapedio-temporale (as reported for pleurodires: Albrecht, 1967, 1976). Among pleurodires, Albrecht (1976) observed that the mandibular artery branches off the stapedial artery and identified two different patterns. In pelomedusids and chelids, with the exception of *Chelodina longicollis*, a large mandibular artery branches off the stapedial artery after the later has exited the skull through the foramen stapedio-temporale. In Chelodina longicollis and podocnemidids, the stapedial artery first gives rise to the external mandibular artery posterior to the cranium, which runs anteroventrally to supply the tissue directly medial to the mandible. After exiting the skull through the foramen stapedio-temporale, the stapedial artery arches anteriorly over the fenestra subtemporalis and gives rise to the internal mandibular artery lateral to the foramen nervi trigemini, that courses ventrally to the fossa Meckelii in the mandible. As either course bypasses bone, we are unable to find osteological correlates that would document this pattern in fossil taxa. When the mandibular artery branches off the stapedial artery within the cavum acusticojugulare (testudinoids, chelydrids, carettochelyids, the posterior (vestigial) mandibular artery of chelonioids, and, potentially, dermatemydids), it takes an anteriorly directed course through the canalis cavernosus. From there, it usually exits the cranium, either through the trigeminal

function of the artery (as in the skull region it supplies with blood) has changed. A similar



1538

1539

1540

1541

1542

1543

1544

1545

1546

1547

1548

1549

1550

1551

1552

1553

1554

1555

1556

1557

1558

1559

foramen or a separate foramen arteriomandibulare. The latter exit has been observed directly from dissections for the posterior (vestigial) mandibular artery of the chelonioid *Chelonia mydas* (Albrecht, 1976) and the mandibular artery of the testudinids *Gopherus berlandieri*, Stigmochelys pardalis, and Chelonoidis denticulatus (McDowell, 1961). The presence of the foramen arteriomandibulare should serve as an excellent osteological correlate for the location of the mandibular artery in the canalis cavernosus. We confirm the previously established presence of this foramen in testudinids (McDowell, 1961), but note that Bramble (1971) and Crumly (1982, 1994) found additional variation, which may have relevance for systematics. Among testudinoids, Evers & Benson (2019) reported a foramen arteriomandibulare for *Platysternon megacephalum*, but we here note by reference to the same specimen, that it is unclear if the slit-like foramina indeed represent a true foramen arteriomandibulare or the incomplete ossification to the anterior wall of the canalis cavernosus. In contrast, we here confirm the exit of the mandibular artery through a separate foramen in Carettochelys insculpta through the presence of a foramen arteriomandibulare in osteological material, as previously reported by Evers & Benson (2019), in combination with personal observations of a stained specimen. This clearly contradicts the speculations of Joyce, Volpato & Rollot (2018) that the mandibular artery of carettochelyids may be fed from the certebral artery. Evers & Benson (2019) also reported the presence of a foramen arteriomandibulare in the pelomedusid *Pelomedusa subrufa*. If correct, this observation would be particularly relevant, as it would indicate a completely different course of the mandibular artery (i.e. through the canalis cavernosus) than usually reported for pleurodires (Albrecht, 1976). Given that dissections by Albrecht (1976) of *Pelomedusa subrufa* show that the canalis cavernosus houses no artery (contradicting ovservations by Evers & Benson, 2019), we re-examined the specimen used by



1561

1562

1563

1564

1565

1566

1567

1568

1569

1570

1571

1572

1573

1574

1575

1576

1577

1578

1579

1580

1581

1582

Evers & Benson (2019: SMF 70504). The 'mandibular artery foramen' of that specimen is highly irregular around its margins, and parallels the anterior portion of the canalis cavernosus, much as in the specimen of *Platysternon megacephalum* mentioned above. We, therefore, here re-interpret the 'foramina' as the incompletely ossified anterior wall of the canalis cavernosus. Although the presence of a foramen arteriomandibulare is the best direct osteological correlate for the course of the mandibular artery, our segmentations show that the course of this artery through the canalis cavernosus is often indicated by a subtle subdivision of the latter, which can serve as a second, more subtle osteological correlate for the placement of the mandibular artery within the canalis cavernosus. Such a subdivision is present in *Carettochelys* insculpta (Fig. 4), Dermatemys mawii (Fig. 7), chelydrids (Fig. 8), cheloniids (Fig. 9), Platysternon megacephalum (Fig. 11), emydids (Fig. 12), testudinids (Fig. 13), and geoemydids (Fig. 14). In these clades the dorsolateral part of the canalis cavernosus is separated from the medioventral part by a longitudinal, dorsal constriction between these subsections of the canal, which is visible on models of the canalis cavernosus as a longitudinal sulcus. In coronal slices of CT scans of these taxa, the canalis cavernosus shows a reniform cross-section. This morphology is developed to different degrees. For instance, it is particularly strong in testudinids (Fig. 13) and geoemydids (Fig. 14). However, there is also within-clade variation to the feature. For instance, the subdivision of the canalis cavernosus is relatively subtle in the geoemydid Geoclemys hamiltonii, but well-developed to the point that almost two canals are developed in sections of the skull in the geoemydids Cyclemys dentata and Pangshura tecta. We suggest the presence of this subdivision within the canalis cavernosus to be an osteological correlate for the condition that a mandibular artery extends through the canalis cavernosus. The slight spatial separation within the canalis cavernosus thereby represents the adjacent pathways for the vena





capitis lateralis and mandibular artery. Two reasons for hypothesizing the subdivision as an indicator for the mandibular artery can be named. The presence of the subdivision of the canalis cavernosus coincides with the passage of the mandibular artery through that structure in all taxa for which direct dissection observations have been made. Additionally, the foramen arteriomandibulare, i.e. a clear indication that the mandibular artery passes through the canalis cavernosus, is only ever present in taxa which also have the subdivision. Thus, the presence of this subdivision provides important information on some clades for which currently no dissection study is available, such as *Dermatemys mawii*. Thus, we speculate that the subdivision of the canalis cavernosus can be useful in the future to investigate the course of the mandibular artery in fossil clades.

In summary, several patterns for the mandibular artery can be identified from the information available and summarized above: (i) the mandibular artery branches off the stapedial artery without running through the canalis cavernosus in pleurodires, and the chelid *Chelodina longicollis* and podocnemidids have a second mandibular artery branch additionally supplying the mandible. In the second pattern (ii), the mandibular artery branches off the stapedial artery within the cavum acustico-jugulare, follows the course of the canalis cavernosus, and exits the skull through the foramen nervi trigemini or a separate foramen arteriomandibulare. This pattern is observed among cryptodires with the exceptions of kinosternids and trionychids. In kinosternids (iii), the mandibular artery does not branch off the stapedial artery but rather from the palatine artery, anterior to the foramen anterius canalis carotici lateralis. Finally (iv), the mandibular artery of trionychids is interpreted to be a modified palatine artery, and extends through the canalis caroticus lateralis.



The facial nerve system of turtles

Gaffney (1979) proposed two main patterns for the course of the facial nerve in pleurodires
and cryptodires, respectively. According to this model, pleurodires have the geniculate ganglion
located at the junction between the canalis nervus facialis and the canalis caroticus internus,
whereas the geniculate ganglion of cryptodires is developed at the point of contact between the
canalis nervus facialis and the canalis cavernosus. This hypothesis was extrapolated from data
collected by Siebenrock (1897) and Soliman (1964) on a few species of cryptodires and
pleurodires. The summary provided by Gaffney (1979) lead to the construction of a phylogenetic
character for the passage of the hyomandibular branch of the facial nerve (e.g., Gaffney, Meylan
& Wyss, 1991). Since, few studies have further scrutinized the proposals of Gaffney (1979) (but
see Evers & Benson, 2019). Here, we propose that two main patterns of the facial nerve system
can be recognized among extant turtles (Fig. 16). These patterns differ from one another in the
relative position of the geniculate ganglion, but, unlike in Gaffney (1979), they do not
correspond closely to the phylogenetic distinction of pleurodires and cryptodires.
Our pattern I is characterized by a geniculate ganglion positioned within the canalis
cavernosus, or at the interface between the canalis nervus facialis and the canalis cavernosus, and
thus outside of the prootic (Fig. 16). Pattern I essentially corresponds to the 'cryptodiran pattern'
of Gaffney (1979). However, pattern I is actually only realized in a subset of cryptodires, namely
in chelydroids (kinosternids, chelydrids, <i>Dermatemys mawii</i>), cheloniids, emysternians
(emydids, Platysternon megacephalum), a subset of trionychids (Apalone spinifera, Apalone
mutica, Amyda cartilaginea, and Pelodiscus sinensis among our sample), a subset of testudinids
(Agrionemys horsfieldii, Gopherus agassizii, Gopherus flavomarginatus, Gopherus polyphemus,
Kinixys erosa, Malacochersus tornieri, and Testudo marginata among our sample), and a subset



1630

1631

1632

1633

1634

1635

1636

1637

1638

1639

1640

1641

1642

1643

1644

1645

1646

1647

1648

1649

1650

1651

of geoemydids (Batagur baska, Cuora amboinensis, Cyclemys dentata, Geoclemys hamiltonii, Geoemyda spengleri, Malayemys subtrijuga, Morenia ocellata, Pangshura tecta, and Siebenrockiella crassicollis among our sample). Our pattern I is further subdivided into three sub-patterns that are distinct in the way the proximal portion of the vidian nerve is transmitted anteriorly. Most turtles with pattern I have a canalis pro ramo nervi vidiani which transmits the vidian nerve from within the canalis cavernosus into the canalis caroticus internus, and we designate this condition as pattern IA. The pattern we name IB is similar in that a canalis pro ramo nervi vidiani is also present, but this canal extends to the canalis caroticus lateralis instead. Thus, the canalis pro ramo nervi vidiani intersects with the carotid canal system slightly more anteriorly than in pattern IA. Pattern IB is seen in the emydid Glyptemys muhlenbergii and the geoemydids Cyclemys dentata and Geoemyda spengleri. We observed a third pattern, named pattern IC, in the testudinids Kinixys erosa and Testudo marginata. These turtles lack a bypassage of the vidian nerve through the canalis caroticus internus or any other canal associated with the carotid arterial system altogether. Instead, the vidian nerve passes directly into the canalis nervus vidianus from the canalis cavernosus. Our pattern II is characterized by a geniculate ganglion position outside the canalis cavernosus and in a more proximal position with regard to the facial nerve stem coming from the brain, and thus within the prootic. All turtles with pattern II have a canalis nervus hyomandibularis proximalis, which transmits the hyomandibular nerve from within the prootic to the canalis cavernosus. However, pattern II can be subdivided according to the course of the vidian nerve. In turtles with the pattern we name IIA, the vidian nerve is contained in a separate canal, the canalis pro ramo nervi vidiani, which extends from the geniculate ganglion to the canalis caroticus internus. The canalis pro ramo nervi vidiani in turtles of pattern IIA always



1653

1654

1655

1656

1657

1658

1659

1660

1661

1662

1663

1664

1665

1666

1667

1668

1669

1670

1671

1672

1673

starts in the prootic, and thus differs slightly from the canal with the same name in turtles of patterns IA and IB, in which the canal diverges from the canalis cavernosus and thus often from within the pterygoid. We retain the same name for all of these canals, as either transmit the vidian nerve toward the carotid arterial system. In pattern IIB, the vidian nerve directly enters the canalis caroticus internus and a canalis pro ramo nervi vidiani is absent. The direct transmission of the vidian nerve is enabled by an intersection of the canalis caroticus internus with the canalis nervus facialis. Patterns IIB and IIC share the direct intersection of the canalis nervus facialis and the canalis caroticus internus. However, in pattern IIC, a separate, anteriorly directed canalis nervus vidianus emerges from the area of the canal intersection. Thus, instead of passing through the carotid canal system, the vidian nerve directly enters its own canal, similar to pattern IB. Pattern IIA is found in podocnemidids, Carettochelys insculpta, some trionychids (Chitra indica, Cyclanorbis senegalensis, Cycloderma frenatum and Lissemys punctata among our sample), some testudinids (Aldabrachelys gigantea, Indotestudo elongata, and Indotestudo forstenii among our sample), and the geoemydid *Mauremys leprosa*. Pattern IIB, which essentially is the 'pleurodiran pattern' of Gaffney (1979), is found in most chelids and *Pelomedusa subrufa*, but additionally also in the cryptodires *Dermochelys coriacea* and *Rhinoclemmys melanosterna*. Pattern IIC is found in the chelid *Chelus fimbriatus* and the pelomedusid *Pelusios subniger*. It is noteworthy that our pattern IIA is basically identical to the facial nerve pattern recognized by Evers & Benson (2019: see character 127.1) for thalassochelydians, which were found to be crownward stem-turtles in that study. Our finding of similar facial nerve patterns in some pleurodires (podocnemidids) and some of the phylogenetically earliest branching cryptodires (some trionychids and Carettochelys insculpta) possibly suggests, that pattern IIA could be





plesiomorphic for crown-group turtles. However, only the re-examination of a broad set of fossil turtles can test this further.

Two additional sources of variation to the facial nerve system are apparent, but these are unrelated to the patterns outlined above. The first kind of variation relates to the posterior (=distal) path of the hyomandibular nerve. In all turtles, the posterior part of the hyomandibular nerve traverses or parallels the canalis cavernosus to reach the cavum acustico-jugulare. However, the posterior course of the nerve may be situated (a) in a separate canal (canalis nervus hyomandibularis distalis); (b) a sulcus in the wall of the canalis cavernosus; or (c) entirely within the canalis cavernosus (Fig. 17). This variation is independent of the presence of a canalis nervus hyomandibularis proximalis in turtles with pattern II, as the canalis nervus hyomandibularis proximalis of pattern II only transmits the proximal part of the hyomandibular nerve toward the canalis cavernosus. This is exemplified by turtles with pattern I that have a separate canalis nervus hyomandibularis distalis for the distal part of the nerve (e.g., Aldabrachelys gigantea, Gopherus polyphemus), or turtles with patterns IIA (e.g., Gopherus agassizii) or IIB (e.g., Pelomedusa subrufa) that have a hyomandibular sulcus irrespective of their canalis nervus hyomandibularis proximalis.

The second source of variation not addressed by our ganglion position patterns comes from the anteriormost (=distal) course of the vidian nerve, which is passed through the canalis nervus vidianus in the majority of turtles. The canalis nervus vidianus is present in all turtle clades but cheloniids and dermochelyids, in which the vidian nerve is inferred to extend through the canalis caroticus internus to the sulcus cavernosus, and then, in *Dermochelys coriacea* at least, to follow the path of the palatine artery (Nick, 1912). However, the path of the vidian nerve is highly variable within and between turtle clades, and several patterns can be identified, depending on



1698

1699

1700

1701

1702

1703

1704

1705

1706

1707

1708

1709

1710

1711

1712

1713

1714

1715

1716

1717

1718

1719

whether the vidian nerve extends through the canalis caroticus internus, canalis caroticus lateralis, and sulcus cavernosus, or a combination of those. Those turtles classified in patterns IC and IIC directly pass the vidian nerve from the geniculate ganglion into the canalis nervus vidianus. In all other turtles, the vidian nerve extends through parts of the canal system that also houses the carotid arterial system. In podocnemidids (pattern IIA), the vidian nerve enters the cavum pterygoidei and likely runs close to the internal carotid artery before entering the canalis nervus vidianus. However, as the interaction between the vidian nerve and the internal carotid artery occurs within the cavum pterygoidei and is not documented in the bony skeleton, we cannot determine with certainty what the pattern for the vidian nerve is. In chelonioids, the vidian nerve is interpreted to follow the course of the palatine artery within the carotid arterial system, as no distinct canalis nervus vidianus can be observed. In turtles showing pattern IB, the vidian nerve is passed directly into the palatine artery canal, from which it either directly enters the canalis nervus vidianus (the geoemydid Geoemyda spengleri), or first exits into the sulcus cavernosus before entering the canalis nervus vidianus (the emydid Glyptemys muhlenbergii). In turtles that exhibit patterns IA, IIA, or IIB, the vidian nerve always extends at least partially through the canalis caroticus internus. In these turtles the vidian nerve extends from the canalis caroticus internus to the canalis nervus vidianus via one of five pathways (Fig. 18): (1) the vidian nerve enters a separate canalis nervus vidianus that directly branches off the internal carotid canal (Pelomedusa subrufa, chelids except for Chelus fimbriatus; Carettochelys insculpta, Platysternon megacephalum, all testudinids but those with pattern IC, the trionychid Cycloderma frenatum, the kinosternid Staurotypus salvinii, the chelydrid Chelydra serpentina, and the geoemydids Malayemys subtrijuga, Pangshura tecta, and Rhinoclemmys melanosterna); (2) the vidian nerve parallels the internal carotid artery up to its split, and then follows the palatine



1721

1722

1723

1724

1725

1726

1727

1728

1729

1730

1731

1732

1733

1734

1735

1736

1737

1738

1739

1740

1741

artery into its canal, from which a separate canalis nervus vidianus diverges (the emydids *Graptemys geographica*, *Pseudemys floridana*, *Terrapene coahuila*, *Terrapene ornata*); (3) the vidian nerve also parallels the palatine artery, but exits the respective canal through the foramen anterius canalis carotici lateralis into the sulcus cavernosus, from which a separate canalis nervus vidianus emerges (all trionychids but Cycloderma frenatum, all kinosternids but Staurotypus salvinii, Dermatemys mawii, the emydids Clemmys guttata, Emydoidea blandingii, and Emys orbicularis, and the geoemydids Batagur baska, Cuora amboinensis, Geoclemys hamiltonii, and Siebenrockiella crassicollis); (4 & 5) the vidian nerve enters the canalis caroticus lateralis, but not via the arterial pathway, but instead via a 'shortcut' canal that connects the internal carotid and palatine artery canals. The vidian nerve then enters the canalis nervus vidianus that (4) either branches directly off the canalis caroticus lateralis (similar to 2; the emydid *Glyptemys* insculpta), or (5) emerges from the sulcus cavernosus after the vidian nerve has left the arterial canal via the foramen anterius canalis caroticus lateralis (similar to 3; the geoemydids *Mauremys* leprosa and Morenia ocellata). The differences between these five patterns are relatively subtle. and seem largely driven by the relative anteroposterior origin of the canalis nervus vidianus. This is possibly best exemplified by our examined specimen of the emydid *Deirochelys reticularia* (FMNH 98754), which exhibits an asymmetric pattern. On the left side of this specimen, the canalis nervus vidianus begins from the canalis caroticus internus (i.e. pattern 1), whereas the canal starts further anteriorly, from the canalis caroticus lateralis on the right side (i.e. pattern 2). Similarly, in a specimen of *Cyclemys dentata* (NHMUK 97.11.22.3), the exit of the canalis nervus vidianus is asymmetric, as it extends into the sulcus cavernosus on the left side, but connects to the canalis caroticus lateralis on the right side. Our patterns of the relative position of



the canalis nervus vidianus are not easily matched with the phylogenetic relationships of turtles, so that the observed variation between taxa does not seem to be systematic.

1744

1745

1746

1747

1748

1749

1750

1751

1752

1753

1754

1755

1756

1757

1758

1759

1760

1761

1762

1763

1764

1742

1743

Canal sizes

The carotid arterial system is the sole source of blood to the cranium and its subordinate arteries supply all major cranial regions. The majority of cranial tissues are supplied by branches of the internal carotid artery, but some parts are also supplied by the branches of the external carotid artery (e.g., Kardong, 1998). Generally, in reptiles, the anterior head region, including the orbit, is supplied by two branches of the common carotid artery; the stapedial artery and at least one major subordinate branch of the medially directed carotid branch that otherwise supplies the brain via the cerebral artery. The subordinate, facially-directed branch of the brain-supplying internal carotid branch is either the orbital artery, which branches off the cerebral artery from within the sella turcica, or the sphenopalatine artery, which branches off the cerebral/internal carotid before the latter enters the basisphenoid (e.g., Albrecht, 1967; Porter & Witmer, 2015; Porter, Sedlmayr & Witmer, 2016). The orbital and sphenopalatine arteries can co-exist (e.g., crocodiles; Sedlmayr, 2002; Porter & Witmer, 2015; most turtles: Albrecht, 1967), but one of these arteries usually dominates in terms of arterial size, and thus blood volume transmitted, so that only one 'medial' artery is of volumetric importance for the blood supply of the anterior skull region. The sphenopalatine artery of turtles is generally called the palatine artery, when present (e.g., Albrecht, 1967; Gaffney, 1979). The orbital artery is usually also present in turtles, albeit as a small artery (Albrecht, 1967). One exception are trionychids, in which the orbital artery (i.e., a branch of the cerebral artery that originates in the sella turcica) is exceptionally large and bifurcates anteriorly within the orbital cavity to supply the orbit (Albrecht, 1967).



1766

1767

1768

1769

1770

1771

1772

1773

1774

1775

1776

1777

1778

1779

1780

1781

1782

1783

1784

1785

1786

1787

Albrecht (1967) used the neologism 'pseudopalatine artery' for the orbital artery of trionychids, although the origination within the sella turcica and from the cerebral artery, as well as its direction toward the orbit are consistent with its identification as the orbital artery, an artery that Albrecht (1967) had also identified in other turtle groups. Thus, the major blood supply for the anterior skull region, including the orbit, is achieved by three different arteries in turtles: either by both the palatine artery and the stapedial artery (when both arteries are well developed, e.g., cheloniids: Albrecht, 1976), or predominantly by the stapedial artery (when the palatine artery is absent or small, e.g., *Chrysemys*: Albrecht, 1967), or predominantly by the palatine artery (when the stapedial artery is reduced or absent, e.g., Sternotherus: Albrecht, 1967), or predominantly by the orbital artery (when the palatine artery is absent and stapedial artery is reduced in size, e.g., trionychids: Albrecht, 1967). Although the origin of the arteries suppling the anterior skull region thus varies across turtles, the terminal patterning of these arteries, such as the development of supra- and infraorbital arteries, are largely consistent (see Albrecht, 1967). Variation as to which artery supplies specific organs is also documented for the mandible in turtles: whereas in non-turtle reptiles and many turtles, the mandibular artery originates as a branch of the stapedial artery (e.g., Albrecht, 1967, 1976; Gaffney, 1979; Porter & Witmer, 2015), the mandibular artery in some turtles may also branch from the palatine artery when the stapedial artery is reduced (e.g., Sternotherus: Albrecht, 1967) or the internal carotid artery when the stapedial and palatine arteries are reduced (e.g., trionychids: Albrecht, 1967). In turtles, both the palatine and stapedial arteries are variably reduced or entirely lost among different clades (e.g., Albrecht, 1967, 1976; Gaffney, 1979; this study). As the above examples show, these arterial reductions affect the blood supply by shifting the origin of arteries supplying the anterior skull region or the mandible to whichever artery is not reduced. Based on his



1789

1790

1791

1792

1793

1794

1795

1796

1797

1798

1799

1800

1801

1802

1803

1804

1805

1806

1807

1808

1809

1810

dissections of a few representatives of most turtle clades, Albrecht (1976) hypothesized that reductions in the size of the stapedial artery are counterbalanced by increases in size of the palatine or orbital arteries to ensure the arterial blood supply for the anterior region of the skull. Although relatively many studies related to the cranial arteries or canals are available, and although qualitative observations for various turtle clades seem to provide support for Albrecht's (1976) hypothesis (e.g., McDowell, 1961), only few publications explicitly compare or quantify canal sizes for a large number of species (e.g., Jamniczky & Russell, 2007). Here, we digitally measured the cross-sectional area of the canalis caroticus internus, the canalis caroticus lateralis, the canalis caroticus basisphenoidalis, and the canalis stapedio-temporalis in our CT-scans (see Methods for further details). These measurements, summarized in Table 2, provide approximate estimates of blood flow, as arterial canal diameter is proportional to arterial size in turtles (Albrecht, 1976, Jamniczky & Russell, 2004). Our PGLS analysis finds strong evidence of a correlation between internal carotid artery size and stapedial artery size (Table 3). Variation in cross-sectional area of the stapedial artery canal explains a large portion of variance in the cross-sectional area of the internal carotid artery canal $(R^2 = 0.73)$. The regression line has an intercept of 1.097 and a slope of 0.776 (Fig. 19 A; Table 3). The relationship between cross-sectional areas of stapedial and internal carotid arteries underwent evolutionary change on the tree, as the phylogenetic signal of this relationship as estimated during the fitting of the regression model is high (lambda = 0.96). Residual internal carotid artery size is consistently larger than zero in three clades, which are trionychians, kinosternoids, and chelonioids (Fig. 19 C). These clades have larger internal carotid cross-sectional diameters than expected by the regression, although this effect is much smaller in chelonioids than in trionychids and kinosternoids, which are visually separated from the



1812

1813

1814

1815

1816

1817

1818

1819

1820

1821

1822

1823

1824

1825

1826

1827

1828

1829

1830

1831

1832

1833

remaining data (Fig. 19 A), but seem to follow a trend parallel to the remaining data. To test if our data can be better explained by a model with different intercepts or slopes or both for the visually separated groups, we performed generalized least-squares phylogenetic analysis of covariance (pANCOVA) using the gls.ancova function of the package evomap (Smaers & Rohlf, 2016; Smaers & Mongle, 2018). We defined a group with consistently positive residuals (i.e. chelonioids, kinosternoids, trionychians) and another with the remaining taxa for which models could be compared. Results of the pANCOVA show that a model with varying intercepts is significantly supported over a single intercept-single slope model (F value = 14.53, p < 0.0003), and that this model is favored over a model with varying slopes and intercept (F = 3.53, p =0.06). These results demonstrate that kinosternoids, chelonioids, and trionychians follow a regression line with an elevated intercept in comparison to other turtles (Fig. 19 B; Table 3). These taxa have larger internal carotid cross-sectional areas than other turtles (as the intercept is elevated), but show the same proportional size increase with increasing stapedial artery size than other turtles (as regression slopes are near identical). These observations quantitatively confirm previous hypotheses, as particularly trionychids and kinosternoids are known for their small stapedial artery canals. However, and somewhat unexpectedly, the same is also true for some taxa with relatively large stapedial arteries, such as carettochelyids or chelonioids, indicating that these taxa have a higher 'medial' blood flow than expected based on their stapedial artery sizes, which are relatively large to begin with. Much of the variation we observe can be attributes to the placement of the mandibular artery, which draws blood from the carotid system, but does not feed the anterior skull region. In trionychids and kinosternoids, the mandibular artery is fed from the lateral branch of the internal carotid artery (Albrecht, 1967, 1976). It is therefore not surprising, that the diameter of the internal carotid artery is larger than expected. The high



1835

1836

1837

1838

1839

1840

1841

1842

1843

1844

1845

1846

1847

1848

residuals found in Carettochelys insculpta, however, cannot be explained by this model, as our observations indicate that the mandible of this taxon is fed by the stapedial artery prior to its passage through the stapedial canal. In chelonioids, the mandible is partially fed from the stapedial artery, but prior to its passing through the stapedial canal, and by the lateral branch of the internal carotid artery (Albrecht, 1976). The internal carotid artery is therefore enlarged again, but not to the extent as seen in trionychids and kinosternids. The opposite situation is seen in chelids, where the mandible is completely fed by the stapedial artery after its passage through the stapedial canal (Albrecht, 1976). The stapedial canal is therefore disproportionally enlarged. A similar enlargement, however, is not apparent for the remaining pleurodires, even though mandibles are fully (Pelomedusidae) or partially (Podocnemididae) fed by the stapedial following is passage through the stapedial canal (Albrecht, 1976). In all remaining turtles, the mandible is fed from the stapedial artery, but prior to its passage through the stapedial canal (Albrecht, 1967 1976). In summary, our canal size data quantitatively confirm that variation in the stapedial artery size is countered by oppositional variation in the internal carotid size and that variation from the mean can partially be explained by the placement of the mandibular artery.

1849

1850

1851

1852

1853

1854

1855

1856

Evolution of the internal carotid arterial system of turtles

Plesiomorphically, the split of the internal carotid artery into its cerebral and palatal branches occurs extracranially (i.e. not embedded in bone), with the palatine branch extending anteriorly through the interpterygoid vacuity, and the cerebral artery extending through the basisphenoid. This condition is known in basal taxa such as *Proganochelys quenstedtii* and *Kayentachelys aprix* (Gaffney, 1990; Sterli & Joyce, 2007; Gaffney & Jenkins, 2010). The plesiomorphic presence of the palatine artery, which leaves no direct osteological correlate in these turtles, is



1858

1859

1860

1861

1862

1863

1864

1865

1866

1867

1868

1869

1870

1871

1872

1873

1874

1875

1876

1877

1878

1879

inferred based on outgroup comparisons (Müller, Sterli & Anguetin, 2011), and the presence of palatine artery canals in slightly derived stem turtles with closed interpterygoid openings. Examples of those are Kallokibotion bajazidi (Gaffney & Meylan, 1992) and Mongolochelys efremovi (Sterli et al., 2010), in which the split of the internal carotid artery into its cerebral and palatal branches still occurs extracranially, but with the closure of the interpterygoid vacuity, a distinct canalis caroticus lateralis is present. As all extant turtles have the internal carotid artery embedded in bone posterior to its split, this condition could be symplesiomorphic for crowngroup turtles, and may possibly have evolved somewhere on the stem-lineage of turtles. Examination of fossil representatives of the stem-lineages for the major turtle subclades will provide important clues as to whether the complete embedding of the carotid system in bone is indeed ancestral for the crown-group. The evolutionary reconstruction of the carotid embedding is also hindered by varying phylogenetic hypotheses regarding the position of several turtle clades as stem or crown-group turtles, including paracryptodires, thalassochelydians, xinjiangchelyids, and sinemydids/macrobaenids (e.g., Joyce, 2007; Sterli, 2010; Anquetin, 2012; Zhou & Rabi, 2015; Cadena & Parham, 2015; Joyce et al., 2016; Evers & Benson, 2019). Partial embedding of the internal carotid artery is observed in macrobaenids/sinemydids such as Dracochelys bicuspis (Gaffney & Ye, 1992), xinjiangchelyids like Xinjiangchelys wusu (Rabi et al., 2013), or thalassochelydians like *Plesiochelys etalloni* (NMS 40870). These turtles all share that the posterior part of the internal carotid is embedded in bone, but the anterior part around the area of the split into palatine and cerebral arteries is exposed in a fenestra caroticus (Rabi et al., 2013). If these turtles are evolutionary intermediates between basal stem-turtles and crown-group turtles with completely embedded carotids, as indicated by some phylogenetic analyses (e.g., Evers & Benson, 2018), their morphology indicates that the encasing of the carotid artery





1881

1882

1883

1884

1885

1886

1887

1888

1889

1890

1891

1892

1893

1894

1895

1896

1897

1898

1899

1900

1901

1902

followed a 'posterior-section-first'-pattern. The converse pattern is observed among some paracryptodires: In the baenid Eubaena cephalica, a short anterior section of the internal carotid artery prior to its entry into the basisphenoid (upon which it becomes the cerebral artery), is embedded by bone (Rollot, Lyson & Joyce, 2018), whereas the palatine artery is absent. This could provide evidence for an 'anterior-section-first' embedding of the internal carotid artery. However, it is questionable if the baenid condition is truly informative about the evolution of crown-group turtles. Baenids are most frequently inferred to be deeply nested within Paracryptodira (e.g., Lyson & Joyce, 2011), but pleurosternids and some of the earliest paracryptodires, such as *Uluops uluops*, have carotid patterns quite distinct from those of baenids (e.g., Anguetin & André, 2020; Evers, Rollot & Joyce, in review). In *Uluops uluops*, the carotid split seems to be exposed (pers. obs. UCM 53971), indicating that no foramen posterius canalis carotici interni is present. The same condition has been reported for *Dorsetochelys typocardium* (Anguetin & André, 2020). In pleurosternids, the far-anteriorly positioned foramen posterius canalis carotici interni has likely been misidentified, and the visible foramen in the suture of the basisphenoid and pterygoid is for the cerebral artery instead, whereas the palatine artery is likely lost (pers. obs. UMZC T1041: Pleurosternon bullockii; Evers, Rollot & Joyce, in review). Thus, *Uluops* and pleurosternids possibly have entirely uncovered internal carotid arteries and therefore the plesiomorphic condition of Testudinata. Depending on paracryptodiran in-group relationships, the loss of the palatine branch of the internal carotid artery has occurred independently at least one time within paracryptodires (Rollot, Lyson & Joyce, 2018), and several times both within extant lineages. The use of CT data will probably yield new results about the cranial morphology and circulation system of turtles. Particularly important will be the inclusion of fossil taxa belonging



to stem lineages of extant clades of Testudines, as those will provide new insights into the evolution of the carotid circulation system of turtles.

1905

1906

1907

1908

1909

1910

1911

1912

1913

1914

1915

1916

1917

1918

1919

1920

1921

1922

1923

1924

1925

1903

1904

CONCLUSIONS

We here describe the carotid circulation and facial nerve systems of all major extant clades of turtles based on micro-CT scans of 69 specimens representing 66 species. Our main results include reinterpretations of the carotid arterial canal system and the facial nerve system and show that some canals pertaining to the facial nerve system have been misinterpreted in the past as carotid canals. Our observations warrant slight nomenclatural updates to previous canal definitions, which facilitate the precise description of the observed disparity. We demonstrate that the complete loss of the palatine artery and the respective canalis caroticus lateralis is more widespread among turtles than previously recognized, and happened independently in pleurodires, carettochelyids, platysternids, testudinids, and some geoemydids. Quantitative canal size data shows that variation of stapedial vs. non-stapedial carotid canal size can largely be attributed to differences in mandible artery course. We review these differences across turtle groups, and add novel observation regarding osteological correlates for the mandibular artery, which help to distinguish mandibular blood supply patterns in cryptodires even in the absence of direct arterial observation. Our data furthermore shows unexpected variation with regard to the canal system for the facial nerve, particularly with respect to the position of the geniculate ganglion, as well as the course of the subordinate facial nerve branches, the vidian and hyomandibular nerves through their specific canals. These data show that previously hypothesized distinctions in the facial nerve system of pleurodires and cryptodires cannot be upheld. The carotid artery and facial nerve systems appear to vary independently from each





other, although the facial nerve and carotid systems in part share the same canals. The carotid circulation and facial nerve systems have been used as a source of phylogenetic characters in many studies, but our observations provide the basis for the revision of previously phrased characters and the conception of new phylogenetic characters. Important future tasks include the integration of fossil data both from stem-lineages of extant groups to facilitate understanding of the evolution of modern diversity regarding these systems, as well from stem-turtles to understand the evolution of the derived arterial embedding found in turtles.

ACKNOWLEDGEMENTS

We would like to acknowledge the curators and staff of museums that provided us access to specimens used in this study, particularly Loïc Costeur (NMB), Alan Resatar (FMNH), Patrick Campbell (NHMUK), Linda Mogk (SMF), Alexander Kupfer (SMNS), and Jason Head (UMZC). We thank research and technical staff and PIs at the CT scanning facilities we used for this research, namely Tom Davies and Ben Moon (University of Bristol), Farah Ahmed (NHMUK), Zhe-Xi Luo and April Isch Neander (University of Chicago), and Ingmar Werneburg (University of Tübingen). We also extend our gratitude to the contributors and curators of MorphoSource.

REFERENCES

Albrecht PW. 1967. The cranial arteries and cranial arterial foramina of the turtle genera *Chrysemys*, *Sternotherus* and *Trionyx*: a comparative study of analysis with possible evolutionary implications. *Tulane Studies in Zoology* **14:**81–99.



Albrecht PW. 1976. The cranial arteries of turtles and their evolutionary significance. <i>Journal of</i>
Morphology 149: 159–182.
Anquetin J, André C. 2020. The last surviving Thalassochelydia—a new turtle cranium from
the Early Cretaceous of the Purbeck Group (Dorset, UK). PaleorXiv.
doi:10.31233/osf.io/7pa5c.
Anquetin J. 2012. Reassessment of the phylogenetic interrelationships of basal turtles
(Testudinata). Journal of Systematic Palaeontology 10:3–45.
Bardet N, Jalil N-E, Lapparent de Broin F de, Germain D, Lambert O, Amaghzaz M. 2013
A giant chelonioid turtle from the Late Cretaceous of Morocco with a suction feeding
apparatus unique among tetrapods. PLoS ONE 8:1-10.
Bender O. 1906. Die Schleimhautnerven des Facialis, Glassopharyngeus und Vagus. Jenaische
Denkschriften 7:343–454.
Benoit J, Manger PR, Rubidge BS. 2016. Palaeoneurological clues to the evolution of defining
mammalian soft tissue traits. Scientific Reports 6:25604.
Benoit J, Angielczky KD, Miyamae JA, Manger P, Fernandez V, Rubridge B. 2018.
Evolution of facial innervation in anomodont therapsids (Synapsida): Insights from X-ray
computerized microtomography. Journal of Morphology 279:673-701.
Bojanus LH. 1819-1821. Anatome testudinis europaeae. Vilna: Joseph Sawadzki.
Brinkman DB, Peng JH. 1993. New material of Sinemys (Testudines, Sinemydidae) from the
early cretaceous of China. Canadian Journal of Earth Sciences 30:2139-2152.
Brinkman DB, Peng JH. 1996. A new species of Zangerlia (Testudines: Nanhsiungchelyidae)
from the Upper Cretaceous redbeds and Bayan Mandahu, Inner Mongolia, and the
relationships of the genus. Canadian Journal of Earth Sciences 33:526-540.



1971	Cadena E, Parham JF. 2015. Oldest known marine turtle? A new protostegid from the Lower
1972	Cretaceous of Colombia. PaleoBios 32:1–421.
1973	Crumly CR. 1982. A cladistic analysis of Geochelone using cranial osteology. Journal of
1974	Herpetology 16: 215–234.
1975	Crumly CR. 1994. Phylogenetic systematics of North American tortoises (Genus Gopherus):
1976	Evidence for their classification. Fish and Wildlife Research 13:7–32.
1977	Dehnhardt G, Mauck B. 2008. Mechanoreception in secondarily aquatic vertebrates. In:
1978	Thewissen JGM, Nummela S, eds. Sensory evolution on the threshold: adaptations in
1979	secondarily aquatic vertebrates. Berkeley: University of California Press, 295–314.
1980	Evans SE. 1987. The braincase of Youngina capensis (Reptilia: Diapsida; Permian). Neues
1981	Jahrbuch für Geologie und Paläontologie-Monatshefte 4:193–203.
1982	Evers SW. 2019. CT scans of extant turtle skulls. MorphoSource. Available at https://www.mor
1983	phosource.org/Detail/ProjectDetail/Show/project_id/769.
1984	Evers SW, Barrett PM, Benson RBJ. 2019. Anatomy of Rhinochelys pulchriceps
1985	(Protostegidae) and marine adaptation during the early evolution of chelonioids. PeerJ
1986	7: e6811
1987	Evers SW, Benson RBJ. 2018. Project: Evers & Benson 2018, Turtle CT data and 3D models.
1988	MorphoSource. Available at
1989	http://www.morphosource.org/Detail/ProjectDetail/Show/project_id/462.
1990	Evers SW, Benson RBJ. 2019. A new phylogenetic hypothesis of turtles with implications for
1991	the number of evolutionary transitions to marine lifestyles supports an Early Cretaceous
1992	origin and rapid diversification of Chelonioidea. Palaeontology 62:93-134.



1993	Evers S, Joyce WG. 2020. A re-descripton of Sandownia harrisi (Testudinata: Sandownidae)
1994	from the Aptian of the Isle of Wight based on computed tomography scans. Royal Society
1995	Open Science 7:191936.
1996	Evers S, Rollot Y, Joyce WG. in review. Cranial osteology of the Early Cretaceous turtle
1997	Pleurosternon bullockii (Paracryptodira: Pleurosternidae).
1998	Felsenstein J. 1985. Phylogenies and the Comparative Method. <i>American Naturalist</i> 125: 1–15.
1999	Fuchs H. 1931. Ueber den Unterkiefer und die Unterkiefernerven (Ramus tertius nervi trigemini
2000	et Chorda tympani) der Arrauschildkröte (Podocnemis expansa), nebst Bemerkungen zur
2001	Kiefergelenksfrage. Zeitschrift für Anatomie und Entwicklungsgeschichte 94:206–274.
2002	Gaffney ES. 1972. An illustrated glossary of turtle skull nomenclature. American Museum
2003	Novitates 2486: 1–33.
2004	Gaffney ES. 1975. A phylogeny and classification of the higher categories of turtles. <i>Bulletin of</i>
2005	the American Museum of Natural History 155:387–436.
2006	Gaffney ES. 1976. Cranial morphology of the European Jurassic turtles <i>Portlandemys</i> and
2007	Plesiochelys. Bulletin of the American Museum of Natural History 157:487–544.
2008	Gaffney ES. 1979. Comparative cranial morphology of recent and fossil turtles. Bulletin of the
2009	American Museum of Natural History 164:69–376.
2010	Gaffney ES. 1983. The cranial morphology of the extinct horned turtle <i>Meiolania platyceps</i> ,
2011	from the Pleistocene of Lord Howe Island, Australia. Bulletin of the American Museum of
2012	Natural History 175: 361–480.
2013	Gaffney ES. 1990. The comparative osteology of the Triassic turtle <i>Proganochelys</i> . Bulletin of
2014	the American Museum of Natural History 194: 1–176.



2015	Gaffney ES. 1996. The postcranial morphology of <i>Meiolania platyceps</i> and a review of the
2016	Meiolaniidae. Bulletin of the American Museum of Natural History 229:1–166.
2017	Gaffney ES, Jenkins FA. 2010. The cranial morphology of Kayentachelys, an Early Jurassic
2018	cryptodire, and the early history of turtles. Acta Zool-Stockholm 91:335–368.
2019	Gaffney ES, Meylan PA. 1988. A phylogeny of turtles. In: Benton MJ, ed. The phylogeny and
2020	classification of the tetrapods, volume 1: amphibians, reptiles, birds. Oxford: Clarendon
2021	Press, 157–219.
2022	Gaffney ES, Meylan PA. 1992. The Transylvanian turtle Kallokibotion, a primitive cryptodire
2023	of cretaceous age. American Museum Novitates 3040:1-37.
2024	Gaffney ES, Meylan PA & Wyss AR. 1991. A computer assisted analysis of the relationships
2025	of the higher categories of turtles. Cladistics 7:313-335.
2026	Gaffney ES, Rich TH, Vickers-Rich P, Constantine A, Vacca R, Kool L. 2007. Chubutemys,
2027	a new eucryptodiran turtle from the early cretaceous of Argentina, and the relationships of
2028	Meiolaniidae. American Museum Novitates 3599:1-35.
2029	Gaffney ES, Tong H, Meylan PA. 2006. Evolution of the side-necked turtles: the families
2030	Bothremydidae, Euraxemydidae, and Araripemydidae. Bulletin of the American Museum of
2031	Natural History 300: 1–698.
2032	Gaffney ES, Ye X. 1992. Dracochelys, a new cryptodiran turtle from the early cretaceous of
2033	China. American Museum Novitates 3048:1–13.
2034	Garbin RC, Ascarrunz E, Joyce WG. 2018. Polymorphic characters in the reconstruction of
2035	the phylogeny of geoemydid turtles. Zoological Journal of the Linnean Society 184:896-918.
2036	Gaupp E. 1888. Anatomische Untersuchungen über die Nervenversorgung der Mund- und
2037	Nasenhöhlendrüsen der Wirbeltiere. Morphologisches Jahrbuch 14:436–489.



2038	George ID, Holliday CM. 2013. Trigeminal nerve morphology in Alligator mississippiensis and
2039	its significance for crocodyliform facial sensation and evolution. Anatomical Record
2040	296: 670–680.
2041	Grafen A. 1989. The phylogenetic regression. Philosophical Transactions of the Royal Society of
2042	London B: Biological Sciences 326: 119–157.
2043	Hanson FB. 1919. The anterior cranial nerves of Chelydra serpentina. Washington University
2044	Studies, Science Series 7:13–41.
2045	Haughton SH. 1929. Notes on some pareiasaurian brain-cases. Annals of the South African
2046	Museum 28: 88–96.
2047	Hermanson G, Iori FV, Evers SW, Langer MC, Ferreira GS. 2020. A small podocnemidoid
2048	(Pleurodira, Pelomedusoides) from the Late Cretaceous of Brazil, and the innervation and
2049	carotid circulation of side-necked turtles. Papers in Paleontology 6:329-347
2050	Hirayama R. 1998. Oldest known sea turtle. Nature 392:705–708.
2051	Hoffmann CK. 1890. Reptilien. I. Schildkröten. In: Bronn HG, ed. Klassen und Ordnungen des
2052	Thier-Reichs, Vol. 6. Leipzig: C. F. Winter'sche Verlagshandlung, 1–442.
2053	Hooks GE. 1998. Systematic revision of the Protostegidae, with a redescription of Calcarichelys
2054	gemma Zangerl, 1953. Journal of Vertebrate Paleontology 18:85–98
2055	Ives AR. 2018. R2s for correlated data: phylogenetic models, LMMs, and GLMMs. Systematic
2056	Biology 68: 234–251.
2057	HA Jamniczky, AP Russell. 2004. Cranial arterial foramen diameter in turtles: a quantitative
2058	assessment of size-independent phylogenetic signal Animal Riology 54:417–436



HA Jamniczky, AP Russell. 2007. Reappraisal of patterns of nonmarine cryptodiran turtle 2059 carotid circulation: evidence from osteological correlates and soft tissues. Journal of 2060 Morphology 268:571-587. 2061 **Jamniczky HA. 2008.** Turtle carotid circulation: a character analysis case study. *Biological* 2062 Journal of the Linnean Society 93:239–256. 2063 **Joyce WG. 2007.** Phylogenetic relationships of Mesozoic turtles. *Bulletin of the Peabody* 2064 Museum of Natural History **48:**3–102. 2065 Joyce WG, Rabi M, Clark JM, Xu X. 2016. A toothed turtle from the Late Jurassic of China 2066 2067 and the global biogeographic history of turtles. BMC Evolutionary Biology 16:236. Joyce WG, Volpato VS, Rollot Y. 2018. The skull of the carettochelyid turtle Anosteira pulchra 2068 from the Eocene (Uintan) of Wyoming and the carotid canal system of carettochelyid turtles. 2069 2070 Fossil Record **21:**301–310. **Kenneth V. 1998.** Vertebrates: Comparative Anatomy, Function, Evolution. 2nd Edition. 2071 Boston, Massachusetts, McGraw-Hill. 2072 **Kear BP**, Lee MSY. 2006. A primitive protostegid from Australia and early sea turtle evolution. 2073 *Biology Letters* **2:**116–119. 2074 **Kesteven HL. 1910.** The anatomy of the head of the green turtle *Chelone midas*, Latr. Part I. 2075 The skull. *Journal and Proceedings of the Royal Society of New South Wales* **44:**368–400. 2076 Lapparent de Broin F de, Werner C. 1998. New late Cretaceous turtles from the Western 2077 2078 Desert, Egypt. Annales de Paléontologie 84:131–214. Lapparent de Broin F de, de la Fuente MS, Fernandez MS. 2007. Notoemys laticentralis 2079 (Chelonii, Pleurodira), Late Jurassic of Argentina: new examination of the anatomical 2080

structures and comparisons. Revue de Paléobiologie 26:99–136.

2081



2082	Lautenschiager 5, Ferreira G5, Werneburg 1. 2016. Sensory evolution and ecology of early
2083	turtles revealed by digital endocranial reconstructions. Frontiers in Ecology and Evolution
2084	6: 7.
2085	Lawson R. 1970. The caecilian cardio-vascular system and intra-amphibian relationships.
2086	Journal of Zoology 160:199–229.
2087	Lipka TR, Therrien F, Weishampel DB, Jamniczky HA, Joyce WG, Colbert MW,
2088	Brinkman DB. 2006. A new turtle from the Arundel Clays (Potomac Formation, Early
2089	Cretaceous) of Maryland, U.S.A. Journal of Vertebrate Paleontology 26:300–307.
2090	Lyson TR, Joyce WG. 2011. Cranial anatomy and phylogenetic placement of the enigmatic
2091	turtle Compsemys victa. Journal of Paleontology 85:789–801.
2092	McDowell SB. 1961. On the major arterial canals in the ear region of testudinoid turtles and the
2093	classification of the Testudinoidea. Bulletin of the Museum of Comparative Zoology 125:23-
2094	39.
2095	Meylan PA. 1987. The phylogenetic relationships of soft-shelled turtles (family Trionychidae).
2096	Bulletin of the American Museum of Natural History 186:1–110.
2097	Meylan PA, Gaffney ES. 1989. The skeletal morphology of the Cretaceous cryptodiran turtle,
2098	Adocus, and the relationships of the Trionychoidea. American Museum Novitates 2941:1-60
2099	Motani R, Schmitz L. 2011. Phylogenetic functional signals in the evolution of form-function
2100	relationships in terrestrial vision. Evolution 65:2245–2257.
2101	Muchlinski MN. 2008. The relationship between the infraorbital foramen, infraorbital nerve,
2102	and maxillary mechanoreception: implications for interpreting the paleoecology of fossil
2103	mammals based on infraorbital foramen size. <i>Anatomical Record</i> 291: 1221–1226.

Müller J, Sterli J, Anguetin J. 2011. Carotid circulation in amniotes and its implications for 2104 turtle relationships. Neues Jahrbuch für Geologie und Paläontologie, Abhandlungen 2105 **261:**289–297. 2106 Nagelkerke NJD. 1991. A note on a general definition of the coefficient of determination. 2107 Biometrika 78:691-692. 2108 2109 Nick L. 1912. Das Kopfskelet von Dermochelys coriacea L. Zoologische Jahrbücher, Abteilung für Anatomie und Ontogenie der Tiere 33:431–552. 2110 Noack T. 1906. Über die Entwicklung des Mittelohres von Emys europaea nebst Bemerkungen 2111 2112 zur Neurologie dieser Schildkröte. Archiv für Mikroskopische Anatomie 69:457–490. O'Keefe R. 2001. A cladistic analysis and taxonomic revision of the Plesiosauria (Reptilia: 2113 Sauropterygia). *Acta Zoologica Fennica* **213:**1–63. 2114 Ogushi K. 1911. Anatomische Studien an der japanischen dreikralligen Lippenschildkröte 2115 (Trionyx japanicus). I. Mitteilung. Morphologisches Jahrbuch 43:1–106 2116 Ogushi K. 1913a. Anatomische Studien an der japanischen dreikralligen Lippenschildkröte 2117 (Trionyx japanicus). II. Mitteilung: Muskel- und peripheres Nervensystem. Morphologisches 2118 *Jahrbuch* **46:**299–562 2119 **Ogushi K. 1913b.** Zur Anatomie der Hirnnerven und des Kopfsympathicus von *Trionyx* 2120 japonicus nebst einigen kritischen Bemerkungen. Morphologisches Jahrbuch 45:441–480 2121 2122 **Pagel MD. 1997.** Inferring evolutionary processes from phylogenies. *Zoologica Scripta* **26:**331– 2123 348. **Pagel MD. 1999.** Inferring the historical patterns of biological evolution. *Nature* **401:**877–884. 2124 Paradis E, Schliep K. 2018. ape 5.0: an environment for modern phylogenetics and 2125 2126 evolutionary analyses in R. Bioinformatics 35:526-528.



212/	Pardo JD, Anderson JS. 2016. Cranial morphology of the Carboniferous-Permian tetrapod
2128	Brachydectes newberryi (Lepospondyli, Lysorophia): new data from μCT. PLoS ONE
2129	11: e0161823.
2130	Paulina-Carabajal A, Sterli J, Georgi J, Poropat SF, Kear BP. 2017. Comparative
2131	neuroanatomy of extinct horned turtles (Meiolaniidae) and extant terrestrial turtles
2132	(Testudinidae), with comments on the palaeobiological implications of selected endocranial
2133	features. Zoological Journal of the Linnean Society 180:930-950.
2134	Pereira AG, Sterli J, Moreira FRR, Schrago CG. 2017. Multilocus phylogeny and statistical
2135	biogeography clarify the evolutionary history of major lineages of turtles. Molecular
2136	Phylogenetics and Evolution 113:59–66
2137	Porter WR, Witmer LM. 2015. Vascular patterns in iguanas and other squamates: blood
2138	vessels and sites of thermal exchange. PLoS ONE 10:e0139215.
2139	Porter WR, Sedlmayr JC, Witmer LM. 2016. Vascular patterns in the heads of crocodilians:
2140	blood vessels and sites of thermal exchange. Journal of Anatomy 229:800-824.
2141	Rabi M, Zhou C-F, Wings O, Ge S, Joyce WG. 2013. A new xinjiangchelyid turtle from the
2142	Middle Jurassic of Xinjiang, China and the evolution of the basipterygoid process in
2143	Mesozoic turtles. BMC Evolutionary Biology 13:203
2144	Revell LJ. 2010. Phylogenetic signal and linear regression on species data. Methods in Ecology
2145	and Evolution 1: 319–329.
2146	Rohlf FJ. 2001. Comparative methods for the analysis of continuous variables: geometric
2147	interpretations. Evolution 55: 2143–2160.



- 2148 Rollot Y, Lyson TR, Joyce WG. 2018. A description of the skull of Eubaena cephalica (Hay,
- 2149 1904) and new insights into the cranial circulation and innervation of baenid turtles. *Journal*
- of Vertebrate Paleontology e1474886.
- 2151 **Ruge G. 1987.** Über das peripherische Gebiet des Nervus facialis bei Wirbeltieren. In:
- Festschrift zum 70. Geburtstag von C. Gegenbaur. Bd. 3. Leipzig: W. Engelmann, 193–348.
- 2153 **Schumacher G-H. 1973.** Die Kopf- und Halsregion der Lederschildkröte Der*mochelys coriacea*
- 2154 (Linnaeus 1766). Abhandlungen der Akademie der Wissenschaften der DDR 2:1–60.
- 2155 **SedImayr JC. 2002.** Anatomy, evolution, and functional significance of cephalic vasculature in
- 2156 Archosauria. PhD Thesis, Ohio University.
- 2157 Shaffer HB, Meylan P, McKnight ML, Larson A. 1997. Tests of turtle phylogeny: molecular,
- 2158 morphological, and paleontological approaches. *Systematic Biology* **46:**235–268.
- 2159 Shiino K. 1913. Beitrag zur Kenntnis der Gehimnerven der Schildkroten. Anatomische Hefte
- **47:**1–34.
- 2161 **Shindo T. 1914.** Zur vergleichenden Anatomie der arteriellen Kopfgefässe der Reptilien.
- 2162 *Anatomische Hefte* **51:**267–356.
- 2163 Shishkin MA. 1968. On the cranial arterial system of the labyrinthodonts. Acta Zoologica 49:1–
- 2164 22.
- 2165 Siebenrock F. 1897. Das Kopfskelet der Schildkröten. Sitzungsberichte der Kaiserlichen
- 2166 Akademie der Wissenschaften 106:245–328.
- 2167 Smaers JB, Mongle CS. 2018. Evomap: R package for the evolutionary mapping of continuous
- 2168 traits. San Francisco: Github.
- 2169 Smaers JB, Rohlf FJ. 2016. Testing species' deviation from allometric predictions using the
- phylogenetic regression. *Evolution* **70:**1145–1149.



2171	Soliman MA. 1964. Die Kopfnerven der Schildkröten. Zeitschrift für Wissenschaftliche
2172	Zoologie 169: 216–312.
2173	Starck D. 1979. Cranio-cerebral relations in recent reptiles. Biology of the Reptilia 9:1-38.
2174	Sterli J, de la Fuente MS. 2010. Anatomy of Condorchelys antiqua Sterli, 2008, and the origin
2175	of the modern jaw closure mechanism in turtles. Journal of Vertebrate Paleontology 30:351-
2176	366.
2177	Sterli J, Joyce WG. 2007. The cranial anatomy of the Early Jurassic turtle Kayentachelys aprix.
2178	Acta Palaeontologica Polonica 52: 675–694.
2179	Sterli J, de la Fuente MS. 2013. New evidence from the Palaeocene of Patagonia (Argentina)
2180	on the evolution and palaeo-biogeography of Meiolaniformes (Testudinata, new taxon name).
2181	Journal of Systematic Palaeontology 11:835–852.
2182	Sterli J, Müller J, Anquetin J, Hilger A. 2010. The parabasisphenoid complex in Mesozoic
2183	turtles and the evolution of the testudinate basicranium. Canadian Journal of Earth Sciences
2184	47: 1337–1346.
2185	Sukhanov VB. 2000. Mesozoic turtles of Middle and Central Asia. In: Benton MJ, Shishkin
2186	MA, Unwin DM, Kurochkin EN, eds. The age of dinosaurs in Russia and Mongolia.
2187	Cambridge: Cambridge University Press, 309–367.
2188	Symonds MRE, Blomberg SP. 2014. A primer on phylogenetic generalised least squares. A
2189	primer on phylogenetic generalised least squares. In: Garamszegi L, eds. Modern
2190	phylogenetic comparative methods and their application in evolutionary biology. Berlin,
2191	Heidelberg: Springer, 105–130.
2192	van der Merwe NJ. 1940. Die Skedelmorfologie van Pelomedusa galeata (Wagler). Tydskrif vir
2193	Wetenskap en Kuns 1: 67–85.



2194	Vogt, C. 1840. Beiträge zur Neurologie der Reptilien. Neue Denkschrift der Allgemeinen
2195	Schweitzerischen Gesellschaft für die gesammten Naturwissenschaften 4:40–55.
2196	Yu E, Ashwell KWS, Shulruf B. 2019 (preprint). Quantitative analysis of arterial supply to the
2197	developing brain in tetrapod vertebrates. Anatomical Record.
2198	Zangerl R. 1953. The vertebrate fauna of the Selma Formation of Alabama. Part IV. The turtles
2199	of the family Toxochelyidae. Fieldiana: Geology Memoirs 3:135–277.
2200	Zhou C-F, Rabi M. 2015. A sinemydid turtle from the Jehol Biota provides insights into the
2201	basal divergence of crown turtles. Scientific Reports 5:16299.
2202	
2203	Figure 1. The carotid circulation and vidian canal system of <i>Chelus fimbriatus</i> (NHMUK
2204	81.9.27.4). Three-dimensional reconstructions of the basisphenoid, right pterygoid, in (A) dorsal,
2205	(B) ventral, and (C) left lateral view. Illustration in dorsal view (D) highlighting the placement of
2206	relevant arteries, nerves, and veins. Dark colors highlight sections fully covered by bone, light
2207	colors partially or fully uncovered sections. Abbreviations: ac = arteria carotis cerebralis; aci =
2208	arteria carotis interna; bs = basisphenoid; 'cc' = secondary canalis cavernosus; ccb = canalis
2209	caroticus basisphenoidalis;; cci = canalis caroticus internus; ccv = canalis cavernosus; cnf =
2210	canalis nervus facialis; cnhp = canalis nervus hyomandibularis proximalis; cnv = canalis nervus
2211	vidianus; faceb = foramen anterius canalis carotici basisphenoidalis; facnv = foramen anterius
2212	canalis nervi vidiani; fpcci = foramen posterius canalis carotici interni; gg = geniculate ganglion;
2213	$pt = pterygoid$; $vcl = vena capitis lateralis$; $VII = nervus facialis$; $VII_{hy} = nervus hyomandibularis$;
2214	VII _{vi} = nervus vidiani.
2215	



Figure 2. The carotid circulation and vidian canal system of <i>Peltocephalus dumerilianus</i>
(NHMUK 60.4.16.9). Three-dimensional reconstructions of the basisphenoid, right pterygoid, in
(A) dorsal, (B) ventral, and (C) left lateral view. Illustration in dorsal view (D) highlighting the
placement of relevant arteries, nerves, and veins. Abbreviations: ac = arteria carotis cerebralis;
aci = arteria carotis interna; bs = basisphenoid; ccb = canalis caroticus basisphenoidalis; ccv =
canalis cavernosus; cnf = canalis nervus facialis; cnhd = canalis nervus hyomandibularis distalis;
cnhp = canalis nervus hyomandibularis proximalis; cnv = canalis nervus vidianus; cprnv =
canalis pro ramo nervi vidiani; faceb = foramen anterius canalis carotici basisphenoidalis; facnv
= foramen anterius canalis nervi vidiani; gg = geniculate ganglion; pt = pterygoid; vcl = vena
capitis lateralis; VII = nervus facialis; VII $_{hy}$ = nervus hyomandibularis; VII $_{vi}$ = nervus vidiani.
Figure 3. The carotid circulation and vidian canal system of <i>Pelusios subniger</i> (NMB
16230). Three-dimensional reconstructions of the basisphenoid, right pterygoid, in (A) dorsal,
(B) ventral, and (C) left lateral view. Illustration in dorsal view (D) highlighting the placement of
relevant arteries, nerves, and veins. Abbreviations: ac = arteria carotis cerebralis; aci = arteria
carotis interna; bs = basisphenoid; ccb = canalis caroticus basisphenoidalis; cnh = canalis nervus
hyomandibularis; cci = canalis caroticus internus; ccv = canalis cavernosus; cnf = canalis nervus
facialis; cnhp = canalis nervus hyomandibularis proximalis; cnv = canalis nervus vidianus; faceb
= foramen anterius canalis carotici basisphenoidalis; facnv = foramen anterius canalis nervi
vidiani; fpcci = foramen posterius canalis carotici interni; gg = geniculate ganglion; pt =
pterygoid; vcl = vena capitis lateralis; VII = nervus facialis; VII $_{hy}$ = nervus hyomandibularis;
$VII_{vi} = nervus \ vidiani.$



Figure 4. The carotid circulation and vidian canal system of Carettochelys insculpta 2239 (NHMUK 1903.7.10.1). Three-dimensional reconstructions of the basisphenoid, right pterygoid, 2240 in (A) dorsal, (B) ventral, and (C) left lateral view. Illustration in dorsal view (D) highlighting 2241 the placement of relevant arteries, nerves, and veins. The red portion of the canalis cavernosus 2242 shows the inferred position of the mandibular artery. Abbreviations: ac = arteria carotis 2243 cerebralis; aci = arteria carotis interna; am = arteria mandibularis; bs = basisphenoid; ccb = 2244 canalis caroticus basisphenoidalis; cci = canalis caroticus internus; ccv = canalis cavernosus; cnf 2245 = canalis nervus facialis; cnv = canalis nervus vidianus; cprnv = canalis pro ramo nervi vidiani; 2246 2247 faceb = foramen anterius canalis carotici basisphenoidalis; facny = foramen anterius canalis nervi vidiani; fpcci = foramen posterius canalis carotici interni; gg = geniculate ganglion; pt = 2248 pterygoid; vcl = vena capitis lateralis; VII = nervus facialis; VII_{hv} = nervus hyomandibularis; 2249 VII_{vi} = nervus vidiani. 2250 2251 Figure 5. The carotid circulation and vidian canal system of Apalone spinifera (FMNH 2252 22178). Three-dimensional reconstructions of the basisphenoid, right pterygoid, in (A) dorsal, 2253 (B) ventral, and (C) left lateral view. Illustration in dorsal view (D) highlighting the placement of 2254 relevant arteries, nerves, and veins. Abbreviations: ac = arteria carotis cerebralis; aci = arteria 2255 carotis interna; am = arteria mandibularis; bs = basisphenoid; ccb = canalis caroticus 2256 basisphenoidalis; cci = canalis caroticus internus; ccl = canalis caroticus lateralis; ccv = canalis 2257 2258 cavernosus; cnf = canalis nervus facialis; cnv = canalis nervus vidianus; faccb = foramen anterius canalis carotici basisphenoidalis; faccl = foramen anterius canalis caroticus lateralis; 2259 facny = foramen anterius canalis nervi vidiani; fpcci = foramen posterius canalis carotici interni; 2260





gg = geniculate ganglion; pt = pterygoid; vcl = vena capitis lateralis; VII = nervus facialis; VII_{hv} 2261 = nervus hyomandibularis; VII_{vi} = nervus vidiani. 2262 2263 Figure 6. The carotid circulation and vidian canal system of Sternotherus minor (FMNH 2264 **211696).** Three-dimensional reconstructions of the basisphenoid, right pterygoid, in (A) dorsal, 2265 2266 (B) ventral, and (C) left lateral view. Illustration in dorsal view (D) highlighting the placement of relevant arteries, nerves, and veins. Abbreviations: ac = arteria carotis cerebralis; aci = arteria 2267 carotis interna; ap = arteria palatina; am = arteria mandibularis; bs = basisphenoid; ccb = canalis 2268 2269 caroticus basisphenoidalis; cci = canalis caroticus internus; ccl = canalis caroticus lateralis; ccv = canalis cavernosus; cnf = canalis nervus facialis; cnv = canalis nervus vidianus; cprnv = canalis 2270 pro ramo nervi vidiani; faceb = foramen anterius canalis carotici basisphenoidalis; facel = 2271 foramen anterius canalis caroticus lateralis; facny = foramen anterius canalis nervi vidiani; fpcci 2272 = foramen posterius canalis carotici interni; gg = geniculate ganglion; pt = pterygoid; vcl = vena 2273 capitis lateralis; VII = nervus facialis; VII_{hv} = nervus hyomandibularis; VII_{vi} = nervus vidiani. 2274 2275 Figure 7. The carotid circulation and vidian canal system of *Dermatemys mawii* (SMF 2276 **59463).** Three-dimensional reconstructions of the basisphenoid, right pterygoid, in (A) dorsal, 2277 (B) ventral, and (C) left lateral view. Illustration in dorsal view (D) highlighting the placement of 2278 relevant arteries, nerves, and veins. The red portion of the canalis cavernosus shows the inferred 2279 2280 position of the mandibular artery. Abbreviations: ac = arteria carotis cerebralis; aci = arteria carotis interna; am-a = anterior arteria mandibularis; am-p = posterior arteria mandibularis; ap = 2281 arteria palatina; bs = basisphenoid; ccb = canalis caroticus basisphenoidalis; cci = canalis 2282 2283 caroticus internus; cel = canalis caroticus lateralis; cev = canalis cavernosus; enf = canalis nervus





facialis; cnv = canalis nervus vidianus; faceb = foramen anterius canalis carotici 2284 basisphenoidalis; facel = foramen anterius canalis caroticus lateralis; facny = foramen anterius 2285 canalis nervi vidiani; fpcci = foramen posterius canalis carotici interni; gg = geniculate ganglion; 2286 pt = pterygoid; vcl = vena capitis lateralis; VII = nervus facialis; VII $_{hv}$ = nervus hyomandibularis; 2287 VII_{vi} = nervus vidiani. 2288 2289 Figure 8. The carotid circulation and vidian canal system of Chelydra serpentina (SMF 2290 **32846).** Three-dimensional reconstructions of the basisphenoid, right pterygoid, in (A) dorsal, 2291 2292 (B) ventral, and (C) left lateral view. Illustration in dorsal view (D) highlighting the placement of relevant arteries, nerves, and veins. The red portion of the canalis cavernosus shows the inferred 2293 position of the mandibular artery. Abbreviations: ac = arteria carotis cerebralis; aci = arteria 2294 carotis interna; ap = arteria palatina; am = arteria mandibularis; bs = basisphenoid; ccb = canalis 2295 caroticus basisphenoidalis; cci = canalis caroticus internus; ccl = canalis caroticus lateralis; ccv = 2296 canalis cavernosus; cnf = canalis nervus facialis; cnv = canalis nervus vidianus; faceb = foramen 2297 anterius canalis carotici basisphenoidalis; faccl = foramen anterius canalis caroticus lateralis; 2298 facny = foramen anterius canalis nervi vidiani; fpcci = foramen posterius canalis carotici interni; 2299 gg = geniculate ganglion; pt = pterygoid; vcl = vena capitis lateralis; VII = nervus facialis; VII_{hv} 2300 = nervus hyomandibularis; VII_{vi} = nervus vidiani. 2301 2302 2303 Figure 9. The carotid circulation and vidian canal system of Eretmochelys imbricata (FMNH 22242). Three-dimensional reconstructions of the basisphenoid, right pterygoid, in (A) 2304 dorsal, (B) ventral, and (C) left lateral view. Illustration in dorsal view (D) highlighting the 2305 2306 placement of relevant arteries, nerves, and veins. The red portion of the canalis cavernosus





shows the inferred position of the posterior mandibular artery. Abbreviations: ac = arteria carotis 2307 cerebralis; aci = arteria carotis interna; ap = arteria palatina; am-a = anterior arteria mandibularis; 2308 am-p = posterior arteria mandibularis; bs = basisphenoid; ccb = canalis caroticus 2309 basisphenoidalis; cci = canalis caroticus internus; ccv = canalis cavernosus; cnf = canalis nervus 2310 facialis; cprny = canalis pro ramo nervi vidiani; faceb = foramen anterius canalis carotici 2311 2312 basisphenoidalis; fpcci = foramen posterius canalis carotici interni; gg = geniculate ganglion; pt = pterygoid; v-am = vestigial arteria mandibularis; vcl = vena capitis lateralis; VII = nervus 2313 facialis; VII_{hv} = nervus hyomandibularis; VII_{vi} = nervus vidiani. 2314 2315 Figure 10. The carotid circulation and vidian canal system of *Dermochelys coriacea* (FMNH 2316 171756). Three-dimensional reconstructions of the basisphenoid, right pterygoid, in (A) dorsal, 2317 (B) ventral, and (C) left lateral view. Illustration in dorsal view (D) highlighting the placement of 2318 relevant arteries, nerves, and veins. Abbreviations: ac = arteria carotis cerebralis; aci = arteria 2319 carotis interna; am = arteria mandibularis; ap = arteria palatina; bs = basisphenoid; cci = canalis 2320 caroticus internus; ccv = canalis cavernosus; cnf = canalis nervus facialis; pt = pterygoid; vcl = 2321 vena capitis lateralis; VII = nervus facialis; VII $_{hv}$ = nervus hyomandibularis; VII $_{vi}$ = nervus 2322 2323 vidiani. Note that we do not highlight the course of the mandibular artery, because the mandibular blood supply of *Dermochelys coriacea* is currently unknown. 2324 2325 2326 Figure 11. The carotid circulation and vidian canal system of *Platysternon megacephalum* (SMF 69684). Three-dimensional reconstructions of the basisphenoid, right pterygoid, in (A) 2327 dorsal, (B) ventral, and (C) left lateral view. Illustration in dorsal view (D) highlighting the 2328 2329 placement of relevant arteries, nerves, and veins. The red portion of the canalis cavernosus



shows the inferred position of the mandibular artery. Abbreviations: ac = arteria carotis cerebralis; aci = arteria carotis interna; am = arteria mandibularis; bs = basisphenoid; ccb = canalis caroticus basisphenoidalis; cci = canalis caroticus internus; ccv = canalis cavernosus; cnf = canalis nervus facialis; cnv = canalis nervus vidianus; cprnv = canalis pro ramo nervi vidiani; faccb = foramen anterius canalis carotici basisphenoidalis; facnv = foramen anterius canalis nervi vidiani; fpcci = foramen posterius canalis carotici interni; gg = geniculate ganglion; pt = pterygoid; vcl = vena capitis lateralis; VII = nervus facialis; VII $_{hy}$ = nervus hyomandibularis; VII $_{vi}$ = nervus vidiani.

Figure 12. The carotid circulation and vidian canal system of *Glyptemys insculpta* (FMNH 22240). Three-dimensional reconstructions of the basisphenoid, right pterygoid, in (A) dorsal, (B) ventral, and (C) left lateral view. Illustration in dorsal view (D) highlighting the placement of relevant arteries, nerves, and veins. The red portion of the canalis cavernosus shows the inferred position of the mandibular artery. Abbreviations: ac = arteria carotis cerebralis; aci = arteria carotis interna; ap = arteria palatina; am = arteria mandibularis; bs = basisphenoid; ccb = canalis caroticus basisphenoidalis; cci = canalis caroticus internus; ccl = canalis caroticus lateralis; ccv = canalis cavernosus; cnf = canalis nervus facialis; cnv = canalis nervus vidianus; cprnv = canalis pro ramo nervi vidiani; faccb = foramen anterius canalis carotici basisphenoidalis; faccl = foramen anterius canalis caroticus lateralis; facnv = foramen anterius canalis nervi vidiani; fpcci = foramen posterius canalis carotici interni; gg = geniculate ganglion; pt = pterygoid; vcl = vena capitis lateralis; VII = nervus facialis; VII_{hy} = nervus hyomandibularis; VII_{vi} = nervus vidiani.



Figure 13. The carotid circulation and vidian canal system of Gopherus agassizii (FMNH 2352 **216746).** Three-dimensional reconstructions of the basisphenoid, right pterygoid, in (A) dorsal, 2353 (B) ventral, and (C) left lateral view. Illustration in dorsal view (D) highlighting the placement of 2354 relevant arteries, nerves, and veins. The red portion of the canalis cavernosus shows the inferred 2355 position of the mandibular artery. Abbreviations: ac = arteria carotis cerebralis; aci = arteria 2356 2357 carotis interna; am = arteria mandibularis; bs = basisphenoid; ccb = canalis caroticus basisphenoidalis; cci = canalis caroticus internus; ccv = canalis cavernosus; cnf = canalis nervus 2358 facialis; cnv = canalis nervus vidianus; faceb = foramen anterius canalis carotici 2359 2360 basisphenoidalis; facny = foramen anterius canalis nervi vidiani; fam = foramen arteriomandibulare; fpcci = foramen posterius canalis carotici interni; gg = geniculate ganglion; 2361 pt = pterygoid; vcl = vena capitis lateralis; VII = nervus facialis; VII_{hy} = nervus hyomandibularis; 2362 VII_{vi} = nervus vidiani. 2363 2364 Figure 14. The carotid circulation and vidian canal system of Batagur baska (NHMUK 2365 **67.9.28.7).** Three-dimensional reconstructions of the basisphenoid, right pterygoid, in (A) dorsal, 2366 (B) ventral, and (C) left lateral view. Illustration in dorsal view (D) highlighting the placement of 2367 relevant arteries, nerves, and veins. The red portion of the canalis cavernosus shows the inferred 2368 position of the mandibular artery. Abbreviations: ac = arteria carotis cerebralis; aci = arteria 2369 carotis interna; ap = arteria palatina; am = arteria mandibularis; bs = basisphenoid; ccb = canalis 2370 2371 caroticus basisphenoidalis; cci = canalis caroticus internus; ccl = canalis caroticus lateralis; ccv = canalis cavernosus; cnf = canalis nervus facialis; cnv = canalis nervi vidiani; cprnv = canalis pro 2372 ramo nervi vidiani; faceb = foramen anterius canalis caroticus cerebralis; facel = foramen 2373 2374 anterius canalis caroticus lateralis; facny = foramen anterius canalis nervi vidiani; fpcci =





2375	foramen posterius canalis carotici interni; gg = geniculate ganglion; pt = pterygoid; vcl = vena
2376	capitis lateralis; VII = nervus facialis; VII $_{hy}$ = nervus hyomandibularis; VII $_{vi}$ = nervus vidiani.
2377	
2378	Figure 15. Asymmetry in osteological correlates for the palatine artery in Manouria
2379	impressa (SMF 69777). (A), dorsal view of horizontally cut basicranium for orientation. (B), as
2380	A, but zoomed in on details of anterior exiting foramina for the carotid arterial system. (C),
2381	cranium in left lateral view, showing position of axial slices shown in D-E. (D), axial CT slice at
2382	position of foramina anterius canalis carotici basisphenoidalis. (E), axial CT slice at position of
2383	carotid split. Note that canals and foramina for the palatine artery are present on the right side,
2384	although the palatine artery is generally absent in testudinids. Abbreviations: bo = blind opening
2385	(opens into bone, but does not connect to blood or nervous system); ccb = canalis caroticus
2386	basisphenoidalis; faceb = foramen anterius canalis carotici basisphenoidalis; facel = foramen
2387	anterius canalis carotici lateralis; r-ccl = right canalis caroticus lateralis; tcb = trabeculae of
2388	cancellous bone (small internal openings not connect to blood or nervous system).
2389	
2390	Figure 16. Schematic overview of patterns pertaining to the split of the facial nerve into its
2391	hyomandibular and vidian branches. Abbreviations: caj = cavum acustico-jugulare; ccv =
2392	canalis cavernosus; cci = canalis caroticus internus; ccl = canalis caroticus lateralis; cnf = canalis
2393	nervus facialis; cnhp = canalis nervus hyomandibularis proximalis; cnv = canalis nervus
2394	vidianus; cprnv = canalis pro ramo nervi vidiani; faf = fossa acustico-facialis; fpcci = foramen
2395	posterius canalis carotici interni; gg = geniculate ganglion; VII = nervus facialis; VII_{hy} = nervus
2396	hyomandibularis; VII_{vi} = nervus vidiani.
2397	



2398

2399

2400

2401

2402

2403

2404

2405

2406

2407

2408

2409

2410

2411

2412

2413

2414

2415

2416

2417

2418

2419

2420

Figure 17. Schematic overview of patterns pertaining to the posterior portion of the **hyomandibular nerve.** The five patterns presented herein only apply to taxa in which the vidian nerve enters the carotid canal system (i.e. turtles with patterns IA, IIA, and IIB). Abbreviations: caj = cavum acustico-jugulare; ccv = canalis cavernosus; cnhd = canalis nervus hyomandibularis distalis; snh = sulcus nervus hyomandibularis; VII_{hv} = nervus hyomandibularis. Figure 18. Schematic overview of patterns pertaining to the anterior portion of the vidian **nerve.** Abbreviations: ccv = canalis cavernosus; cci = canalis caroticus internus; ccl = canalis caroticus lateralis; cnv = canalis nervus vidianus; fpcci = foramen posterius canalis carotici interni; scc = "short cut canal". Figure 19. Relationship of internal carotid artery size and stapedial artery size in turtles. (A), PGLS regression of log₁₀-cross-sectional diameter of internal carotid artery canal on log₁₀cross-sectional diameter of stapedial artery canal. Solid grey line is the regression line describing a model with a single slope and intercept for all taxa. Dashed the lines are regression lines for subsets of the data (see text and table 3 for details). (B), plot showing which data points were used as subsets for the multiple regression model test. (C), residual plot of PGLS regression of the full dataset, ordered by clades. Symbols in A and C denote clade attributions. Table 1. List of specimens used in this study. Abbreviations: FMNH, Field Museum of Natural History, Chicago, IL, USA; NHMUK, Natural History Museum London, London, England; NMB, Naturhistorisches Museum Basel, Basel, Switzerland; PCHP, Chelonian Research Institute, Oviedo, FL, USA; PIMUZ, Paläontologisches Museum Zürich, Zürich,





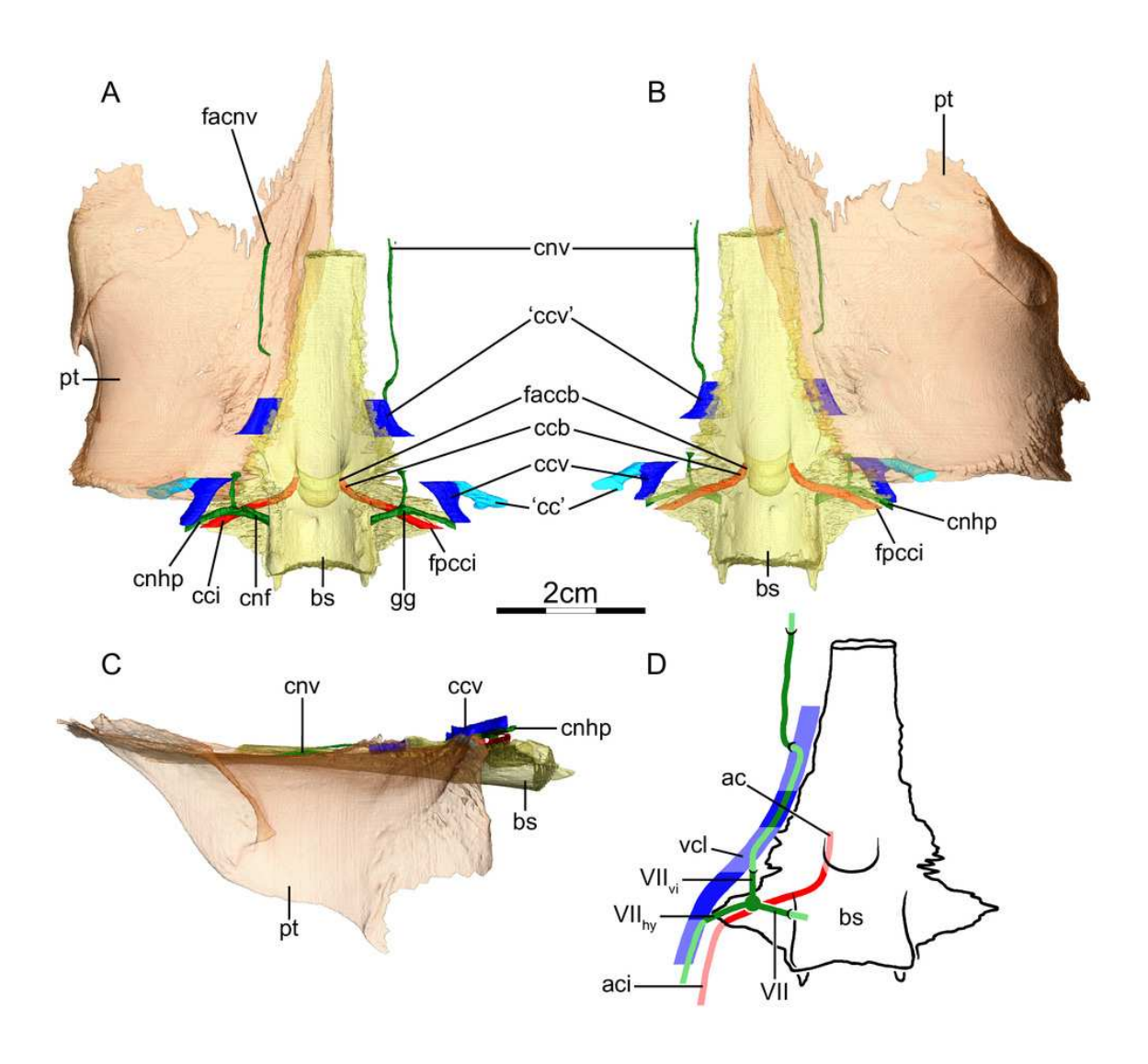
2421	Switzerland; SMF, Senckenberg Naturmuseum Frankfurt, Frankfurt am Main, Germany;
2422	SMNS, Staatliches Museum für Naturkunde Stuttgart, Stuttgart, Germany; UF, Florida Museum
2423	of Natural History, Gainesville, FL, USA; UMZC, University Museum of Zoology Cambridge,
2424	Cambridge, England.
2425	
2426	Table 2. Surface values (μm^2) of the stapedial and carotid artery canals. Abbreviations:
2427	CCB, canalis caroticus basisphenoidalis; CCI, canalis caroticus internus; CCL, canalis caroticus
2428	lateralis; CST, canalis stapedio-temporalis. Note that value 0 is used when the canalis caroticus
2429	lateralis and arteria palatina are known to be absent, whereas NA (non-applicable) is only used
2430	for chelonioids, in which the palatine artery is present but does not extend through its own canal,
2431	preventing us to make any measurement of the latter.
2432	
2433	Table 3. Results of PGLS regressions of internal carotid artery size on stapedial artery size.
2434	CCI stands for cross-sectional area of the internal carotid artery canal. CST stands for cross-
2435	sectional area of stapedial artery canal. CTK-abbreviated model describes model only including
2436	chelonioids, trionychians, and kinosternoids. Remaining-abbreviated model includes all taxa not
2437	included in the CTK-model. Phylogenetic signal (lambda) was estimated during model fitting.
2438	R2 is the generalized coefficient of determination described by Nagelkerke (1991).



The carotid circulation and vidian canal system of *Chelus fimbriatus* (NHMUK 81.9.27.4).

Three-dimensional reconstructions of the basisphenoid, right pterygoid, in (A) dorsal, (B) ventral, and (C) left lateral view. Illustration in dorsal view (D) highlighting the placement of relevant arteries, nerves, and veins. Dark colors highlight sections fully covered by bone, light colors partially or fully uncovered sections. Abbreviations: ac = arteria carotis cerebralis; aci = arteria carotis interna; bs = basisphenoid; 'cc' = secondary canalis cavernosus; ccb = canalis caroticus basisphenoidalis; cci = canalis caroticus internus; ccv = canalis cavernosus; cnf = canalis nervus facialis; cnhp = canalis nervus hyomandibularis proximalis; cnv = canalis nervus vidianus; faccb = foramen anterius canalis carotici basisphenoidalis; facnv = foramen anterius canalis nervi vidiani; fpcci = foramen posterius canalis carotici interni; gg = geniculate ganglion; pt = pterygoid; vcl = vena capitis lateralis; VII = nervus facialis; VII_{vv} = nervus hyomandibularis; VII_{vi} = nervus vidiani.



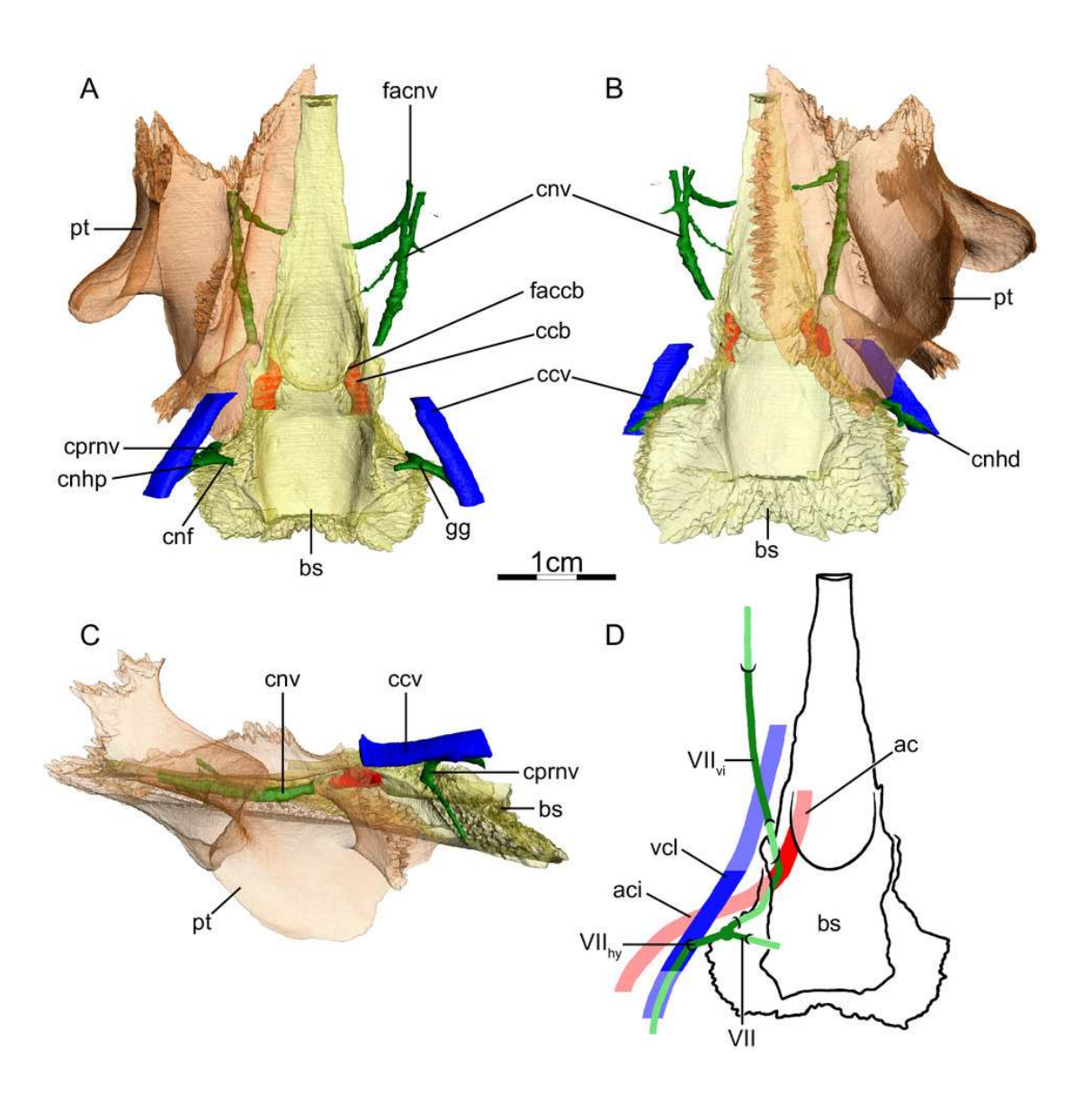




The carotid circulation and vidian canal system of *Peltocephalus dumerilianus* (NHMUK 60.4.16.9).

Three-dimensional reconstructions of the basisphenoid, right pterygoid, in (A) dorsal, (B) ventral, and (C) left lateral view. Illustration in dorsal view (D) highlighting the placement of relevant arteries, nerves, and veins. Abbreviations: ac = arteria carotis cerebralis; aci = arteria carotis interna; bs = basisphenoid; ccb = canalis caroticus basisphenoidalis; ccv = canalis cavernosus; cnf = canalis nervus facialis; cnhd = canalis nervus hyomandibularis distalis; cnhp = canalis nervus hyomandibularis proximalis; cnv = canalis nervus vidianus; cprnv = canalis pro ramo nervi vidiani; faccb = foramen anterius canalis carotici basisphenoidalis; facnv = foramen anterius canalis nervi vidiani; gg = geniculate ganglion; pt = pterygoid; vcl = vena capitis lateralis; VII = nervus facialis; VII_{hy} = nervus hyomandibularis; VII_{yi} = nervus vidiani.



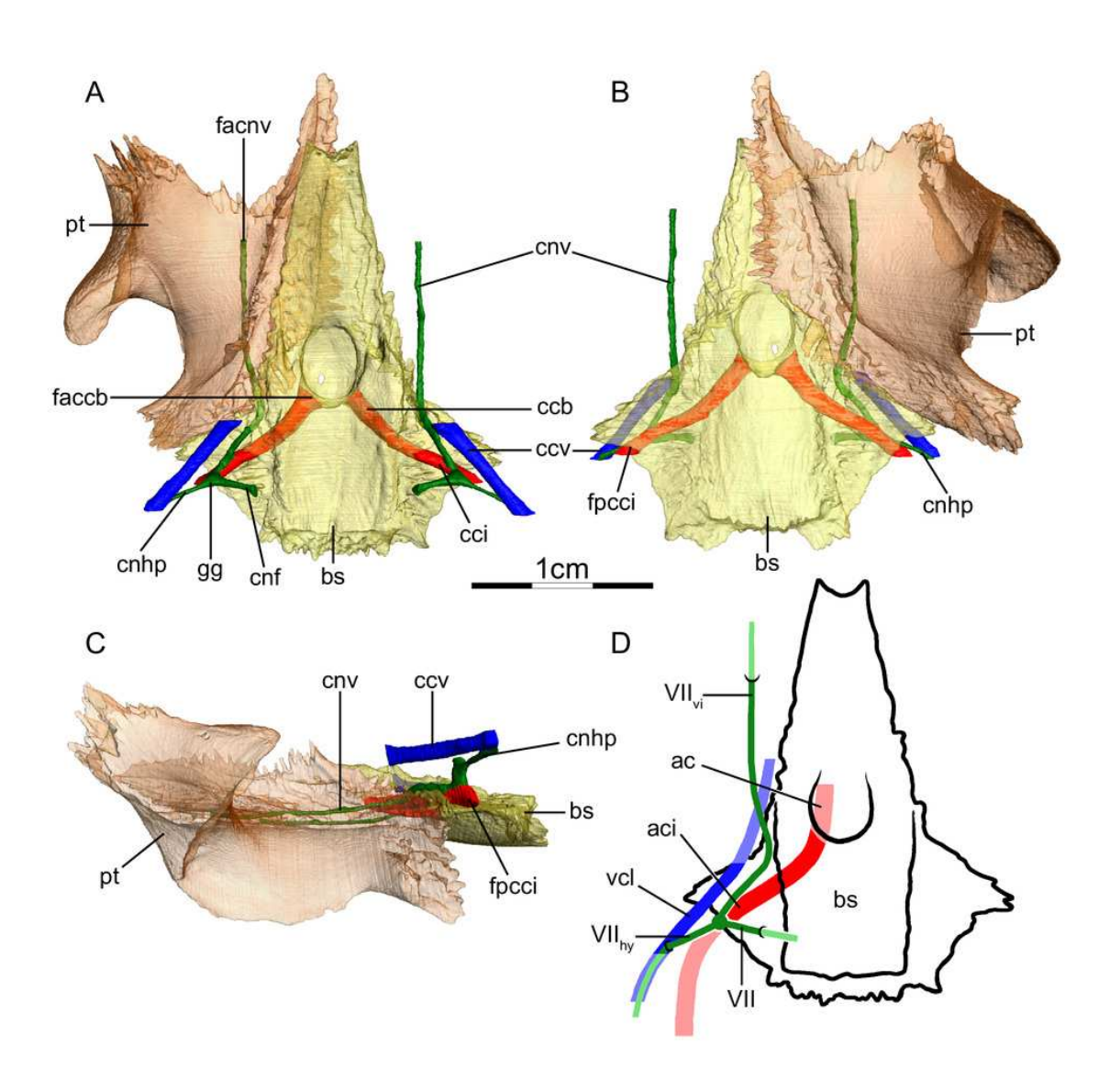




The carotid circulation and vidian canal system of *Pelusios subniger* (NMB 16230).

Three-dimensional reconstructions of the basisphenoid, right pterygoid, in (A) dorsal, (B) ventral, and (C) left lateral view. Illustration in dorsal view (D) highlighting the placement of relevant arteries, nerves, and veins. Abbreviations: ac = arteria carotis cerebralis; aci = arteria carotis interna; bs = basisphenoid; ccb = canalis caroticus basisphenoidalis; cnh = canalis nervus hyomandibularis; cci = canalis caroticus internus; ccv = canalis cavernosus; cnf = canalis nervus facialis; cnhp = canalis nervus hyomandibularis proximalis; cnv = canalis nervus vidianus; faccb = foramen anterius canalis carotici basisphenoidalis; facnv = foramen anterius canalis nervi vidiani; fpcci = foramen posterius canalis carotici interni; gg = geniculate ganglion; pt = pterygoid; vcl = vena capitis lateralis; VII = nervus facialis; VII_{hy} = nervus hyomandibularis; VII_{vi} = nervus vidiani.



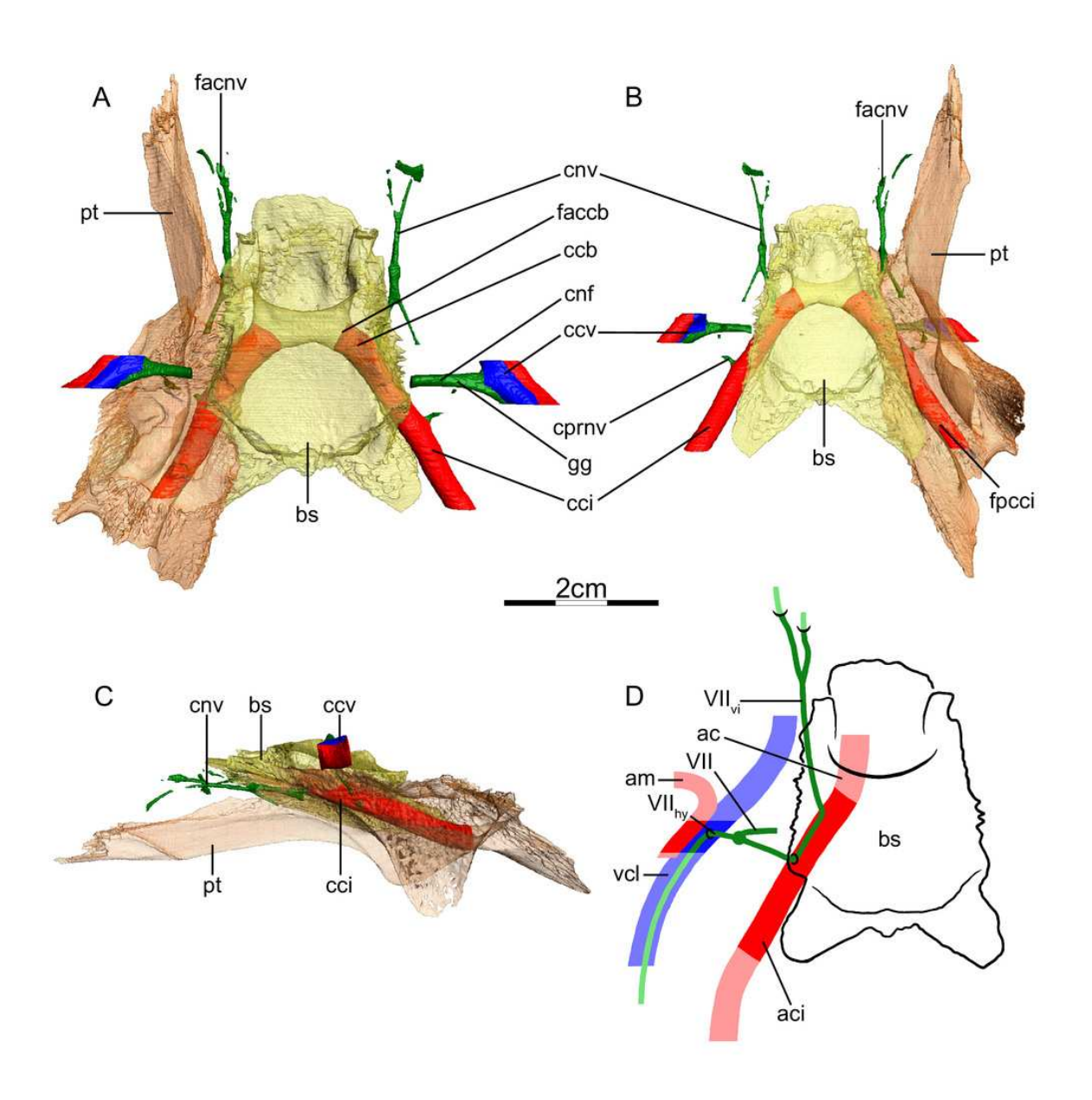




The carotid circulation and vidian canal system of *Carettochelys insculpta* (NHMUK 1903.7.10.1).

Three-dimensional reconstructions of the basisphenoid, right pterygoid, in (A) dorsal, (B) ventral, and (C) left lateral view. Illustration in dorsal view (D) highlighting the placement of relevant arteries, nerves, and veins. The red portion of the canalis cavernosus shows the inferred position of the mandibular artery. Abbreviations: ac = arteria carotis cerebralis; aci = arteria carotis interna; am = arteria mandibularis; bs = basisphenoid; ccb = canalis caroticus basisphenoidalis; cci = canalis caroticus internus; ccv = canalis cavernosus; cnf = canalis nervus facialis; cnv = canalis nervus vidianus; cprnv = canalis pro ramo nervi vidiani; faccb = foramen anterius canalis carotici basisphenoidalis; facnv = foramen anterius canalis nervi vidiani; fpcci = foramen posterius canalis carotici interni; gg = geniculate ganglion; pt = pterygoid; vcl = vena capitis lateralis; VII = nervus facialis; VII_{hy} = nervus hyomandibularis; VII_{yi} = nervus vidiani.



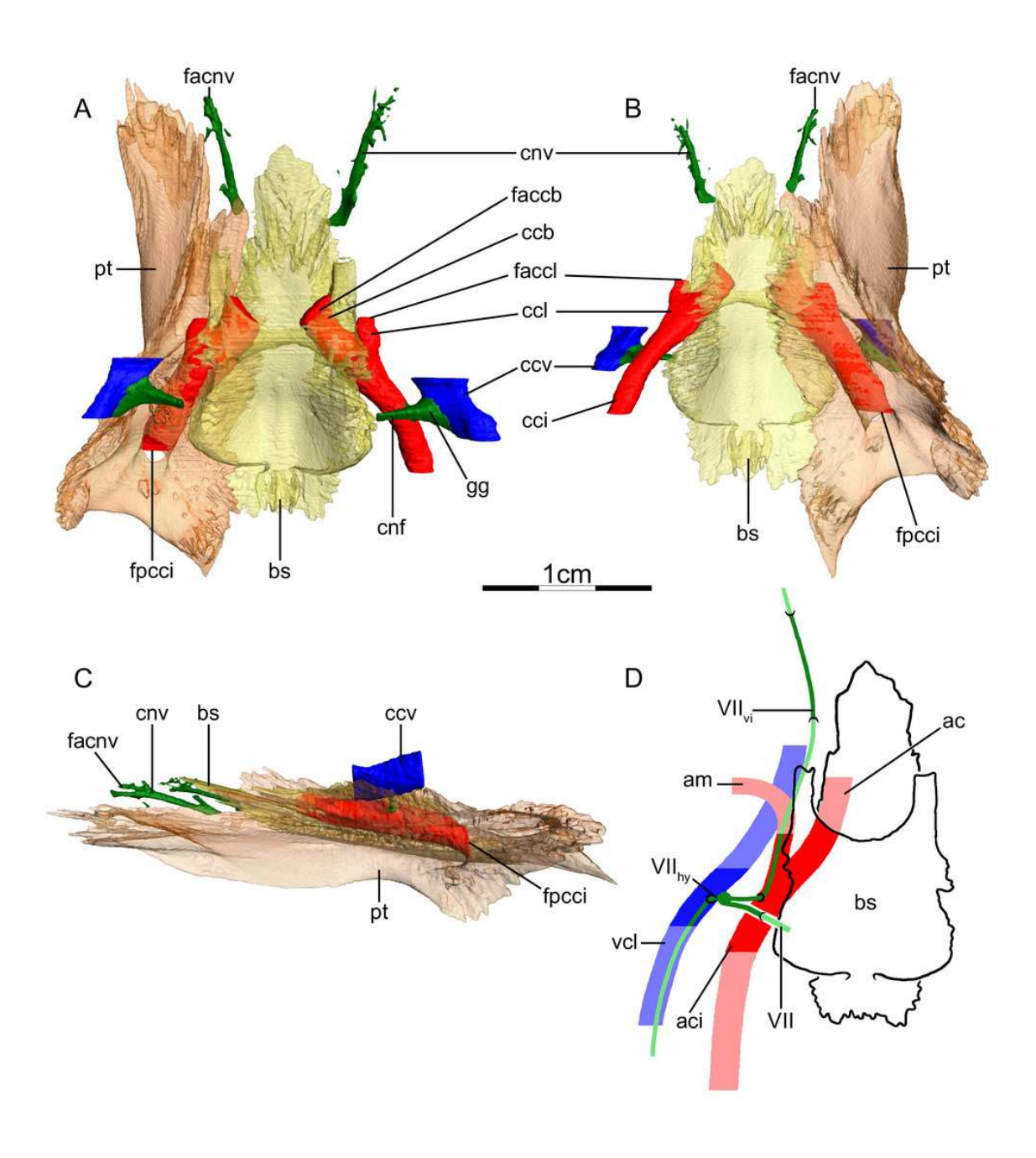




The carotid circulation and vidian canal system of Apalone spinifera (FMNH 22178).

Three-dimensional reconstructions of the basisphenoid, right pterygoid, in (A) dorsal, (B) ventral, and (C) left lateral view. Illustration in dorsal view (D) highlighting the placement of relevant arteries, nerves, and veins. Abbreviations: ac = arteria carotis cerebralis; aci = arteria carotis interna; am = arteria mandibularis; bs = basisphenoid; ccb = canalis caroticus basisphenoidalis; cci = canalis caroticus internus; ccl = canalis caroticus lateralis; ccv = canalis cavernosus; cnf = canalis nervus facialis; cnv = canalis nervus vidianus; faccb = foramen anterius canalis carotici basisphenoidalis; faccl = foramen anterius canalis caroticus lateralis; facnv = foramen anterius canalis nervi vidiani; fpcci = foramen posterius canalis carotici interni; gg = geniculate ganglion; pt = pterygoid; vcl = vena capitis lateralis; VII = nervus facialis; VII_{hv} = nervus hyomandibularis; VII_{vi} = nervus vidiani.



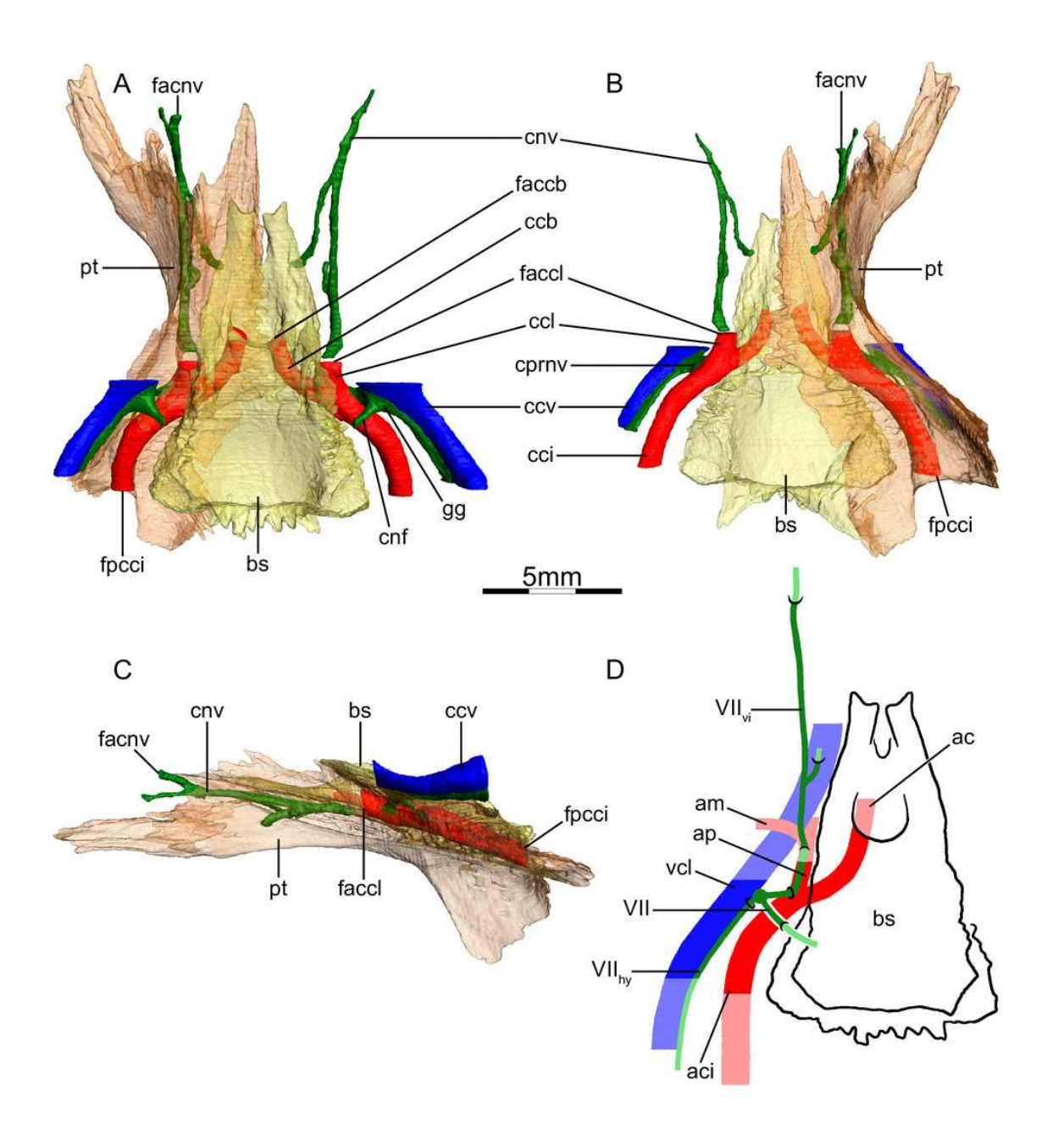




The carotid circulation and vidian canal system of *Sternotherus minor* (FMNH 211696)

Three-dimensional reconstructions of the basisphenoid, right pterygoid, in (A) dorsal, (B) ventral, and (C) left lateral view. Illustration in dorsal view (D) highlighting the placement of relevant arteries, nerves, and veins. Abbreviations: ac = arteria carotis cerebralis; aci = arteria carotis interna; ap = arteria palatina; am = arteria mandibularis; bs = basisphenoid; ccb = canalis caroticus basisphenoidalis; cci = canalis caroticus internus; ccl = canalis caroticus lateralis; ccv = canalis cavernosus; cnf = canalis nervus facialis; cnv = canalis nervus vidianus; cprnv = canalis pro ramo nervi vidiani; faccb = foramen anterius canalis carotici basisphenoidalis; faccl = foramen anterius canalis caroticus lateralis; facnv = foramen anterius canalis nervi vidiani; fpcci = foramen posterius canalis carotici interni; gg = geniculate ganglion; pt = pterygoid; vcl = vena capitis lateralis; VII = nervus facialis; VII_{hy} = nervus hyomandibularis; VII_{yi} = nervus vidiani.



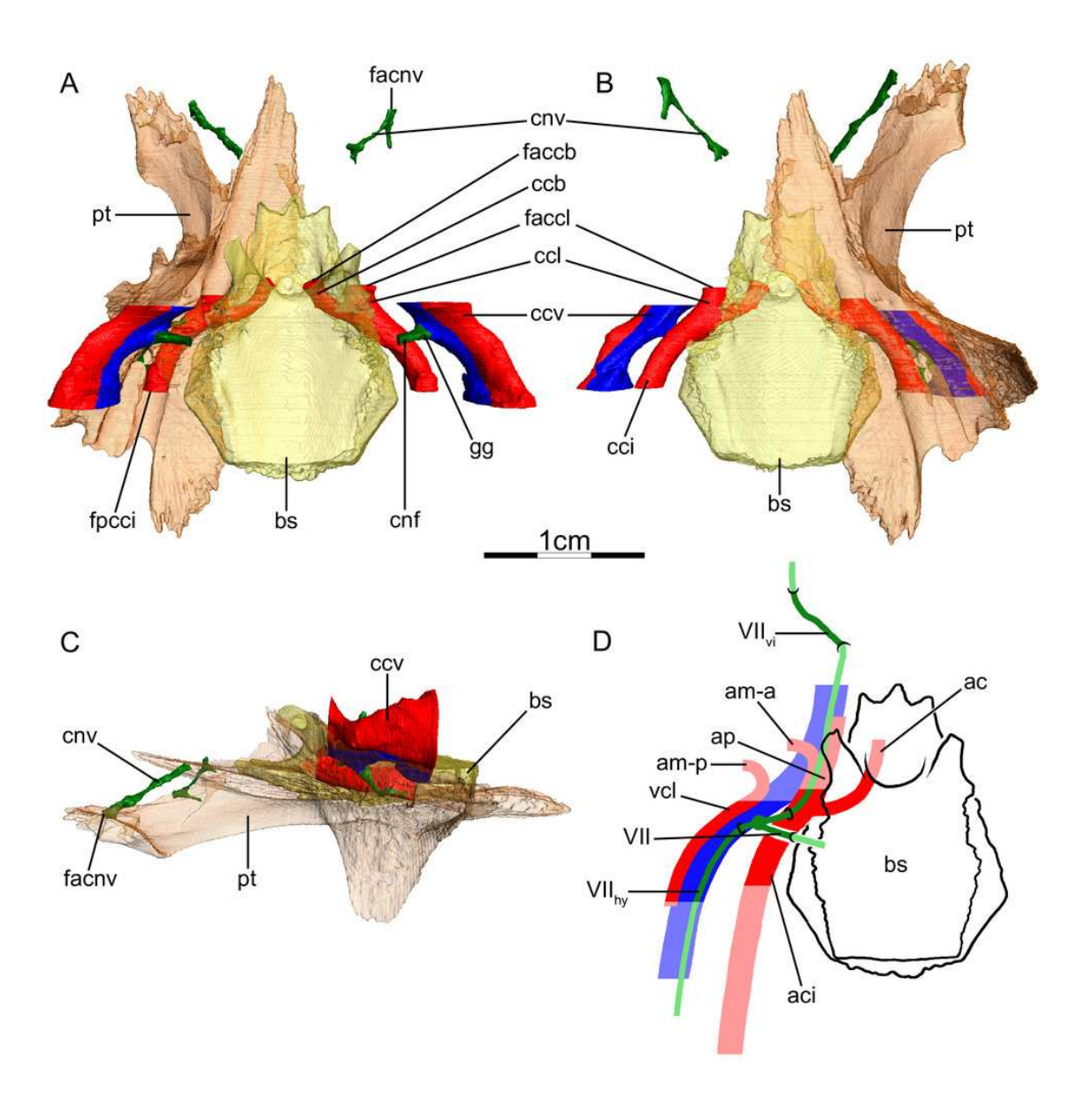




The carotid circulation and vidian canal system of *Dermatemys mawii* (SMF 59463).

Three-dimensional reconstructions of the basisphenoid, right pterygoid, in (A) dorsal, (B) ventral, and (C) left lateral view. Illustration in dorsal view (D) highlighting the placement of relevant arteries, nerves, and veins. The red portion of the canalis cavernosus shows the inferred position of the mandibular artery. Abbreviations: ac = arteria carotis cerebralis; aci = arteria carotis interna; am-a = anterior arteria mandibularis; am-p = posterior arteria mandibularis; ap = arteria palatina; bs = basisphenoid; ccb = canalis caroticus basisphenoidalis; cci = canalis caroticus internus; ccl = canalis caroticus lateralis; ccv = canalis cavernosus; cnf = canalis nervus facialis; cnv = canalis nervus vidianus; faccb = foramen anterius canalis carotici basisphenoidalis; faccl = foramen anterius canalis caroticus lateralis; facnv = foramen anterius canalis nervi vidiani; fpcci = foramen posterius canalis carotici interni; gg = geniculate ganglion; pt = pterygoid; vcl = vena capitis lateralis; VII = nervus facialis; VII_{bv} = nervus hyomandibularis; VII_{vi} = nervus vidiani.



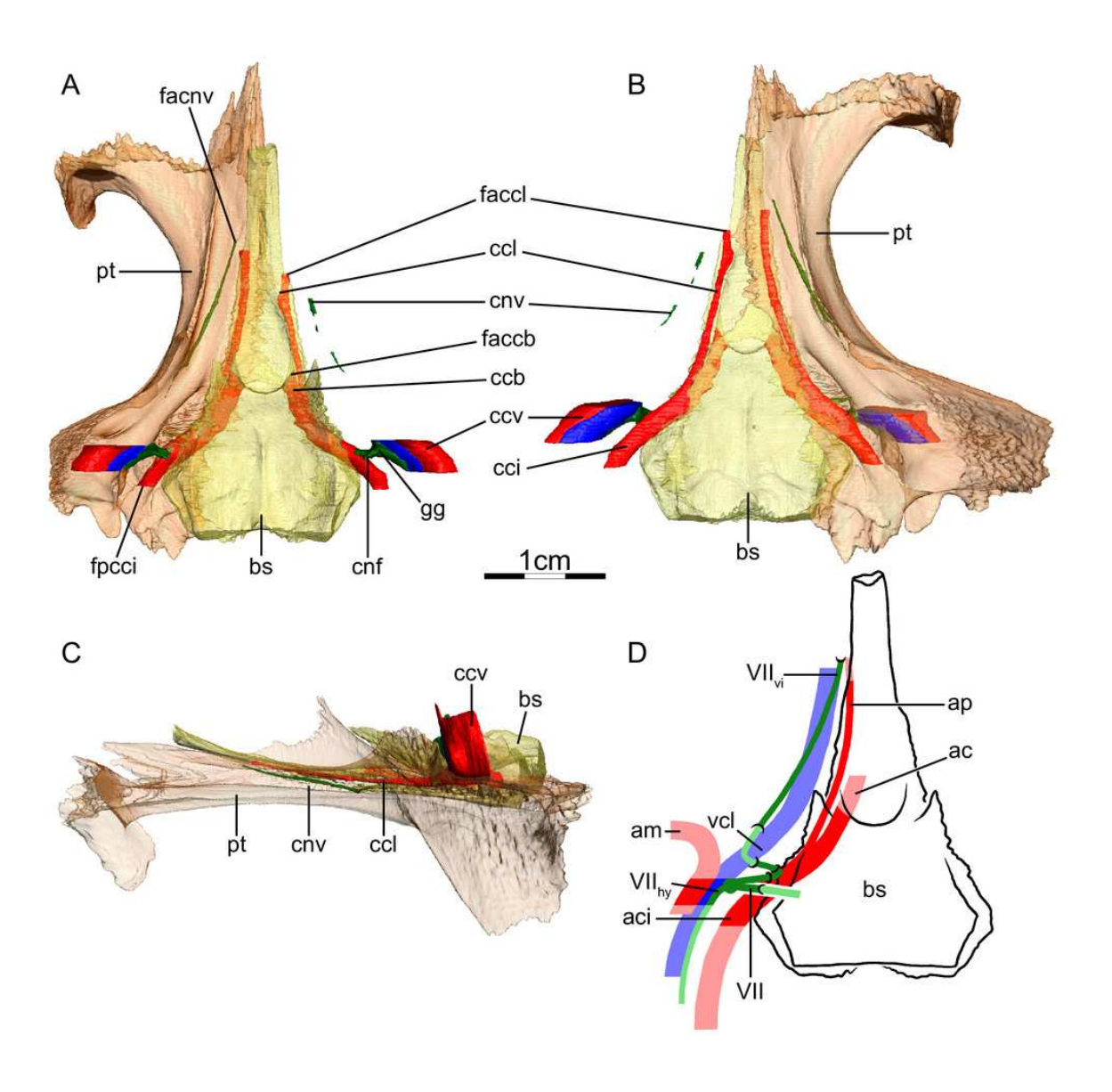




The carotid circulation and vidian canal system of Chelydra serpentina (SMF 32846).

Three-dimensional reconstructions of the basisphenoid, right pterygoid, in (A) dorsal, (B) ventral, and (C) left lateral view. Illustration in dorsal view (D) highlighting the placement of relevant arteries, nerves, and veins. The red portion of the canalis cavernosus shows the inferred position of the mandibular artery. Abbreviations: ac = arteria carotis cerebralis; aci = arteria carotis interna; ap = arteria palatina; am = arteria mandibularis; bs = basisphenoid; ccb = canalis caroticus basisphenoidalis; cci = canalis caroticus internus; ccl = canalis caroticus lateralis; ccv = canalis cavernosus; cnf = canalis nervus facialis; cnv = canalis nervus vidianus; faccb = foramen anterius canalis carotici basisphenoidalis; faccl = foramen anterius canalis caroticus lateralis; facnv = foramen anterius canalis nervi vidiani; fpcci = foramen posterius canalis carotici interni; gg = geniculate ganglion; pt = pterygoid; vcl = vena capitis lateralis; VII = nervus facialis; VII_{hy} = nervus hyomandibularis; VII_{vi} = nervus vidiani.



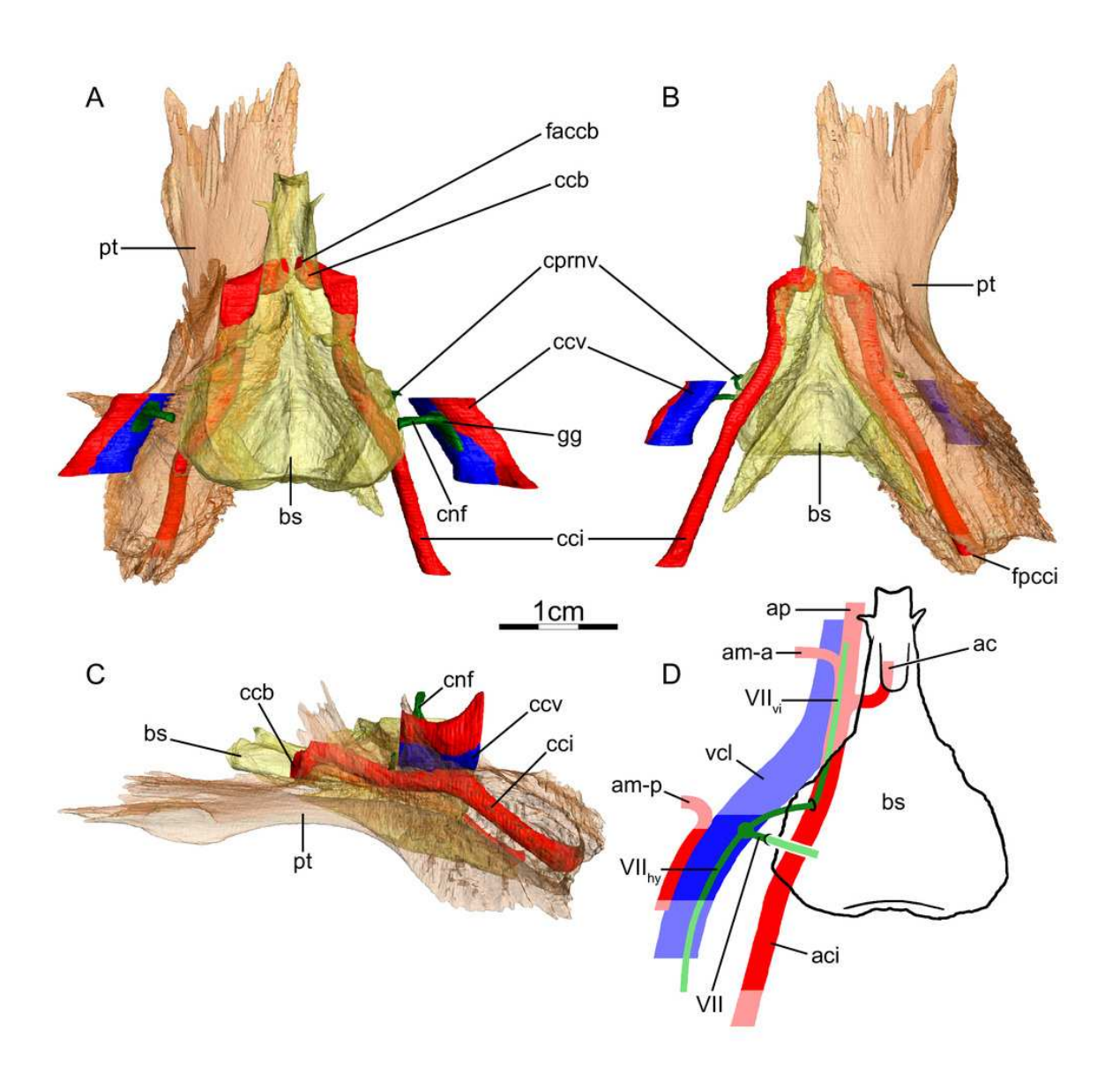




The carotid circulation and vidian canal system of *Eretmochelys imbricata* (FMNH 22242).

Three-dimensional reconstructions of the basisphenoid, right pterygoid, in (A) dorsal, (B) ventral, and (C) left lateral view. Illustration in dorsal view (D) highlighting the placement of relevant arteries, nerves, and veins. The red portion of the canalis cavernosus shows the inferred position of the posterior mandibular artery. Abbreviations: ac = arteria carotis cerebralis; aci = arteria carotis interna; ap = arteria palatina; am-a = anterior arteria mandibularis; am-p = posterior arteria mandibularis; bs = basisphenoid; ccb = canalis caroticus basisphenoidalis; cci = canalis caroticus internus; ccv = canalis cavernosus; cnf = canalis nervus facialis; cprnv = canalis pro ramo nervi vidiani; faccb = foramen anterius canalis carotici basisphenoidalis; fpcci = foramen posterius canalis carotici interni; gg = geniculate ganglion; pt = pterygoid; v-am = vestigial arteria mandibularis; vcl = vena capitis lateralis; VII = nervus facialis; VII_{ny} = nervus hyomandibularis; VII_{vi} = nervus vidiani.



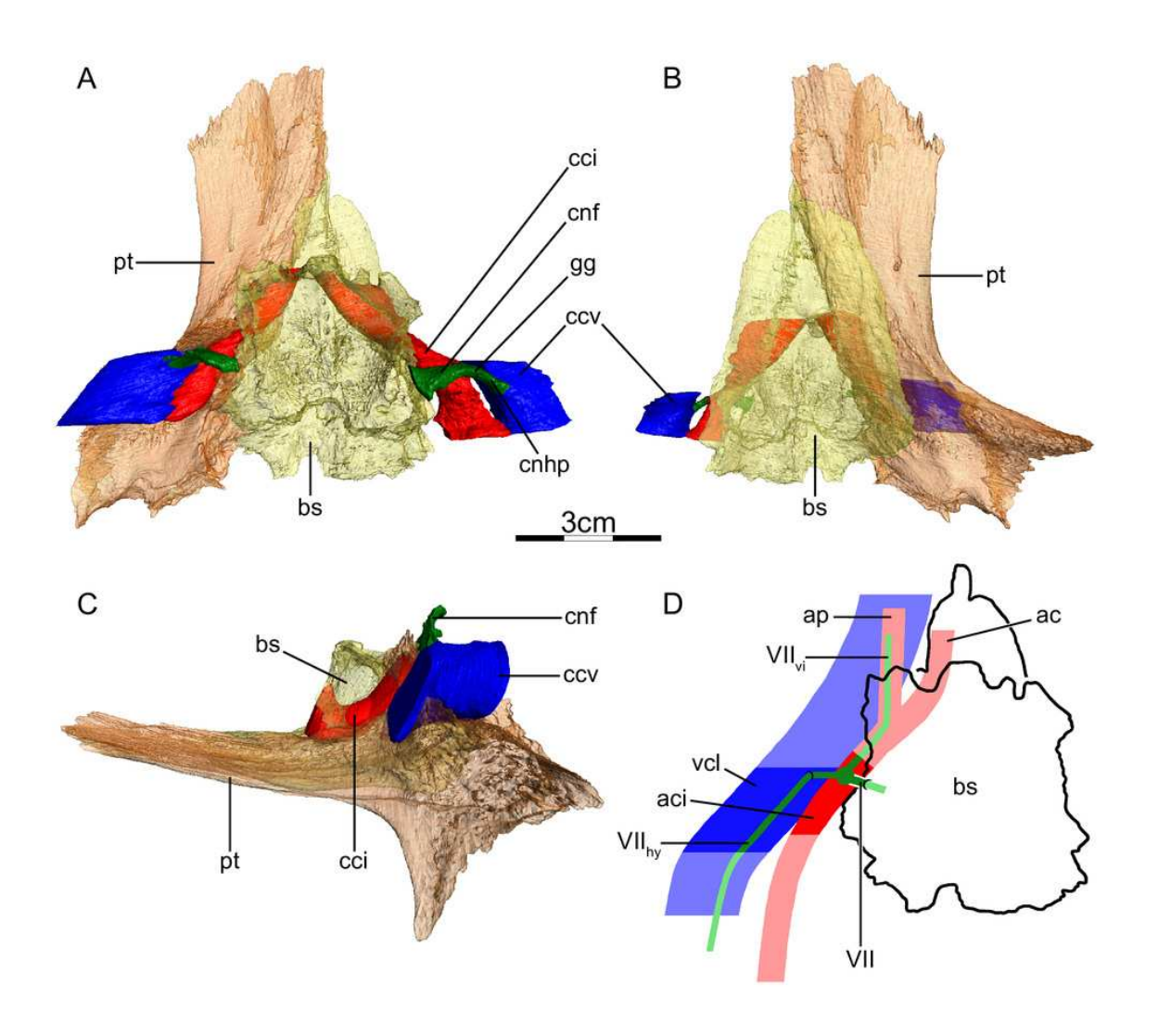




The carotid circulation and vidian canal system of *Dermochelys coriacea* (FMNH 171756).

Three-dimensional reconstructions of the basisphenoid, right pterygoid, in (A) dorsal, (B) ventral, and (C) left lateral view. Illustration in dorsal view (D) highlighting the placement of relevant arteries, nerves, and veins. Abbreviations: ac = arteria carotis cerebralis; aci = arteria carotis interna; am = arteria mandibularis; ap = arteria palatina; bs = basisphenoid; cci = canalis caroticus internus; ccv = canalis cavernosus; cnf = canalis nervus facialis; pt = pterygoid; vcl = vena capitis lateralis; VII = nervus facialis; VII $_{\rm hy}$ = nervus hyomandibularis; VII $_{\rm vi}$ = nervus vidiani. Note that we do not highlight the course of the mandibular artery, because the mandibular blood supply of *Dermochelys coriacea* is currently unknown.



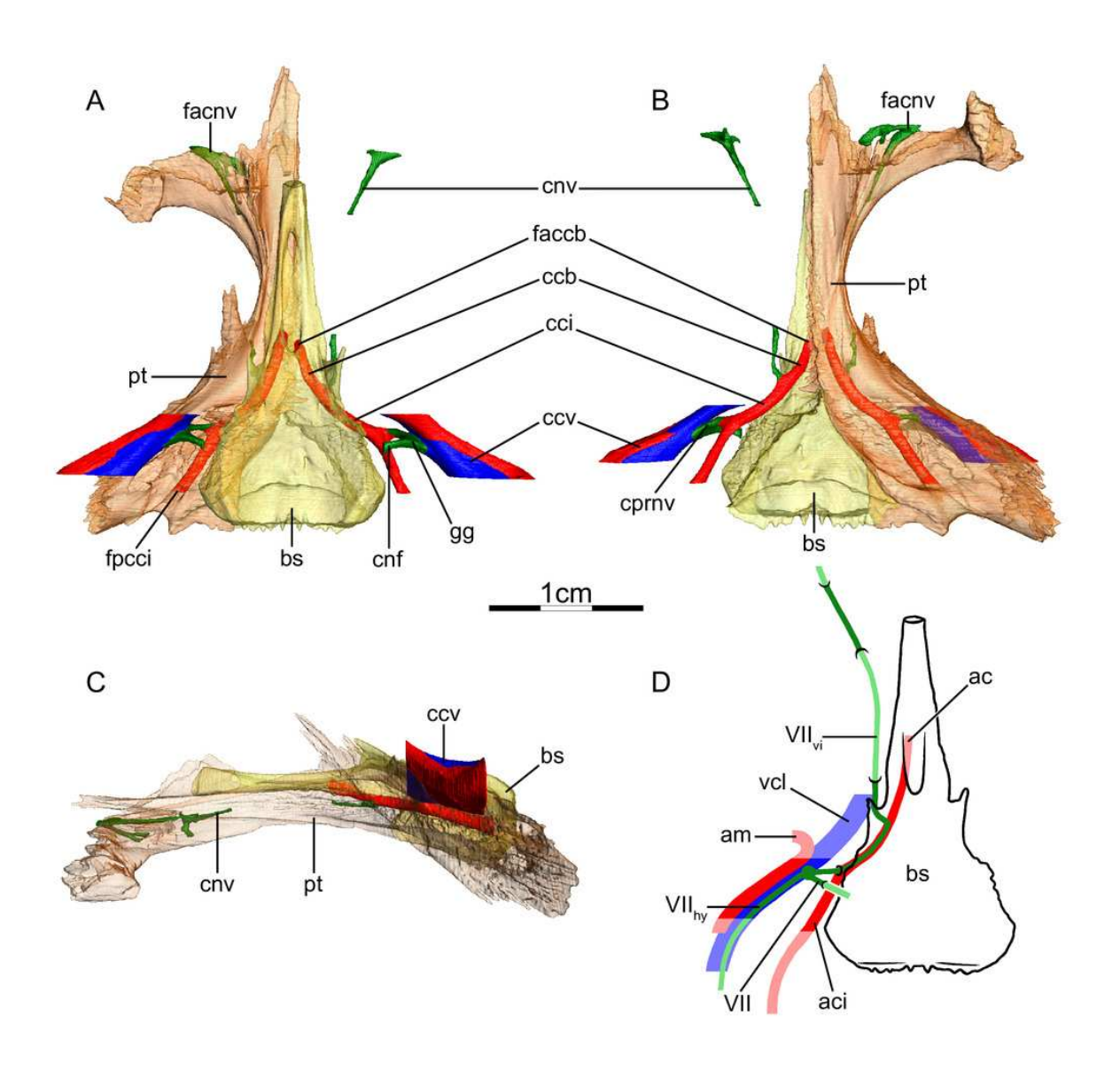




The carotid circulation and vidian canal system of *Platysternon megacephalum* (SMF 69684).

Three-dimensional reconstructions of the basisphenoid, right pterygoid, in (A) dorsal, (B) ventral, and (C) left lateral view. Illustration in dorsal view (D) highlighting the placement of relevant arteries, nerves, and veins. The red portion of the canalis cavernosus shows the inferred position of the mandibular artery. Abbreviations: ac = arteria carotis cerebralis; aci = arteria carotis interna; am = arteria mandibularis; bs = basisphenoid; ccb = canalis caroticus basisphenoidalis; cci = canalis caroticus internus; ccv = canalis cavernosus; cnf = canalis nervus facialis; cnv = canalis nervus vidianus; cprnv = canalis pro ramo nervi vidiani; faccb = foramen anterius canalis carotici basisphenoidalis; facnv = foramen anterius canalis nervi vidiani; fpcci = foramen posterius canalis carotici interni; gg = geniculate ganglion; pt = pterygoid; vcl = vena capitis lateralis; VII = nervus facialis; VII_{hy} = nervus hyomandibularis; VII_{yi} = nervus vidiani.



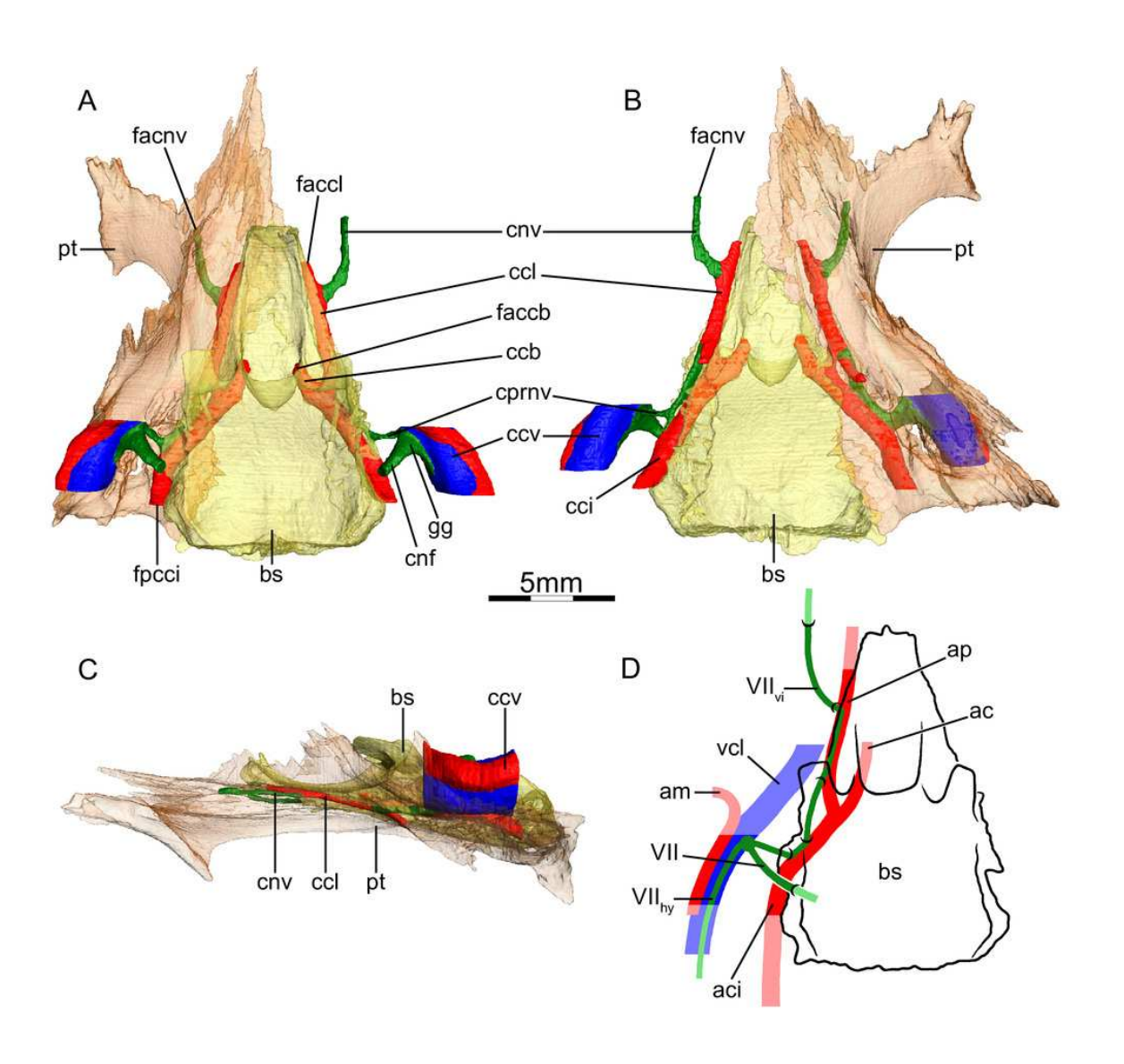




The carotid circulation and vidian canal system of *Glyptemys insculpta* (FMNH 22240).

Three-dimensional reconstructions of the basisphenoid, right pterygoid, in (A) dorsal, (B) ventral, and (C) left lateral view. Illustration in dorsal view (D) highlighting the placement of relevant arteries, nerves, and veins. The red portion of the canalis cavernosus shows the inferred position of the mandibular artery. Abbreviations: ac = arteria carotis cerebralis; aci = arteria carotis interna; ap = arteria palatina; am = arteria mandibularis; bs = basisphenoid; ccb = canalis caroticus basisphenoidalis; cci = canalis caroticus internus; ccl = canalis caroticus lateralis; ccv = canalis cavernosus; cnf = canalis nervus facialis; cnv = canalis nervus vidianus; cprnv = canalis pro ramo nervi vidiani; faccb = foramen anterius canalis carotici basisphenoidalis; faccl = foramen anterius canalis caroticus lateralis; facnv = foramen anterius canalis nervi vidiani; fpcci = foramen posterius canalis carotici interni; gg = geniculate ganglion; pt = pterygoid; vcl = vena capitis lateralis; VII = nervus facialis; VII_{by} = nervus hyomandibularis; VII_{yi} = nervus vidiani.



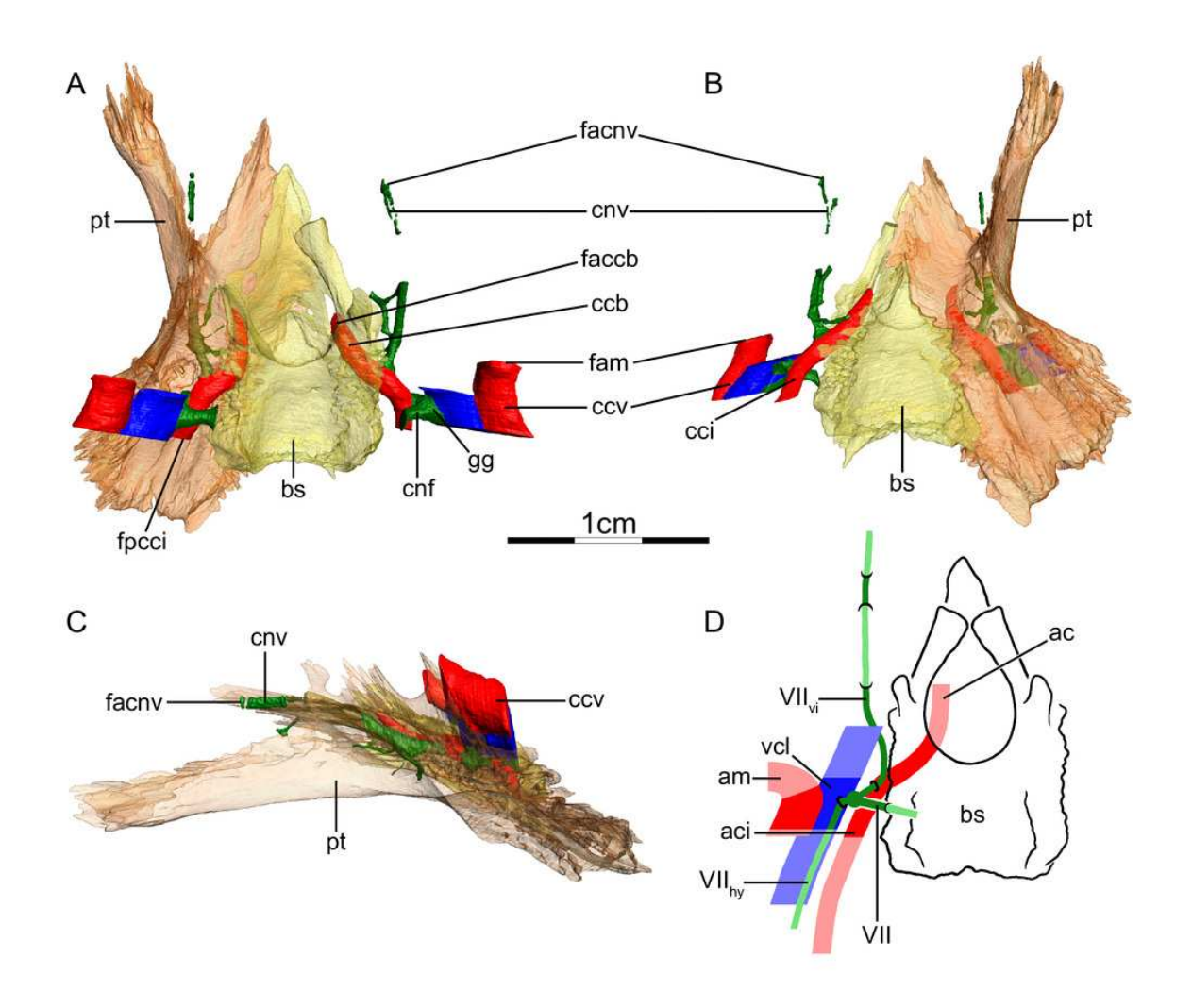




The carotid circulation and vidian canal system of Gopherus agassizii (FMNH 216746).

Three-dimensional reconstructions of the basisphenoid, right pterygoid, in (A) dorsal, (B) ventral, and (C) left lateral view. Illustration in dorsal view (D) highlighting the placement of relevant arteries, nerves, and veins. The red portion of the canalis cavernosus shows the inferred position of the mandibular artery. Abbreviations: ac = arteria carotis cerebralis; aci = arteria carotis interna; am = arteria mandibularis; bs = basisphenoid; ccb = canalis caroticus basisphenoidalis; cci = canalis caroticus internus; ccv = canalis cavernosus; cnf = canalis nervus facialis; cnv = canalis nervus vidianus; faccb = foramen anterius canalis carotici basisphenoidalis; facnv = foramen anterius canalis nervi vidiani; fam = foramen arteriomandibulare; fpcci = foramen posterius canalis carotici interni; gg = geniculate ganglion; pt = pterygoid; vcl = vena capitis lateralis; VII = nervus facialis; VII_{hy} = nervus hyomandibularis; VII_{vi} = nervus vidiani.



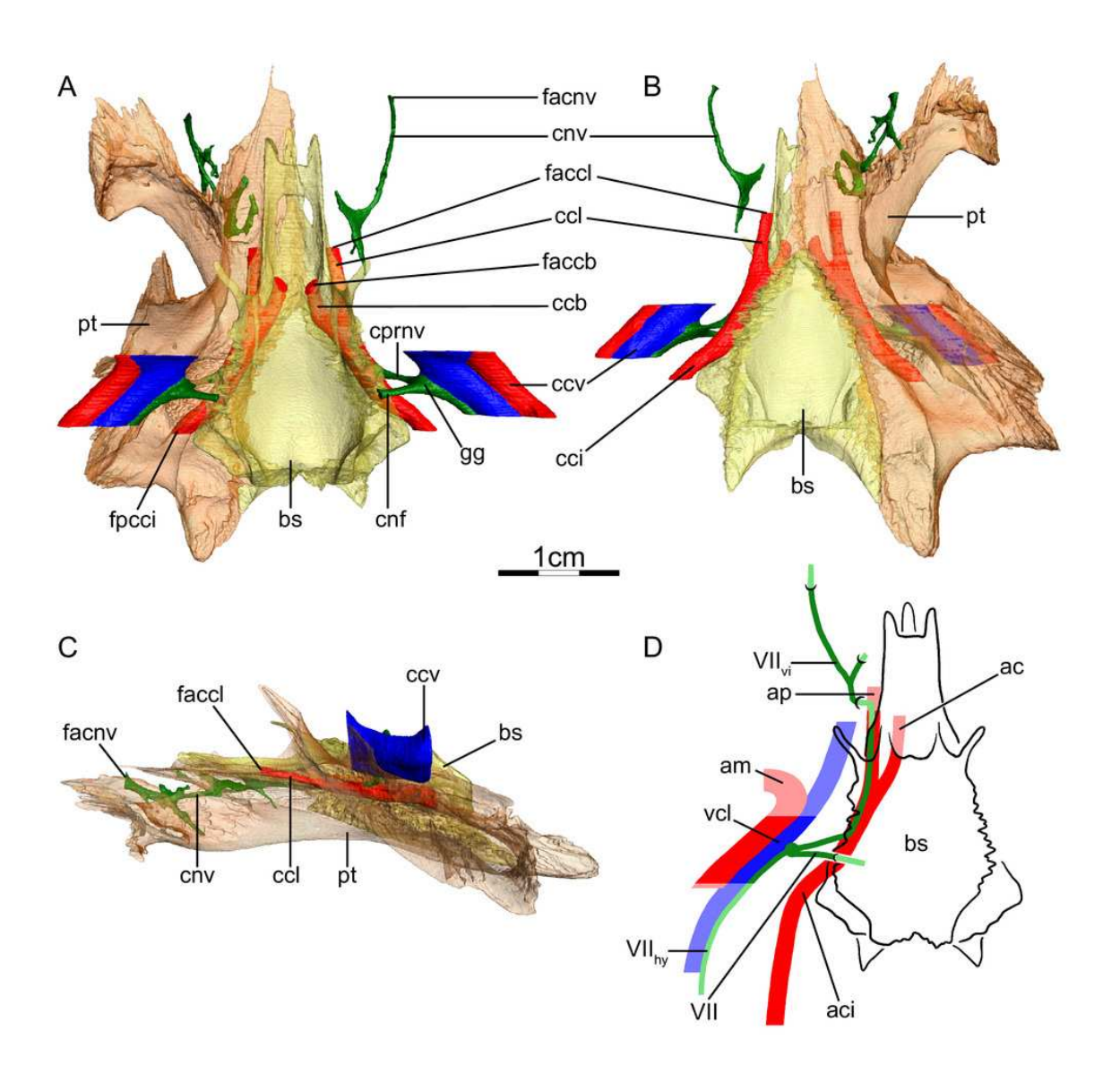




The carotid circulation and vidian canal system of Batagur baska (NHMUK 67.9.28.7).

Three-dimensional reconstructions of the basisphenoid, right pterygoid, in (A) dorsal, (B) ventral, and (C) left lateral view. Illustration in dorsal view (D) highlighting the placement of relevant arteries, nerves, and veins. The red portion of the canalis cavernosus shows the inferred position of the mandibular artery. Abbreviations: ac = arteria carotis cerebralis; aci = arteria carotis interna; ap = arteria palatina; am = arteria mandibularis; bs = basisphenoid; ccb = canalis caroticus basisphenoidalis; cci = canalis caroticus internus; ccl = canalis caroticus lateralis; ccv = canalis cavernosus; cnf = canalis nervus facialis; cnv = canalis nervi vidiani; cprnv = canalis pro ramo nervi vidiani; faccb = foramen anterius canalis caroticus cerebralis; faccl = foramen anterius canalis caroticus lateralis; facnv = foramen anterius canalis nervi vidiani; fpcci = foramen posterius canalis carotici interni; gg = geniculate ganglion; pt = pterygoid; vcl = vena capitis lateralis; VII = nervus facialis; VII_{hy} = nervus hyomandibularis; VII_{vi} = nervus vidiani.

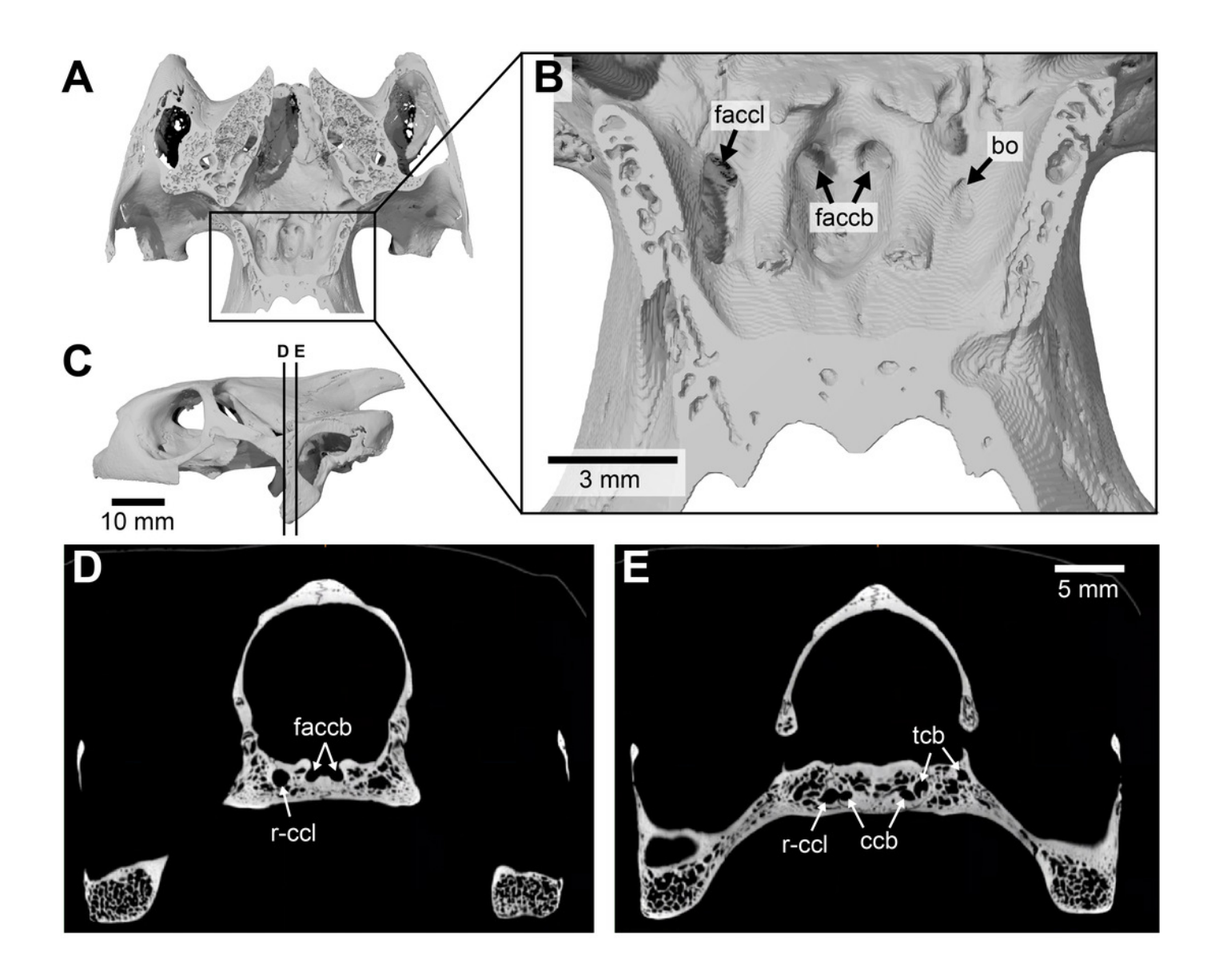






Asymmetry in osteological correlates for the palatine artery in *Manouria impressa* (SMF 69777).

(A), dorsal view of horizontally cut basicranium for orientation. (B), as A, but zoomed in on details of anterior exiting foramina for the carotid arterial system. (C), cranium in left lateral view, showing position of axial slices shown in D-E. (D), axial CT slice at position of foramina anterius canalis carotici basisphenoidalis. (E), axial CT slice at position of carotid split. Note that canals and foramina for the palatine artery are present on the right side, although the palatine artery is generally absent in testudinids. Abbreviations: bo = blind opening (opens into bone, but does not connect to blood or nervous system); ccb = canalis caroticus basisphenoidalis; faccb = foramen anterius canalis carotici basisphenoidalis; faccl = foramen anterius canalis carotici lateralis; r-ccl = right canalis caroticus lateralis; tcb = trabeculae of cancellous bone (small internal openings not connect to blood or nervous system).

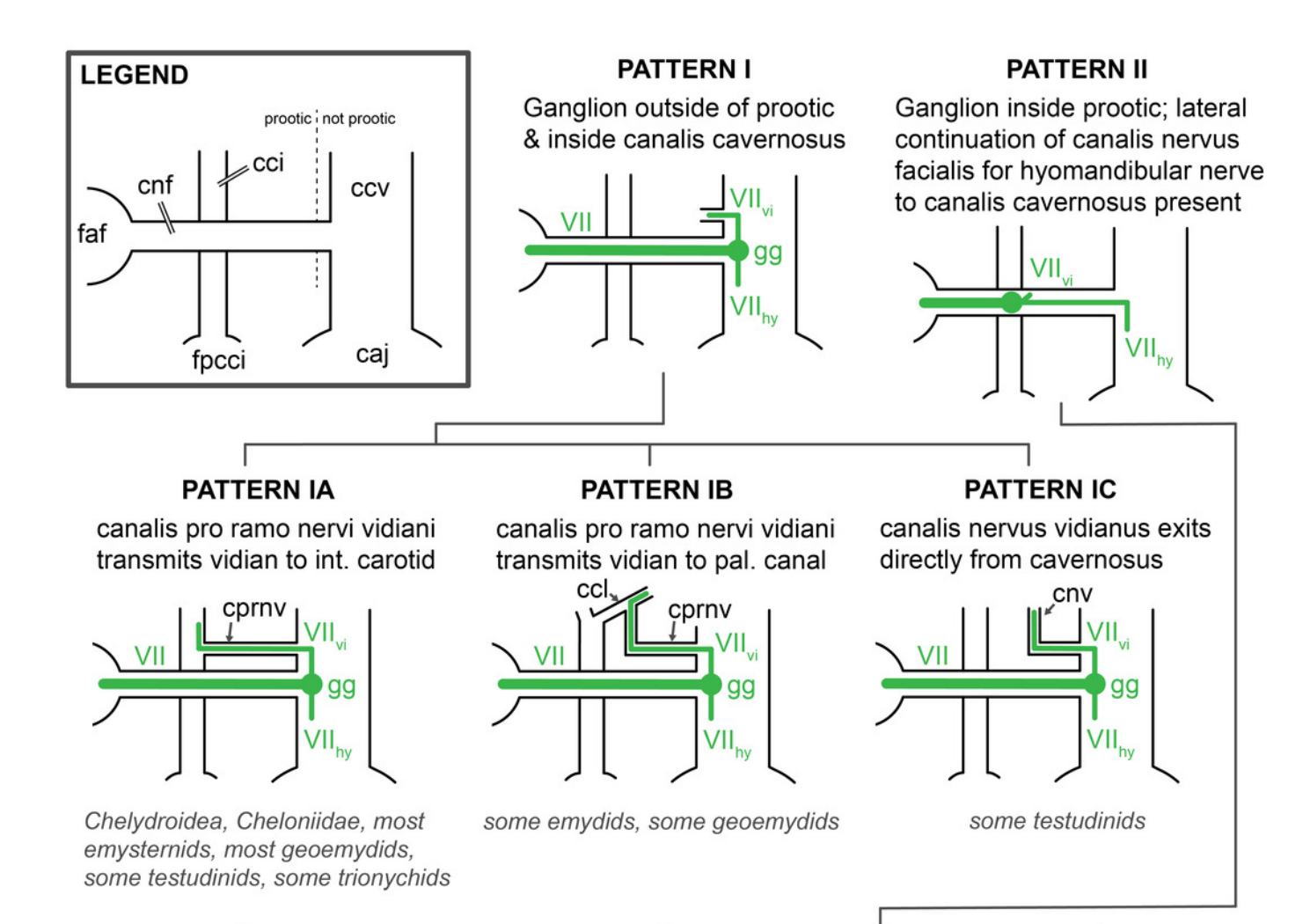




Schematic overview of patterns pertaining to the split of the facial nerve into its hyomandibular and vidian branches.

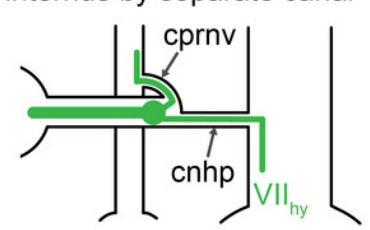
Abbreviations: caj = cavum acustico-jugulare; ccv = canalis cavernosus; cci = canalis caroticus internus; ccl = canalis caroticus lateralis; cnf = canalis nervus facialis; cnhp = canalis nervus hyomandibularis proximalis; cnv = canalis nervus vidianus; cprnv = canalis pro ramo nervi vidiani; faf = fossa acustico-facialis; fpcci = foramen posterius canalis carotici interni; gg = geniculate ganglion; VII = nervus facialis; VII $_{hy}$ = nervus hyomandibularis; VII $_{vi}$ = nervus vidiani.





PATTERN IIA

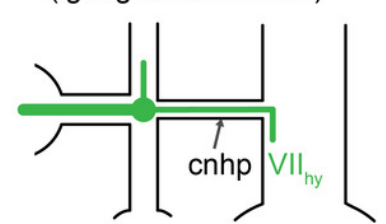
Vidian nerve transmitted from ganglion to canalis caroticus internus by separate canal



Carettochelys insculpta, some trionychids, some testudinids, podocnemidids

PATTERN IIB

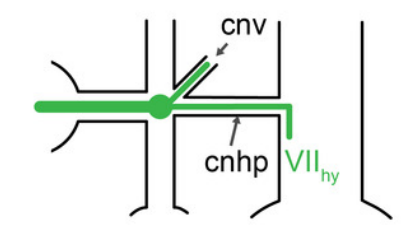
Vidian nerve enters canalis caroticus internus directly ('ganglion within cci')



most chelids, Pelomedusa subrufa Dermochelys coriacea

PATTERN IIC

Vidian nerve enters canalis nervus vidianus directly



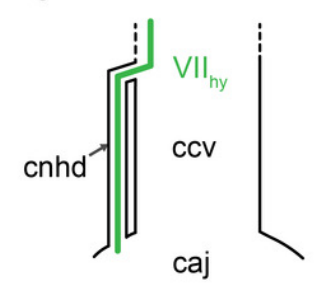
Chelus fimbriatus, Pelusios subniger

Schematic overview of patterns pertaining to the posterior portion of the hyomandibular nerve.

The five patterns presented herein only apply to taxa in which the vidian nerve enters the carotid canal system (i.e. turtles with patterns IA, IIA, and IIB). Abbreviations: caj = cavum acustico-jugulare; ccv = canalis cavernosus; cnhd = canalis nervus hyomandibularis distalis; $snh = sulcus nervus hyomandibularis; VII_{hv} = nervus hyomandibularis.$

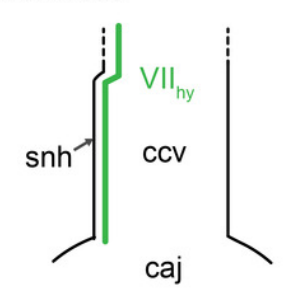
PATTERN a

Distal part of hyomandibular nerve in separate canal paralleling canalis cavernosus



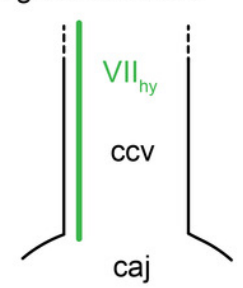
PATTERN b

Distal part of hyomandibular nerve in sulcus in wall of canalis cavernosus



PATTERN c

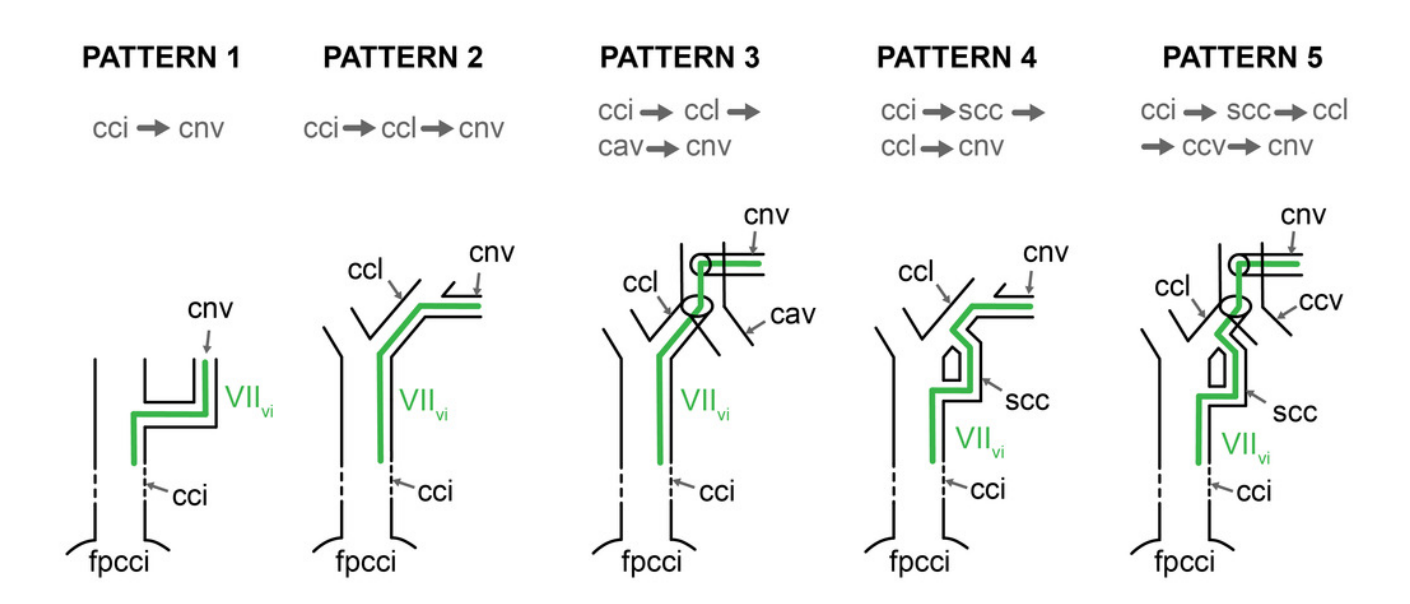
Distal part of hyomandibular nerve in canalis cavernosus; no osteological correlate





Schematic overview of patterns pertaining to the anterior portion of the vidian nerve.

Abbreviations: ccv = canalis cavernosus; cci = canalis caroticus internus; ccl = canalis caroticus lateralis; cnv = canalis nervus vidianus; fpcci = foramen posterius canalis carotici interni; scc = "short cut canal".





Relationship of internal carotid artery size and stapedial artery size in turtles.

(A), PGLS regression of \log_{10} -cross-sectional diameter of internal carotid artery canal on \log_{10} -cross-sectional diameter of stapedial artery canal. Solid grey line is the regression line describing a model with a single slope and intercept for all taxa. Dashed grey lines are regression lines for subsets of the data (see text and table 3 for details). (B), plot showing which data points were used as subsets for the multiple regression model test. (C), residual plot of PGLS regression of the full dataset, ordered by clades. Symbols in A and C denote clade attributions.

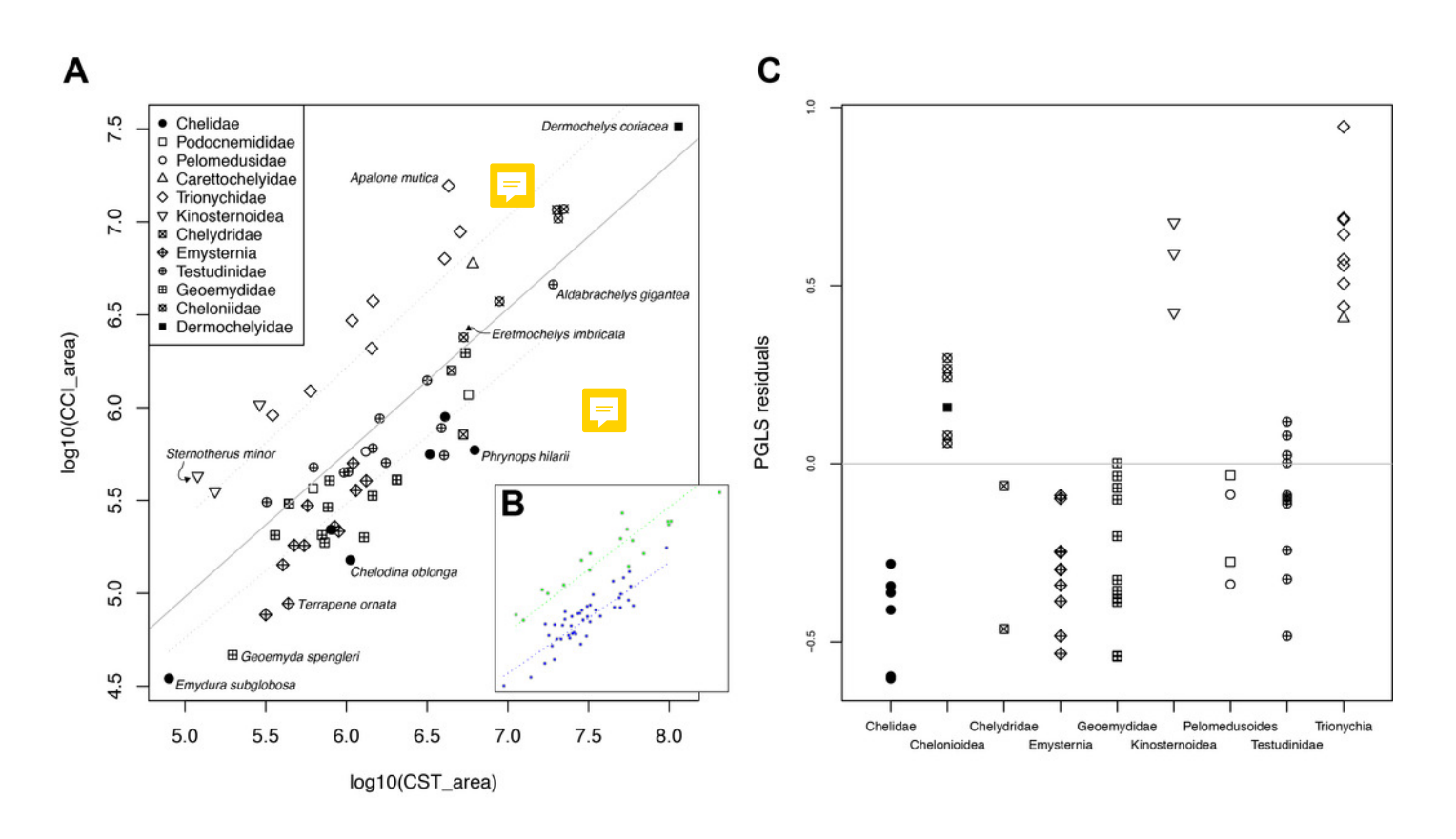




Table 1(on next page)

List of specimens used in this study.

Abbreviations: **FMNH**, Field Museum of Natural History, Chicago, IL, USA; **NHMUK**, Natural History Museum London, London, England; **NMB**, Naturhistorisches Museum Basel, Basel, Switzerland; **PCHP**, Chelonian Research Institute, Oviedo, FL, USA; **PIMUZ**, Paläontologisches Museum Zürich, Zürich, Switzerland; **SMF**, Senckenberg Naturmuseum Frankfurt, Frankfurt am Main, Germany; **SMNS**, Staatliches Museum für Naturkunde Stuttgart, Stuttgart, Germany; **UF**, Florida Museum of Natural History, Gainesville, FL, USA; **UMZC**, University Museum of Zoology Cambridge, Cambridge, England.

PeerJ

Taxon	Specimen(s) used	Repository	Project	Media accession number	Citation/Source
Carettochelyidae					
Carettochelys insculpta	NHMUK 1903.7.10.1	MorphoSource	P769	M42840	Evers (2019)
Carettochelys insculpta	SMF 56626	none	NA	NA	shared by I. Werneburg
Chelidae					
Chelodina oblonga	NHMUK 64.12.22	MorphoSource	P769	M42849	Evers (2019)
Chelus fimbriatus	NHMUK 81.9.27.4	MorphoSource	P769	M42856	Evers (2019)
Emydura subglobosa	PIMUZ lab# 2009.37	none	NA	NA	Lautenschlager et al. (2018)
Hydromedusa tectifera	SMF 70500	none	NA	NA	shared by I. Werneburg
Phrynops geoffroanus	SMF 45470	MorphoSource	P462	M22118	Evers & Benson (2018)
Phrynops hilarii	NHMUK 91.3.16.1	MorphoSource	P769	M42860	Evers (2019)
Cheloniidae					
Caretta caretta	NHMUK 1938.1.9.1	MorphoSource	P769	M42843	Evers (2019)
Caretta caretta	NHMUK 1940.3.15.1	MorphoSource	P769	M42844	Evers (2019)
Chelonia mydas	NHMUK 1969.776	MorphoSource	P769	M42846	Evers (2019)
Eretmochelys imbricata	FMNH 22242	MorphoSource	P769	M42863	Evers (2019)
Lepidochelys olivacea	SMNS 11070	MorphoSource	P462	M22068	Evers & Benson (2018)
Natator depressus	R112123	none	NA	NA	Jones et al. (2012)
Chelydridae					
Chelydra serpentina	SMF 32846	none	NA	NA	shared by I. Werneburg
Macrochelys temminckii	FMNH 22111	MorphoSource	P769	M42869	Evers (2019)
Dermatemydidae					
Dermatemys mawii	SMF 59463	none	NA	NA	shared by I. Werneburg
Dermochelyidae					
Dermochelys coriacea	FMNH 171756	MorphoSource	P769	M42864	Evers (2019)
Dermochelys coriacea	UMZC R3031	MorphoSource	P462	M22024	Evers & Benson (2018)
Emydidae					
Clemmys guttata	FMNH 22114	MorphoSource	P769	M42870	Evers (2019)
Deirochelys reticularia	FMNH 98754	MorphoSource	P769	M42883	Evers (2019)
Emydoidea blandingii	FMNH 22144	MorphoSource	P769	M42871	Evers (2019)
Emys orbicularis	SMF 1987	none	NA	NA	Lautenschlager et al. (2018)

PeerJ

Glyptemys insculpta	FMNH 22240	MorphoSource	P769	M42873	Evers (2019)
Glyptemys muhlenbergii	UF 85274	Digimorph	NA	NA	shared by J. Olori
Graptemys geographica	NHMUK 55.12.6.11	MorphoSource	P769	M42847	Evers (2019)
Pseudemys floridana	FMNH 8222	MorphoSource	P769	M42882	Evers (2019)
Terrapene coahuila	FMNH 47372	MorphoSource	P769	M42881	Evers (2019)
Terrapene ornata	FMNH 23014	MorphoSource	P769	M42875	Evers (2019)
Geoemydidae					
Batagur baska	NHMUK 67.9.28.7	MorphoSource	P769	M42851	Evers (2019)
Cuora amboinensis	NHMUK 69.42.145	MorphoSource	P769	M42852	Evers (2019)
Cyclemys dentata	NHMUK 97.11.22.3	MorphoSource	P769	M42861	Evers (2019)
Geoclemys hamiltonii	NHMUK 87.9.30.1	MorphoSource	P769	M42859	Evers (2019)
Geoemyda spengleri	FMNH 260381	MorphoSource	P769	M42877	Evers (2019)
Malayemys subtrijuga	NHMUK 1920.1.20.2545	MorphoSource	P769	M42841	Evers (2019)
Mauremys leprosa	NHMUK unnumbered	MorphoSource	P769	M42862	Evers (2019)
Morenia ocellata	NHMUK 87.3.11.7	MorphoSource	P769	M42858	Evers (2019)
Pangshura tecta	NHMUK 1889.2.6.1	MorphoSource	P769	M42839	Evers (2019)
Rhinoclemmys melanosterna	FMNH 44446	MorphoSource	P769	M42879	Evers (2019)
Siebenrockiella crassicollis	NHMUK 1864.9.2.47	MorphoSource	P769	M42837	Evers (2019)
Kinosternidae					
Kinosternon baurii	FMNH 211705	MorphoSource	P769	M42865	Evers (2019)
Kinosternon scorpioides	SMF 71893	none	NA	NA	shared by I. Werneburg
Kinosternon subrubrum hippocrepis	FMNH 211711	MorphoSource	P769	M42866	Evers (2019)
Staurotypus salvinii	NHMUK 1879.1.7.5	MorphoSource	P769	M42838	Evers (2019)
Sternotherus minor	FMNH 211696	MorphoSource	P462	M22123	Evers & Benson (2018)
Pelomedusidae					
Pelomedusa subrufa	NMB 16229	none	NA	NA	scanned at University of Fribourg
Pelusios subniger	NMB 16230	none	NA	NA	scanned at University of Fribourg
Platysternidae					
Platysternon megacephalum	SMF 69684	none	NA	NA	shared by I. Werneburg
Podocnemididae					
Peltocephalus dumerilianus	NHMUK 60.4.16.9	MorphoSource	P769	M42848	Evers (2019)
Podocnemis unifilis	FMNH 45657	MorphoSource	P769	M42880	Evers (2019)

PeerJ

_		
Testu	din	achir

Agrionemys horsfieldii	PCHP 2929	Digimorph	NA	NA	shared by H. Jamniczky
Aldabrachelys gigantea	NHMUK 77.11.12.2	MorphoSource	P769	M42855	Evers (2019)
Gopherus agassizii	FMNH 216746	MorphoSource	P769	M42868	Evers (2019)
Gopherus flavomarginatus	FMNH 98916	MorphoSource	P769	M42884	Evers (2019)
Gopherus polyphemus	FMNH 211815	MorphoSource	P462	M22041	Evers & Benson (2018)
Indotestudo elongata	SMF 71585	none	NA	NA	shared by I. Werneburg
Indotestudo forstenii	SMF 73257	none	NA	NA	shared by I. Werneburg
Kinixys erosa	SMF 40166	none	NA	NA	shared by I. Werneburg
Malacochersus tornieri	SMF 58702	none	NA	NA	Lautenschlager et al. (2018)
Psammobates tentorius verroxii	SMF 57142	none	NA	NA	shared by I. Werneburg
Testudo marginata	FMNH 51672	MorphoSource	P769	M42885	Evers (2019)
Trionychidae					
Amyda cartilaginea	FMNH 244117	MorphoSource	P769	M42876	Evers (2019)
Apalone mutica	PCHP 2746	Digimorph	NA	NA	shared by H. Jamniczky
Apalone spinifera emoryi	FMNH 22178	MorphoSource	P462	M22038	Evers & Benson (2018)
Chitra indica	NHMUK 1926.12.16.1	MorphoSource	P769	M42842	Evers (2019)
Cyclanorbis senegalensis	NHMUK 65.5.9.21	MorphoSource	P769	M42850	Evers (2019)
Cycloderma frenatum	NHMUK 84.2.4.1	MorphoSource	P769	M42857	Evers (2019)
Lissemys punctata	SMF 74141	none	NA	NA	shared by I. Werneburg
Pelodiscus sinensis	IW576-2b	none	NA	NA	Lautenschlager et al. (2018)



Table 2(on next page)

Surface values (μm^2) of the stapedial and carotid artery canals.

Abbreviations: **CCB**, canalis caroticus basisphenoidalis; **CCI**, canalis caroticus internus; **CCL**, canalis caroticus lateralis; **CST**, canalis stapedio-temporalis. Note that value 0 is used when the canalis caroticus lateralis and arteria palatina are known to be absent, whereas NA (non-applicable) is only used for chelonioids, in which the palatine artery is present but does not extend through its own canal, preventing us to make any measurement of the latter.



Specimen number	Clade	CST (µm²)	CCI (µm²)	CCL (µm²)	CCB (µm²)
NHMUK 64.12.22	Chelidae	1 058 910	150 952	0	226 210
NHMUK 81.9.27.4	Chelidae	4 085 377	892 145	0	735 967
PIMUZ lab 2009.37	Chelidae	79 531	34 767	0	48 407
SMF 70500	Chelidae	809 644	219 930	0	129 035
SMF 45470	Chelidae	3 287 280	559 981	0	360 356
NHMUK 91.3.16.1	Chelidae	6 239 953	590 788	0	645 906
NHMUK 60.4.16.9	Podocnemididae	5 715 929	0	0	1 171 054
FMNH 45657	Podocnemididae	622 116	0	0	366 395
NMB 16229	Pelomedusidae	800 031	220 484	0	214 207
NMB 16230	Pelomedusidae	1 317 192	579 301	0	539 570
NHMUK 1903.7.10.1	Carettochelyidae	6 037 962	5 492 060	0	5 946 210
SMF 56626	Carettochelyidae	6 073 891	5 924 760	0	5 758 653
FMNH 244117	Trionychidae	4 050 871	6 345 134	2 472 623	8 542 707
PCHP 2746	Trionychidae	4 294 390	15 625 225	5 531 628	15 083 901
FMNH 22178	Trionychidae	1 083 662	2 942 414	1 085 638	3 592 534
NHMUK 1926.12.16.1	Trionychidae	1 433 582	2 082 272	1 321 450	3 189 755
NHMUK 65.5.9.21	Trionychidae	1 462 382	3 750 276	2 133 552	2 899 158
NHMUK 84.2.4.1	Trionychidae	5 057 276	8 859 103	3 025 341	8 682 245
SMF 74141	Trionychidae	598 611	1 227 979	662 055	1 106 322
IW576-2b	Trionychidae	348 972	910 693	538 326	1 070 091
FMNH 211705	Kinosternoidea	6 887	296 351	284 037	204 334
SMF 71893	Kinosternoidea	0	389 035	324 601	253 329
FMNH 211711	Kinosternoidea	153 559	354 306	426 087	192 819
NHMUK 1879.1.7.5	Kinosternoidea	289 782	1 037 615	1 109 716	430 654
FMNH 211696	Kinosternoidea	119 665	427 605	617 472	253 623
SMF 59463	Kinosternoidea	0	1 956 557	2 431 274	619 092
SMF 32846	Chelydridae	4 474 201	1 585 832	298 793	892 542
FMNH 22111	Chelydridae	5 301 958	715 698	331 401	526 512
SMF 69684	Emysternia	1 326 669	403 520	0	423 613
FMNH 22114	Emysternia	315 976	76 772	21 190	68 564
FMNH 98754	Emysternia	573 476	296 410	25 414	239 791
FMNH 22144	Emysternia	844 910	228 468	109 072	166 938
SMF 1987	Emysternia	547 409	180 790	51 255	175 723
FMNH 22240	Emysternia	1 144 915	357 824	108 998	197 169
UF 85274	Emysternia	1 102 125	501 052	99 906	589 908
NHMUK 55.12.6.11	Emysternia	404 097	142 127	59 958	74 399
FMNH 8222	Emysternia	897 674	215 901	35 132	171 386
FMNH 47372	Emysternia	474 363	181 076	48 008	164 677
FMNH 23014	Emysternia	436 725	87 948	14 436	74 255
PCHP 2929	Testudinidae	3 165 141	1 403 465	0	619 523
NHMUK 77.11.12.2	Testudinidae	19 119 633	4 600 686	0	1 803 844
FMNH 216746	Testudinidae	4 029 636	552 921	0	312 752
FMNH 98916	Testudinidae	3 878 526	775 653	0	628 089
FMNH 211815	Testudinidae	1 460 433	604 499	0	292 845



SMF 71585	Testudinidae	1 610 958	873 682	0	605 264
SMF 73257	Testudinidae	626 304	476 457	0	525 015
SMF 40166	Testudinidae	1 027 408	451 262	0	448 521
SMF 58702	Testudinidae	965 106	447 165	0	223 974
SMF 57142	Testudinidae	320 876	309 491	0	279 191
FMNH 51672	Testudinidae	1 753 928	504 385	0	290 444
NHMUK 67.9.28.7	Geoemydidae	5 452 221	1 966 423	755 435	1 059 290
NHMUK 69.42.145	Geoemydidae	733 274	187 661	93 272	132 423
NHMUK 97.11.22.3	Geoemydidae	705 719	205 409	11 538	250 573
NHMUK 87.9.30.1	Geoemydidae	1 284 666	200 522	100 544	232 274
FMNH 260381	Geoemydidae	197 252	46 546	3 301	45 749
NHMUK 1920.1.20.2545	Geoemydidae	784 335	404 425	0	412 694
NHMUK unnumbered	Geoemydidae	766 806	291 204	66 746	180 330
NHMUK 87.3.11.7	Geoemydidae	1 452 138	334 818	109 244	201 610
NHMUK 1889.2.6.1	Geoemydidae	2 049 189	408 694	0	354 358
FMNH 44446	Geoemydidae	440 261	303 083	0	180 061
NHMUK 1864.9.2.47	Geoemydidae	361 209	205 648	79 943	128 400
NHMUK 1938.1.9.1	Cheloniidae	26 309 163	11 101 359	NA	5 080 248
NHMUK 1940.3.15.1	Cheloniidae	20 113 757	11 617 628	NA	5 565 138
NHMUK 1969.776	Cheloniidae	22 229 237	11 714 676	NA	3 359 440
FMNH 22242	Cheloniidae	5 323 654	2 387 389	NA	1 457 179
SMNS 11070	Cheloniidae	8 862 496	3 736 567	NA	1 944 444
R112123	Cheloniidae	20 561 877	10 457 393	NA	3 623 651
FMNH 171756	Dermochelyidae	114 071 530	32 495 529	NA	NA
UMZC R3031	Dermochelyidae	94 063 561	32 012 524	NA	NA

1



Table 3(on next page)

Results of PGLS regressions of internal carotid artery size on stapedial artery size.

CCI stands for cross-sectional area of the internal carotid artery canal. CST stands for cross-sectional area of stapedial artery canal. CTK-abbreviated model describes model only including chelonioids, trionychians, and kinosternoids. Remaining-abbreviated model includes all taxa not included in the CTK-model. Phylogenetic signal (lambda) was estimated during model fitting. R2 is the generalized coefficient of determination described by Nagelkerke (1991).



Model	Lambda	Variable	Coefficient	R ²
$(\log 10(\text{CCI}) \sim \log 10(\text{CST}))_{\text{alltaxa}}$	0,957	Intercept	1,098	0,73
		Slope	0,776	
$(\log 10(CCI) \sim \log 10(CST))_{ctk}$	0,738	Intercept	1,84	0,89
		Slope	0,735	
(log10(CCI) ~ log10(CST)) _{remaining}	0,4	Intercept	0,892	0,75
<u> </u>		Slope	0,764	